



City Research Online

City, University of London Institutional Repository

Citation: Bazargan, M. (1981). Simultaneous heat and mass transfer in an inclined rectangular cavity and its application to solar distillation.. (Unpublished Doctoral thesis, The City University)

This is the accepted version of the paper.

This version of the publication may differ from the final published version.

Permanent repository link: <https://openaccess.city.ac.uk/id/eprint/34302/>

Link to published version:

Copyright: City Research Online aims to make research outputs of City, University of London available to a wider audience. Copyright and Moral Rights remain with the author(s) and/or copyright holders. URLs from City Research Online may be freely distributed and linked to.

Reuse: Copies of full items can be used for personal research or study, educational, or not-for-profit purposes without prior permission or charge. Provided that the authors, title and full bibliographic details are credited, a hyperlink and/or URL is given for the original metadata page and the content is not changed in any way.

City Research Online:

<http://openaccess.city.ac.uk/>

publications@city.ac.uk

SIMULTANEOUS HEAT AND MASS TRANSFER
IN AN INCLINED RECTANGULAR CAVITY AND ITS APPLICATION TO
SOLAR DISTILLATION

by

Mehdi Bazargan

A Thesis submitted for the Degree of
Doctor of Philosophy
of

The City University, London

The Department
of
Mechanical Engineering

July 1981

The following appendices have been removed for copyright reasons:

Appendix 2 - pp. 178-196

Appendix 6 - pp. 203-207

Appendix 9 - pp. 233-239

Appendix 10 - pp. 240-243

CONTENTS

	32
	52
	57
	Page
	59
LIST OF TABLES	6
LIST OF FIGURES	8
ACKNOWLEDGEMENTS	10
ABSTRACT	12
NOMENCLATURE	13
1. INTRODUCTION	16
1.1 SCOPE OF THE TREATMENT	18
1.2 LITERATURE REVIEW	19
1.2.1 SIMULTANEOUS HEAT AND MASS TRANSFER	19
1.2.2 SOLAR DISTILLATION	23
=====	
PART 1 SIMULTANEOUS HEAT AND MASS TRANSFER IN AN	27
INCLINED RECTANGULAR CAVITY	27
=====	
2. MATHEMATICAL FORMULATION	25
2.1 EQUATIONS OF CHANGE	25
2.1.1 SET 1 OF THE EQUATIONS	26
2.1.2 SET 2 OF THE EQUATIONS	28
2.2 BOUNDARY CONDITIONS	30
2.3 NORMALIZATION	31

3. METHOD OF SOLUTION	35
3.1 GRID	35
3.2 FINITE DIFFERENCE EQUATION OF ENERGY	37
3.3 FINITE DIFFERENCE EQUATIONS OF MOMENTUM AND	
DIFFUSION	40
3.4 FINITE DIFFERENCE EQUATION OF CONTINUTY	44
3.5 BOUNDARY CONDITIONS	46
3.6 SOLUTION PROCEDURE	48

4. HEAT TRANSFER IN AN INCLINED RECTANGULAR CAVITY	50
4.1 EQUATIONS TO BE SOLVED	50
4.2 RESULTS AND COMPARISONS FOR THE CASE OF A	102

VERTICAL CAVITY	52
4.2.1 TEMPERATURE DISTRIBUTION	52
4.2.2 HEAT TRANSFER RATE	57
4.3 RESULTS AND COMPARISONS FOR THE CASE OF INCLINED CAVITIES	59
4.4 CONCLUSIONS	59

5. WATER DISTILLATION IN A VERTICAL RECTANGULAR CAVITY	61
5.1 NATURE OF THE PROCESS	61
5.2 PREPARATION OF THE COMPUTER PROGRAM	62
5.3 CASES UNDER CONSIDERATION	62
5.4 RESULTS AND COMPARISONS	63
5.4.1 MASS TRANSFER	63
5.4.2 HEAT TRANSFER	70
5.4.3 DISCUSSION OF THE RESULTS	73
5.5 IMPROVEMENT OF THE SOLUTION	73
5.5.1 EFFECT OF TANGENTIAL VELOCITY AT THE HOT BOUNDARY	76
5.5.2 EFFECT OF VARIABLE PROPERTIES	77
5.5.3 PHASE CHANGE	77
5.6 FINAL SOLUTION	82
5.6.1 RESULTS AND COMPARISONS	82
5.6.2 DISCUSSION OF THE FINAL RESULTS	86
5.7 HEAT AND MASS TRANSFER CORRELATIONS	87
5.7.1 NORMALIZATION OF THE EQUATIONS OF CHANGE	87
5.7.2 MODELS OF CORRELATIONS	88
5.7.2.a TYPE 1	88
5.7.2.b TYPE 2	90
5.7.3 METHOD OF CORRELATION	91
5.7.4 RESULTS OF CORRELATION	92
5.7.4.a CORRELATIONS OF TYPE 1	92
5.7.4.b CORRELATIONS OF TYPE 2	98
5.7.5 DISCUSSION OF THE CORRELATIONS	98

6. CORRELATION OF HEAT AND MASS TRANSFER IN AN INCLINED CAVITY	102
6.1 RESULTS AND DISCUSSIONS	102
6.1.1 HEAT AND MASS TRANSFER RATES	102

6.1.2 CORRELATIONS OF HEAT AND MASS TRANSFER	103
10.1 EFFECT OF ATMOSPHERIC VARIABLES	150
10.1.1 SOLAR RADIATION	150
10.1.2 AMBIENT TEMPERATURES	150
=====	
PART 2 SOLAR DISTILLATION	
=====	
7. SOLAR STILLS	111
7.1 BASIC OPERATION	111
7.2 ROOF-TYPE STILLS	111
7.3 FLAT TILTED SOLAR STILLS	113
7.4 MULTIPLE EFFECT SOLAR STILLS	114

8. SOLAR RADIATION	115
8.1 SOLAR RADIATION REACHING THE EARTH	115
8.2 DIRECT AND DIFFUSE RADIATION	116
8.3 GEOMETRY OF DIRECT AND DIFFUSE RADIATION	117
8.3.1 DIRECT RADIATION	117
8.3.2 DIFFUSE RADIATION	118
8.4 RADIATION ON A HORIZONTAL AND ON A TILTED SURFACE	119
8.5 ESTIMATION OF DAILY TOTAL RADIATION ON A HORIZONTAL SURFACE	120
8.5.1 DAILY EXTRATERRESTRIAL RADIATION	122
8.5.2 SUNSHINE HOURS AS PERCENTAGE OF MAXIMUM	122
8.5.3 CONSTANTS 'a' AND 'b'	123
8.6 HOURLY RADIATION ON A HORIZONTAL SURFACE	125
8.7 HOURLY RADIATION ON A TILTED SURFACE	131
8.8 MONTHLY AND ANNUAL RADIATION ON A TILTED SURFACE	132
8.9 TRANSMISSION AND ABSORPTION	133

9. SIMULTANEOUS HEAT AND MASS TRANSFER IN A TILTED SOLAR STILL	139
9.1 ATTENUATION AND DISSIPATION OF SOLAR INCIDENT RADIATION	139
9.2 STEADY STATE, HOURLY ENERGY BALANCE	141
9.2.1 COVER ENERGY BALANCE	141
9.2.2 LINER-WATER ENERGY BALANCE	144
9.3 METHOD OF SOLUTION	145
9.4 EXAMPLES OF NUMERICAL SOLUTIONS	146

10. PERFORMANCE OF A TILTED SOLAR STILL	149
10.1 EFFECT OF ATMOSPHERIC VARIABLES	150
10.1.1 SOLAR RADIATION	150
10.1.2 AMBIENT TEMPERATURE	150
10.1.3 WIND VELOCITY	152
10.2 EFFECTS OF DESIGN FACTORS	155
10.2.1 ANGLE OF INCLINATION	156
10.2.2 ASPECT RATIO	157
10.3 EFFECTS OF OPERATIONAL TECHNIQUES	159
10.4 PRODUCTIVITY OF A MODIFIED FLAT TILTED STILL	161
=====	
DISCUSSION	164
CONCLUSIONS	170
RECOMENDATION FOR FURTHER WORK	173
=====	
APPENDIX [1] FINITE DIFFERENCE EQUATIONS FOR BOUNDARIES	174
APPENDIX [2] PRINT-OUT OF THE COMPUTER PROGRAM (THE PROGRAM WHICH SOLVES SET 2 OF THE EQUATIONS OF CHANGE)	177
APPENDIX [3] PHYSICAL PROPERTIES	197
APPENDIX [4] SOLUTION OF ENERGY EQUATION (5.8) (SET 3 OF THE EQUATIONS OF CHANGE)	199
APPENDIX [5] DEFINITION OF SHERWOOD AND NUSSELT NUMBERS	202
APPENDIX [6] PRINT-OUT OF PROGRAM 'COR'	204
APPENDIX [7] PREDICTED HEAT AND MASS TRANSFER RATES IN AN INCLINED RECTANGULAR CAVITY (WATER DISTILLATION)	211
APPENDIX [8] CALCULATIN OF DECLINATION	231
APPENDIX [9] PRINT-OUT OF PROGRAM 'SOLAR'	233
APPENDIX [10] PRINT-OUT OF PROGRAM 'STILL'	240
APPENDIX [11] PREDICTED DISTILLATION RATES IN A TILTED FLAT SOLAR STILL	244
=====	
REFERENCES	264

LIST OF TABLES

	page
Table 4.1 Predicted and reported heat transfer rates in a vertical rectangular cavity	58
Table 4.2 Predicted and reported Nusselt Numbers for an inclined rectangular cavity	60
Table 5.1 Cases under consideration	64
Table 5.2 Predicted mass transfer rates; vertical cavity; Conduction-Diffusion regime	71
Table 5.3 Predicted mass transfer rates; vertical cavity; Transient regime	71
Table 5.4 Predicted mass transfer rates; vertical cavity; Boundary regime	72
Table 5.5 Predicted heat transfer rates; vertical cavity; Conduction-Diffusion regime	74
Table 5.6 Predicted heat transfer rates; vertical cavity; Transient regime	74
Table 5.7 Predicted heat transfer rates; vertical cavity; Boundary regime	75
Table 5.8 Effect of tangential velocity on mass transfer rates (Run 62)	78
Table 5.9 Effect of variable physical and transport properties on mass transfer rate (Run 62)	78
Table 5.10 Mass transfer rates obtained from Set 3 of the equations of change	83
Table 5.11 Heat transfer rates obtained from Set 3 of the equations of change	84
Table 5.12 Nusselt numbers obtained from calculation and correlation Type 1	96
Table 5.13 Sherwood numbers obtained from calculation and correlation Type 1	93
Table 5.14 Nusselt numbers obtained from calculation and correlation Type 2	99
Table 5.15 Sherwood numbers obtained from calculation and correlation Type 2	100
Table 6.1 Predicted heat and mass transfer rates in an inclined rectangular cavity (Run 62)	104
Table 6.2 Heat transfer correlations in a	

	rectangular cavity with different angles of inclination (Type 1)	107
Table 6.3	Mass transfer correlations in a rectangular cavity with different angles of inclination (Type 1)	108
Table 6.4	Heat transfer correlations in a rectangular cavity with different angles of inclination (Type 2)	109
Table 6.5	Mass transfer correlations in a rectangular cavity with different angles of inclination (Type 2)	110
Table 8.1	Climate Constants for use in Equation (8.11)	124
Table 8.2	Monthly incident radiation (Kw-hr/m ²) on an inclined surface with different angles of inclination	134
Table 8.3	Monthly radiation (Kw-hr/m ²) transmitted through a tilted surface with different angles of inclination	137
Table 9.1	Daily distillation rates for a flat tilted solar still	148
Table 10.1	Monthly and annual distillation rates for an adjustable tilted solar still with recirculating system of feeding	163

LIST OF FIGURES

	page
Figure 2.1 Simultaneous heat and mass transfer in an inclined rectangular cavity	26
Figure 3.1 The grid and different types of control volumes	36
Figure 3.2 Notation for a scalar control volume	39
Figure 3.3 Notation for a u-control volume	42
Figure 3.4 Notation for a v-control volume	43
Figure 4.1 Physical model of heat transfer in an inclined rectangular cavity	51
Figure 4.2 Temperature profiles in Conduction regime of flow in a vertical cavity (Width=0.7 in.; Height=14.0 in.)	53
Figure 4.3 Temperature profiles in Transient regime of flow in a vertical cavity (Width=1.4 in.; Height=14.0 in.)	55
Figure 4.4 Temperature profiles in Boundary regime of flow in a vertical cavity (Width=1.4 in.; Height=14.0 in.)	56
Figure 5.1 Mass fraction distribution at mid-height across a vertical cavity in Conduction-Diffusion regime of flow	66
Figure 5.2 Mass fraction distribution at mid-height across a vertical cavity in Transient regime of flow	67
Figure 5.3 Mass fraction distribution at mid-height across a vertical cavity in Boundary regime of flow	68
Figure 5.4 Normal velocity distribution at different heights across a vertical cavity in Boundary regime of flow	69
Figure 5.5 Temperature profiles at different heights	85
Figure 5.6 Variation of Nusselt number with combined Grashof number	93
Figure 5.7 Variation of Sherwood number with combined Grashof number	95
Figure 6.1 Variation of Sherwood number ratio	

with angle of inclination	105
Figure 7.1 Cross section of a roof type solar still mounted on the ground	112
Figure 8.1 Insolation profile for the intermittency function with V equal to 0 and 31 (Equation 8.14)	126
Figure 8.2 Insolation profile for a day with light cloud ($Q_t/Q_{cl}=0.83$; Equ. 8.19)	129
Figure 8.3 Insolation profile for a densely clouded day ($Q_t/Q_{cl}=0.33$; Equ. 8.20)	130
Figure 8.4 Monthly mean of daily radiation in Tehran on clear days (Latitude=35.6 N; Angle of inclination=35.0 deg.; Azimuth angle=0.0)	135
Figure 9.1 Energy transfer process in a tilted solar still	140
Figure 10.1 Effect of Insolation rate on productivity	151
Figure 10.2 Effect of Ambient temperature on productivity	153
Figure 10.3 Effect of Wind velocity on productivity	154
Figure 10.4 Effect of Width on productivity	158
Figure 10.5 Effect of Temperature difference ($T_{in}-T_{out}$) on productivity	160

ACKNOWLEDGEMENTS

I offer my sincere thanks to my supervisor Dr J. R. Simonson for his supervision and continous advice and encouragement throughout this project.

I would also like to thank Dr M. W. Collins and Dr I. K. Smith for their helpful advice.

Finally many thanks to Mr. M. Norton for his help and advice during the preparation of this script.

ABSTRACT

In the first part of this work the problem of simultaneous heat and mass transfer in an air-water vapour mixture is considered. The physical model is an inclined rectangular cavity with the two longer parallel faces maintained at constant and different temperatures. A film of water flows over the lower and hotter parallel face of the cavity. Evaporation takes place from this face, and at the same time condensation occurs on the upper and cooler parallel face. A natural recirculating flow is established in the cavity, and the equations of continuity, momentum, energy and diffusion are solved numerically. The air in the cavity is assumed dry. In an initial part the procedure is applied to pure heat transfer in an inclined rectangular cavity. Secondly, the problem of water distillation in a vertical cavity is examined. In both cases results are compared with the

I hereby declare that powers of discretion is granted to The City University Librarian to allow the thesis to be copied in whole or in part without further reference to the author. This permission covers only single copies made for study purposes, subject to normal conditions of acknowledgement.

global radiation reaching the earth is examined. A computer simulation method for predicting the solar energy availability is given along with the results of applying the method to the Persian Gulf.

The relationship between the solar energy absorbed by a tilted solar still and other interrelated parameters is investigated. The distillation rate, as a function of solar radiation and other parameters, is obtained. Finally the performance of a tilted solar still, and the effect of atmospheric variables, design factors and operational conditions are examined.

Abstract

In the first part of this work the problem of simultaneous heat and mass transfer in an air water vapour mixture is considered. The physical model is an inclined rectangular cavity with the two longer parallel faces maintained at constant and different temperatures. A film of water flows over the lower and hotter parallel face of the cavity. Evaporation takes place from this face, and at the same time condensation occurs on the upper and cooler parallel face. A natural recirculating flow is established in the cavity, and the equations of continuity, momentum, energy and diffusion are solved numerically. The air in the cavity is assumed non-soluble. As an initial test the procedure is applied to pure heat transfer in an inclined rectangular cavity. Secondly, the problem of water distillation in a vertical cavity is examined. In both cases results are compared with the pertinent previously reported data. Finally the procedure is applied to distillation in an inclined cavity at 10 degrees increments of inclination between 0 and 90 degrees. In each case two types of correlation model are obtained.

In the second part of the work the results of the first part are applied to solar distillation of saline water, in which the evaporative cavity face is heated by incident solar radiation. In conjunction with this work global radiation reaching the earth is examined. A computer simulation method for predicting the solar energy availability is given along with the results of applying the method to the Persian Gulf.

The relationship between the solar energy absorbed by a tilted solar still and other interrelated components of energy transfer is formulated. The distillation rate, as a function of solar radiation and other parameters, is obtained. Finally the performance of a tilted solar still, and the effect of atmospheric variables, design factors and operational conditions are examined.

NOMENCLAURE

- A = area
- $a_1, a_2, k_1, k_2, n_1, n_2, m_1, m_2$ = constants of correlations
- a = climate type constant
- Abp = percentage of absorbed solar radiation
- b = vegetation type constant
- Co = concentration at mean temperature
- Cp = specific heat at constant pressure
- Cp = coefficient of pressure in finite difference equations
- CT = coefficient of temperature in finite difference equations
- Cu = coefficient of u in finite difference equations
- Cv = coefficient of v in finite difference equations
- CW = coefficient of W in finite difference equations
- D = diffusion coefficient
- D = conductive flux
- d = cavity width
- Distil = rate of distillation
- e = emissivity
- F = convective flux
- F = geometric configuration factor
- Feed = saline water feed rate
- g = gravitational acceleration
- Hcl = hourly total radiation on a horizontal surface for clear sky condition
- HD = hourly direct radiation on a horizontal surface
- HDi = hourly direct radiation on an inclined surface
- Hdi = hourly diffuse radiation on an inclined surface
- Hi = hourly total radiation on an inclined surface
- Hlow = lower limit profile of hourly solar radiation
- Hre = reflected hourly radiation
- Ht = hourly total radiation on a horizontal surface
- Hup = upper limit profile of hourly solar radiation
- h = convection coefficient
- h = latent enthalpy of evaporation
- K = thermal conductivity
- l = cavity height
- L = cavity height, dimensionless = Asp (aspect ratio)
- Length = top to bottom distance of still

M = molar mass
 n = mass flux
 n = day of year
 " = pressure
 p = combined pressure, $p = [\rho g(d-x) \sin(\alpha) + \rho g(1-y) \cos(\alpha)]$
 \dot{p} = pressure term in pressure correction finite difference equation
 P = dimensionless pressure
 q = heat transfer per unit area and time
 q = convective + conductive flux
 Qd = daily diffuse radiation on a horizontal surface
 Qe = daily extraterrestrial radiation on a horizontal surface
 Qt = daily total radiation on a horizontal surface
 R = rate of phase change, mass per unit volume and unit time
 RD = conversion factor for direct radiation
 Rd = conversion factor for diffuse radiation
 ST = source term in energy finite difference equation
 Su = source term in u- finite difference equation
 Sv = source term in v- finite difference equation
 T = temperature
 Thick = thickness of insulator
 To = mean temperature
 T1 = temperature at hot side
 T2 = temperature at cold side
 Trn = percentage of transmitted solar radiation through still's transparent cover
 Ts = day length, hours
 ts = actual hours of sunshine
 u = x-velocity
 U = dimensionless X-velocity
 U1 = dimensionless normal velocity at hot wall
 U2 = dimensionless normal velocity at cold wall
 v = y-velocity
 V = dimensionless Y-velocity
 V1 = dimensionless tangential velocity at hot wall
 V2 = dimensionless tangential velocity at cold wall
 V = intermittency factor
 Vw = wind velocity

W = mass fraction
 w = hour angle
Width = distance between cover and bottom of still
 W_{sat} = saturated mass fraction
 x = horizontal coordinate, linear dimension
 X = horizontal coordinate, dimensionless
 XW = mole fraction
 XW_0 = mole fraction at T_0
 XW_1 = mole fraction at T_1
 XW_2 = mole fraction at T_2
 XW_{sat} = saturated mole fraction
 y = vertical coordinate, linear dimension
 Y = vertical coordinate, dimensionless
 α = angle of inclination
 α = thermal diffusivity
 β = thermal coefficient of volumetric expansion
 $\beta_0 = \beta$ at T_0
 δ = concentration coefficient of volumetric expansion
 $\delta_0 = \delta$ at T_0
 δ = surface azimuth angle
 ΔT = temperature difference between outlet and inlet saline water
 δx = grid spacing
 δ = declination, i.e., angular position of the sun
 ξ = ground reflectance factor
 θ = temperature, dimensionless
 θ = angle of incidence of direct radiation
 μ = viscosity
 $\mu_0 = \mu$ at T_0
 $\nu = \mu/\rho$ = kinematic viscosity
 $\nu_0 = \nu$ at T_0
 $\pi = 3.14159\dots$
 ρ = density
 $\rho_0 = \rho$ at T_0
 σ = Stefan-Boltzmann constant
 ϕ = dimensionless mass fraction
 ϕ = latitude
 ϕ_i = incidence angle of diffuse radiation

BZ = phase change number, $h_{\text{yap}}/C_p (W_1 - W_2)/(T_1 - T_2)$
 GrT = heat Grashof number, $d^3 g \beta_o (T_1 - T_2) / \nu_o^2$
 GrXW = mass Grashof number, $d^3 g \delta_o (W_1 - W_2) / \nu_o^2$
 Nu = Nusselt number, hd/K
 Pr = Prandtl number, $C_p \mu / K$
 Ra = Rayleigh number, $GrT \cdot Pr$
 Sc = Schmidt number, ν / D
 Sh = Sherwood number

Suffices

a = air
 AW = air, water in binary mixture of humid air
 ca = convection between cover and ambient
 cond-conv = heat transfer by conduction-convection
 cond-conv, lat = heat transfer by conduction-convection
 and evaporation
 g = at glass surface
 gas = gas substance
 GV = species in binary mixture of gas and vapour
 H2O = quantity evaluated for water vapour
 insul = insulator
 l = based on cavity height
 mix = quantity evaluated for mixture
 vap = vapour substance
 w = at saline water surface
 W, P, E, S and N = quantity evaluated for corresponding
 nodes
 w, e, s and n = quantity evaluated at w, e, s and n
 of scalar-cell
 wu, eu, su and nu = quantity evaluated at wu, eu, su and
 nu of u-cell
 wv, ev, sv and nv = quantity evaluated at wv, ev, sv and
 nv of v-cell

1. INTRODUCTION

Solar distillation of saline or brackish water is one of the many methods employed for producing drinkable water. The method is specially suitable for remote villages in arid tropical areas. Many such villages may be found near the Persian Gulf. In recent years the desire to provide drinkable water in these locations has led the author to the present study.

Although the process of solar distillation has been known for almost a century it was not until the early 1950's that active investigation began. During the following 20 year period extensive experimental work was carried out. In many hundreds of installations, mostly in the United States and Australia, experiments were devised to examine almost all aspects of solar distillation. The purpose was to find out the important variables affecting the productivity of the stills. It was assumed that using the information obtained, a cost effective solar still could be designed. Unfortunately attempts failed and although some improvements were made, the process was not shown to be economical. The reason was that the kind of accurate information necessary for progressive designs could not be provided by empirical methods alone. A thorough theoretical investigation was necessary to understand the nature of the internal energy transfer within the stills.

The process of water distillation in solar stills is one of simultaneous heat and mass transfer in a binary

mixture. In such situations the process results when a gas (i.e. air) is confined between two surfaces of a liquid (water) each maintained at different temperature. The gas is essentially insoluble in the liquid. The matter transferred is the substance comprising the liquid phase which evaporates from the hotter liquid surface (saline or brackish water) and condenses on the cooler liquid surface (distilled water). Because of the important and diverse applications of the process in mechanical and chemical engineering, and lack of sufficient information in the pertinent literature, most of the the present work has been directed towards studying the process of simultaneous heat and mass transfer in the aforementioned systems. This forms the first objective of the present work.

Of the many types of solar still, the "flat tilted still" has attracted the most attention due to its relatively higher productivity and efficiency; low capital cost and the potential flexibility in being modified to more advanced stills. For these reasons the geometry considered throughout the present work is that of an inclined rectangular cavity. Consequently the performance of a flat tilted solar still is studied. This forms the second objective of the present work.

It should be noted that the solution to the process of simultaneous heat and mass transfer submitted in the present work is by no means restricted to a rectangular cavity or to the given binary mixture (air-water vapour). The solution is flexible and can be easily extended to any other geometrical shape and binary mixture.

1.1 SCOPE OF THE TREATMENT

The present work is a theoretical investigation and consists of Part 1 (Chapters 2, 3, 4, 5 and 6) and Part 2 (Chapters 7, 8, 9 and 10):

In the first part, Chapter 2 gives the mathematical formulation of the process of simultaneous heat and mass transfer in a binary mixture. The scope of treatment is limited to: a) a laminar two dimensional steady state flow; b) an inclined rectangular cavity with the two longer, parallel faces maintained at different and constant temperatures. The method of solving the equations obtained in this chapter is discussed in Chapter 3, using a newly devised advanced numerical method for treating laminar recirculating flows. In Chapter 4, the procedure is tested by applying it to the problem of pure heat transfer in an inclined cavity; the predicted results are compared with the available experimental data. The process of water distillation in a vertical cavity is considered in Chapter 5. In this chapter the mathematical model suggested in Chapter 2 is re-examined and improvements are made by introducing mathematical expressions of "phase change phenomena" in the binary mixtures into the equations. In Chapter 6, the modified solution obtained in Chapter 5 is applied to an inclined cavity at 10 increments of inclination between 0.0 and 90.0 degrees. In each case two types of correlation model of heat and mass transfer are obtained. The results are to be used in the next part of the work.

In the second part, Chapter 7 gives a brief summary of some of the important types of solar still. In chapter 8

the availability of solar energy as a function of the angle of inclination of the irradiated surface, latitude, vegetation and climate type, etc. are examined. Empirical equations for estimating the amount of solar energy available to a solar still in hourly, daily and monthly bases are provided. The aim of Chapter 9 is to formulate the model of the process of solar distillation in a flat tilted still. The energy components involved in the overall process are introduced and related by using the correlations obtained in Chapter 6 of the first part. The resulting equations are solved numerically as an example in Chapter 10 where the performance of a flat tilted solar still is illustrated. On an hourly basis the effect of atmospheric, design and operational variables on the performance are investigated.

1.2 LITERATURE REVIEW

For convenience, the review given below is divided into two parts:

- a) In the first part references on simultaneous heat and mass transfer in laminar free convection inside a rectangular cavity are reviewed;
- b) In the second part references on solar distillation are given.

1.2.1 SIMULTANEOUS HEAT AND MASS TRANSFER

There are not many related investigations, theoretical or experimental, in the pertinent literature. It appears that the only available related works are those of Davis [1] and Hu [2], which consider the problem in a vertically positioned rectangular cavity. These two works have been

the main references in the first part of the present investigation.

Davis [1] in his pioneering analytical-experimental work considered the process of "partial pressure" water distillation in a vertical cavity. In the experimental part, for a number of cases, the rates of distillation, total heat transfer and the temperature distribution across the cavity were obtained. Because of some difficulties in controlling experimental conditions the results achieved were not very accurate. Nevertheless his findings form the basis for evaluating the results predicted in the first part of the present work. By direct measurement of the local temperatures in different heights of the cavity, he discovered three regimes of fluid flow in the field. The regimes of flow were essentially similar to those reported by Carlson [3] in an experimental interferometerical investigation into the problem of convective heat transfer in a vertical rectangular cavity. In the theoretical part of his work an unsuccessful attempt was made to solve the problem analytically. The idea was to treat the original system of the flow as two separate boundary layers formed on two parallel infinite plates. [The method was later employed by Chu and Emery [4] for convective pure heat transfer in a vertical rectangular cavity.]. The inherent disadvantage of this approach is that the effect of the recirculation of the fluid resulting from the enclosure of the cavity by the top and the bottom walls can not be taken into account.

It was not until the development of the numerical analysis of the finite difference techniques that the

investigation of natural convective flows within the enclosures was accelerated. Hellums [5] and Churchill [6] were the first to apply an explicit transient numerical method to the solution of natural convection in a long horizontal cylinder. For a rectangular enclosure a number of other investigators employed similar or modified versions of the method of Hellums [5] and Churchill [6]. These investigators include: Wilkes and Churchill [7], De Vahl Davis and Kettleborough [8], Elder [9], Wilkes and Churchill [10], Samuel and Churchill [11], De Vahl Davis [12] and Elder [13]. The main feature of the methods exercised in these references is that the original equations of change were rewritten in terms of vorticity function or stream function or both; the velocity components and the pressure terms being eliminated from the equations before the solutions were sought.

Only after the numerical procedures for solving convective flow in a process of pure heat transfer inside a vertical cavity became practicable, the work by Hu [2] for solving the problem of simultaneous heat and mass transfer in a vertical cavity was initiated. In the theoretical part of his work, he used the method developed by Samuel and Churchill [11], i.e., solution of the finite difference equations of change (in terms of vorticity and stream functions) using the alternating direction implicit method of Peaceman and Ruchford [14]. Assuming no phase change in the field, examples of numerical solutions for binary mixtures of water vapour-air and normal heptane-air were produced. For the case of water vapour-air, comparisons were made between the predicted results and those reported

experimentally by Davis [1]: calculated values were up to 30% higher than the experimental ones. In the experimental part of his work, an optical observation of the fluid flow in a binary mixture of normal heptane-air was made. Three regimes of flow reported by Carlson [3] (in a pure convective heat flow) and by Davis [1] (in a simultaneous convective heat and mass flow), were reported.

The numerical method used by Hu [2] and other similar methods employed in the references cited above, generally run into the problem of convergence and stability. A large number of these methods do not guarantee unconditional convergence; usually convergence capabilities are restricted by critical values of non-dimensional parameters such as Rayleigh number or Grashof number. In addition, using vorticity and stream functions instead of primitive variables (velocity components and pressure) in the equation of change, makes it difficult to account for all phenomena involved in the corresponding process, e.g., phase change of the substance vapour in the binary mixture during the process of heat and mass transfer. However, improvements in fast digital computers and numerical methods in the past ten years have helped to resolve most of these difficulties: the hybrid formula of central and upwind finite differences proposed by Spalding [15] provides a highly stable solution to the equations involved: the numerical scheme presented by Spalding, Gosman, Ruchford et al [16] (based on the hybrid formula of Spalding [15]) is capable of solving the complete and general forms of the equations of change. The numerical scheme used in the first part of the present work is based

on those of Spalding, Gosman, Ruchford et al [16].

1.2.2 SOLAR DISTILLATION

As mentioned earlier, there are not many articles in the literature presenting a theoretical investigation into the problem of solar distillation. Of those which do, the most comprehensive ones include the works by Telkes [17], Dunkle [18], MacLeod and Mc Craken [19], Baum and Bairamov [20], Grune et al [21], Hollands [22], Morse and Read [23], Sheridan et al [24], Close [25] and Cooper [26]. Among these, only a few are concerned with the process of simultaneous heat and mass transfer inside the still envelopes. However, they have employed basically similar methods for treating the process. A brief synopsis of their work is given below:

Dunkle [18] was one of the first investigators of solar distillation who attempted to analyse the internal heat transfer by convection(a) and evaporation(b) in a horizontally positioned solar still:

- a) For heat transfer by convection a correlation similar to that proposed by Jakob [27], for pure heat transfer in a horizontal enclosure, was used. The effect of mass transfer on the mechanism of convection was accounted for by using a modified temperature difference between the evaporating and condensing surfaces in the still. For this purpose the original temperatures were combined with the partial pressures of the water vapour at the water surfaces;
- b) Heat of evaporation was derived from a correlation presented by Bowen [28] which gives the ratio of heat

transfer by convection to that by evaporation from any water surface in contact with the atmosphere.

The overall equations were applied to an idealised still with infinite parallel sides.

MacLeod and McCracken [19] used a correlation for internal convection similar to that used by Dunkle [18] except that it applied to a vertical air space. For the evaporation the absolute humidity difference of the water vapour next to the evaporating and condensing surfaces was used to represent the driving force for mass transfer. The effects of temperature, geometry and heat capacity on the performance of a single effect solar still was illustrated.

Cooper [26] submitted one of the most comprehensive and serious theoretical works in solar distillation. Using a digital simulation technique a detailed study of a transient solar system was produced accompanied by an experimental work. Although almost all of the problems associated with solar stills were elaborated, for internal heat and mass transfer he used the previous correlations suggested by Dunkle [18]. The instantaneous energy balances over different parts of the still were formulated to relate the various heat transfer modes. The resultant equations were solved to produce the relative effects of different parameters on the performance of stills. His work has been one of the main references in the second part of the present work.

2. MATHEMATICAL FORMULATION

In this chapter a mathematical model of the process of simultaneous heat and mass transfer inside an enclosure is considered. The physical model which is of particular interest in this work is shown in Figure 2.1. That is, an inclined rectangular cavity with the two longer parallel faces maintained at constant and different temperatures. A film of liquid flows over the lower and hotter parallel face of the cavity. Evaporation takes place from this face, and at the same time condensation occurs on the upper and cooler parallel side. All other sides are adiabatic and impermeable to both heat and mass transfer respectively. A large concentration of a non-soluble gas is contained within the cavity so that the gas phase is a binary mixture of the vapour substance and a non-condensable gas.

2.1 EQUATIONS OF CHANGE

Derivation of the equations of change describing the process of simultaneous heat and mass transfer in a binary mixture is subject to assumptions which are made. It is obvious that the fewer the number of assumptions, the more accurate the equations obtained. However, neglecting insignificant terms which have little effect on the results is convenient from the computing point of view. For example, viscous dissipation terms in the problems involving low viscosity fluid flow are quite justifiably ignored. Deciding which assumptions are reasonable remains to be verified by solving the different sets of equations

obtained under various sets of assumptions and comparing the results with experimental ones (if these are any available). In the present chapter two sets of equations are derived, these are as below.

2.1.1 SET 1 OF THE EQUATIONS

- In deriving the equations for the present set of change, the following assumptions are made:
- (1) The motion of the fluid during the process is laminar, steady and two dimensional.
 - (2) There are no external forces other than gravity.
 - (3) There is no phase change or chemical reaction in the field.
 - (4) Viscous heat dissipation and mixing are negligible.
 - (5) The medium is transparent to radiative energy.
 - (6) Bulk thermal and pressure expansion are negligible.

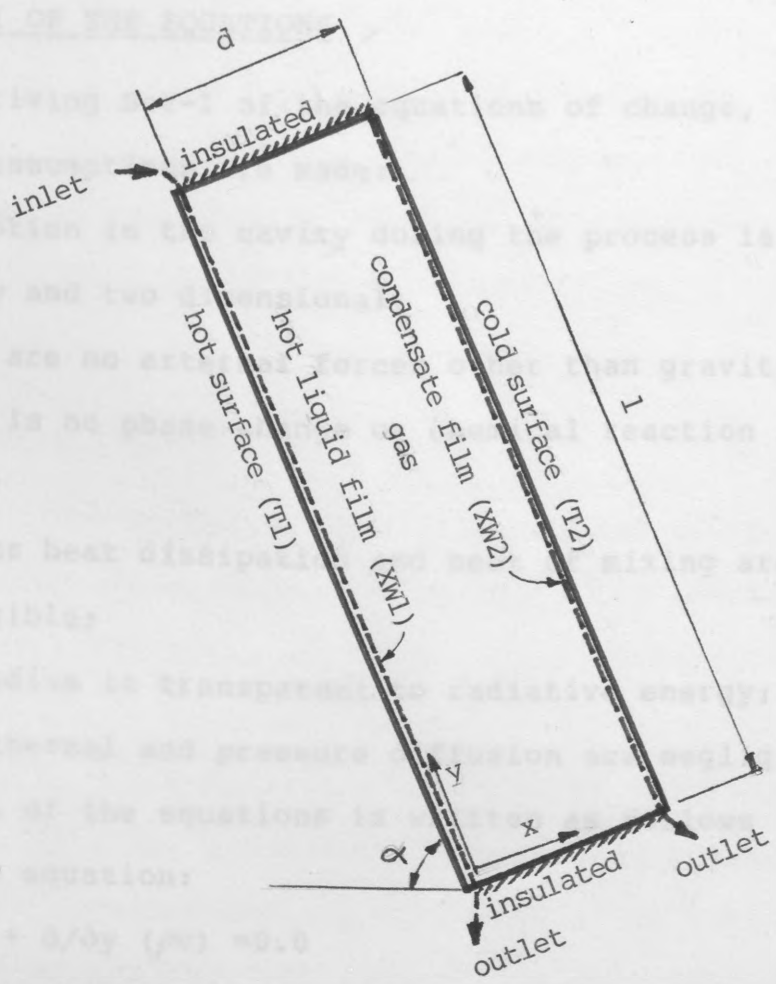


Figure 2.1 Simultaneous heat and mass transfer in an inclined rectangular cavity

Continuity equation:

$$\frac{\partial u}{\partial x} + \frac{\partial v}{\partial y} = 0$$

Momentum equation x-component:

$$\rho u \frac{\partial u}{\partial x} + \rho v \frac{\partial u}{\partial y} = -\frac{\partial p}{\partial x} + \mu \left(\frac{\partial^2 u}{\partial x^2} + \frac{\partial^2 u}{\partial y^2} \right) + \rho g \cos(\phi)$$

Momentum equation y-component:

$$\rho u \frac{\partial v}{\partial x} + \rho v \frac{\partial v}{\partial y} = -\frac{\partial p}{\partial y} + \mu \left(\frac{\partial^2 v}{\partial x^2} + \frac{\partial^2 v}{\partial y^2} \right) - \rho g \sin(\phi)$$

Energy equation:

$$\rho u \frac{\partial T}{\partial x} + \rho v \frac{\partial T}{\partial y} = \frac{\partial}{\partial x} \left(k \frac{\partial T}{\partial x} \right) + \frac{\partial}{\partial y} \left(k \frac{\partial T}{\partial y} \right) + \rho c_p \dot{m}''_1 (T_1 - T) + \rho c_p \dot{m}''_2 (T_2 - T)$$

obtained under various sets of assumptions and comparing the results with experimental ones (if there are any available). In the present chapter two sets of equations are derived, these are as below.

2.1.1 SET 1 OF THE EQUATIONS

In deriving Set-1 of the equations of change, the following assumptions are made:

- (1) The motion in the cavity during the process is laminar, steady and two dimensional;
- (2) There are no external forces other than gravity;
- (3) There is no phase change or chemical reaction in the field;
- (4) Viscous heat dissipation and heat of mixing are negligible;
- (5) The medium is transparent to radiative energy;
- (6) Both thermal and pressure diffusion are negligible.

Then Set-1 of the equations is written as follows [29]:

Continuity equation:

$$\frac{\partial}{\partial x} (\rho u) + \frac{\partial}{\partial y} (\rho v) = 0.0 \quad (2.1)$$

Momentum equation x-component:

$$\rho u \frac{\partial u}{\partial x} + \rho v \frac{\partial u}{\partial y} = -\frac{\partial p}{\partial x} + \quad (2.2)$$

$$\frac{\partial}{\partial x} [2\mu \frac{\partial u}{\partial x} - 2/3 \mu \text{div}(v)] + \frac{\partial}{\partial y} [\mu(\frac{\partial u}{\partial y} + \frac{\partial v}{\partial x})] - \rho g \cos(\alpha)$$

Momentum equation y-component:

$$\rho u \frac{\partial v}{\partial x} + \rho v \frac{\partial v}{\partial y} = -\frac{\partial p}{\partial y} + \quad (2.3)$$

$$\frac{\partial}{\partial y} [2\mu \frac{\partial v}{\partial y} - 2/3 \mu \text{div}(v)] + \frac{\partial}{\partial x} [\mu(\frac{\partial v}{\partial x} + \frac{\partial u}{\partial y})] - \rho g \sin(\alpha)$$

Energy equation:

$$\frac{\partial}{\partial x} (\rho u C_p T) + \frac{\partial}{\partial y} (\rho v C_p T) = \quad (2.4)$$

$$\frac{\partial}{\partial x} (K \frac{\partial T}{\partial x}) + \frac{\partial}{\partial y} (K \frac{\partial T}{\partial y}) + u \frac{\partial p}{\partial x} + v \frac{\partial p}{\partial y}$$

Diffusion equation:

$$\rho u \partial W / \partial x + \rho v \partial W / \partial y = \partial / \partial x (\rho D_{GV} \partial W / \partial x) + \partial / \partial y (\rho D_{GV} \partial W / \partial y) \quad (2.5)$$

In the energy equation, (2.4), the heat capacity of the mixture is defined as:

$$C_p = (n_{\text{gas}} C_{p_{\text{gas}}} + n_{\text{vap}} C_{p_{\text{vap}}}) / (n_{\text{gas}} + n_{\text{vap}}) \quad (2.6)$$

where n_{gas} and n_{vap} are mass fluxes of the gas and vapour respectively. Also in the momentum equations, (2.2)-(2.3), α is the angle of inclination which the y axis makes with the horizon. (See list of Nomenclatures for other variables.).

2.1.2 SET 2 OF THE EQUATIONS

To reduce the number of the variables and being similar to those assumptions made by Davis [1] and Hu [2] in their theoretical parts of their works, assumptions (7) and (8) are added as follows:

(7) All physical and transport properties of the fluid, except density for its effect in producing buoyancy force, are constant and are evaluated at T_0 (the mean temperature) and X_{W0} (the equilibrium mole fraction corresponding to T_0).

(8) The fluid is incompressible, i.e., the density variation due to change in pressure is negligible. Expanding the density, ρ , in the gravity force terms of the momentum equations, in a double Taylor series in T and X_W about T_0 and X_{W0} yields:

$$\rho = \rho_0 - \rho_0 \beta_0 (T - T_0) - \rho_0 \delta_0 (X_W - X_{W0}) \quad (2.7)$$

where,

ρ_0 = density of the fluid at temperature T_0 ;

β_0 = thermal coefficient of volumetric expansion,
defined by $\beta = -1/\rho (\partial\rho/\partial T)_p$ and evaluated at T_0 ;

δ_0 = concentration coefficient of volumetric expansion,
defined by $\delta = -1/\rho (\partial\rho/\partial XW)_T$ and evaluated at T_0 .

Applying assumptions (7) and (8) to the momentum equations, (2.2)-(2.3), gives:

Momentum equation x-component:

$$\rho_0 u \frac{\partial u}{\partial x} + \rho_0 v \frac{\partial u}{\partial y} = -\frac{\partial p''}{\partial x} + \quad (2.8)$$

$$\mu_0 (\frac{\partial^2 u}{\partial x^2} + \frac{\partial^2 u}{\partial y^2}) - \rho_0 g \cos(\alpha) [1.0 + \beta_0(T-T_0) + \delta_0(XW-XW_0)]$$

Momentum equation y-component:

$$\rho_0 u \frac{\partial v}{\partial x} + \rho_0 v \frac{\partial v}{\partial y} = -\frac{\partial p''}{\partial y} + \quad (2.9)$$

$$\mu_0 (\frac{\partial^2 v}{\partial x^2} + \frac{\partial^2 v}{\partial y^2}) - \rho_0 g \sin(\alpha) [1.0 + \beta_0(T-T_0) + \delta_0(XW-XW_0)]$$

Since the terms $\rho_0 g \cos(\alpha)$ and $\rho_0 g \sin(\alpha)$ are constant, they can be combined with the pressure gradient by defining:

$$p = p'' - [\rho_0 g(d-x) \cos(\alpha) + \rho_0 g(1-y) \sin(\alpha)] \quad (2.10)$$

where p represents the excess of the actual pressure p'' over the static pressure $[\rho_0 g(d-x) \cos(\alpha) + \rho_0 g(1-y) \sin(\alpha)]$.

Differentiating (2.10) with respect to y and x give

(2.11) and (2.12) respectively:

$$\frac{\partial p}{\partial y} = \frac{\partial p''}{\partial y} + \rho_0 g \sin(\alpha) \quad (2.11)$$

$$\frac{\partial p}{\partial x} = \frac{\partial p''}{\partial x} + \rho_0 g \cos(\alpha) \quad (2.12)$$

By applying (2.11) and (2.12) to the momentum equations (2.8)-(2.9) and also applying assumptions (7)-(8) to the continuity, diffusion and energy equations given in Set 1, Set 2 of the equations of change would be as follows:

Continuity equation:

$$\frac{\partial u}{\partial x} + \frac{\partial v}{\partial y} = 0.0 \quad (2.13)$$

Momentum equation x-component:

$$\rho_0 u \frac{\partial u}{\partial x} + \rho_0 v \frac{\partial u}{\partial y} = \mu_0 (\frac{\partial^2 u}{\partial x^2} + \frac{\partial^2 u}{\partial y^2}) - \quad (2.14)$$

$$\frac{\partial p}{\partial x} + \rho_0 g \cos(\alpha) \beta_0 (T - T_0) + \rho_0 g \cos(\alpha) \gamma_0 (XW - XW_0)$$

Momentum equation y-component:

$$\rho_0 u \frac{\partial v}{\partial x} + \rho_0 v \frac{\partial v}{\partial y} = \mu_0 (\frac{\partial^2 v}{\partial x^2} + \frac{\partial^2 v}{\partial y^2}) - \quad (2.15)$$

$$\frac{\partial p}{\partial y} + \rho_0 g \sin(\alpha) \beta_0 (T - T_0) + \rho_0 g \sin(\alpha) \gamma_0 (XW - XW_0)$$

Energy equation:

$$\rho_0 u C_p \frac{\partial T}{\partial x} + \rho_0 v C_p \frac{\partial T}{\partial y} = K (\frac{\partial^2 T}{\partial x^2} + \frac{\partial^2 T}{\partial y^2}) \quad (2.16)$$

Diffusion equation:

$$\rho_0 u \frac{\partial W}{\partial x} + \rho_0 v \frac{\partial W}{\partial y} = \rho_0 D_{GV} (\frac{\partial^2 W}{\partial x^2} + \frac{\partial^2 W}{\partial y^2}) \quad (2.17)$$

2.2 BOUNDARY CONDITIONS

Two types of boundary conditions, different only in the velocity conditions at the vertical walls are considered. These are similar to those employed by Hu [2] in the theoretical part of his work. In the first type of boundary conditions, only the normal components of the interfacial velocities are taken into account, the tangential components are neglected. In the second type of boundary conditions the tangential component velocity at the evaporating side, v_1 , is also included. The normal component velocities are obtained by applying the diffusion equation at the evaporating and condensing boundaries. It can be shown [30] that for the evaporating side:

$$u_1 = -1 / [\rho_{vap} (1 - W_1)] D_{GV} \frac{\partial W}{\partial x} \Big|_{x=0.0} \quad (2.18)$$

and for the condensing side:

$$u_2 = -1 / [\rho_{vap} (1 - W_2)] D_{GV} \frac{\partial W}{\partial x} \Big|_{x=d} \quad (2.19)$$

The tangential velocity is taken to be equal to the liquid film velocity at the interface, that is, no-slip condition is assumed. Since the condensing rate is very

small, the tangential component velocity at the interface of the condensing side, v_2 , is negligible.

The complete boundary conditions are given below:

For $0.0 \leq x \leq d$, $y=0.0$ and $y=1$

$$u, v=0.0, \quad \partial T/\partial y=\partial W/\partial y=0.0$$

so top and bottom are considered perfect insulators to both heat and mass transfer.

For $x=d$, $0.0 \leq y \leq 1$

$$v=v_2=0.0 \quad \text{Tangential velocity at the cold wall}$$

$$T=T_2 \quad \text{Temperature at the cold wall}$$

$$W=W_2 \quad \text{Mass fraction at the cold wall}$$

$$u=u_2 \quad \text{Normal velocity at the cold wall}$$

For $y=0.0$ and $y=1$, $0.0 \leq x \leq d$

$$u=v=0.0$$

$$\partial T/\partial y=\partial W/\partial y=0.0$$

For $x=0.0$, $0.0 \leq y \leq 1$

Case 1:

$$v=v_1=0.0$$

$$u=u_1$$

$$T=T_1$$

$$W=W_1$$

Case 2:

$$v=v_1$$

$$u=u_1$$

$$T=T_1$$

$$W=W_1$$

2.3 NORMALIZATION

Equations such as (2.13)-(2.17) are usually converted

to dimensionless forms to generalise the solution of the problem. According to Buckingham Pi Theorem, appearance of dimensionless parameters in a normalized equation show that a relationship between another dependent dimensionless parameter and those independent ones in the equation can be set up; this is now considered in this section. The following dimensionless variables are introduced:

$$\begin{aligned} X=x/d, Y=y/d & \quad \text{normalized space coordinates;} \\ U=ud/v_o, V=vd/v_o & \quad \text{normalized fluid velocities;} \\ \Theta=(T-T_o)/(T_2-T_o) & \quad \text{normalized fluid temperature;} \\ \Phi=(W-W_o)/(W_2-W_o) & \quad \text{normalized vapour mass fraction;} \\ P=pd^2/\rho_o v_o^2 & \quad \text{normalized pressure.} \end{aligned}$$

Inserting the above dimensionless variables in Set 2 of the equations of change results in the following normalized equations:

Continuity equation:

$$\partial U/\partial X + \partial V/\partial Y = 0.0 \quad (2.20)$$

Momentum equation X-component:

$$\begin{aligned} U \partial U/\partial X + V \partial U/\partial Y = -\partial P/\partial X + \partial^2 U/\partial X^2 + \partial^2 U/\partial Y^2 & \quad (2.21) \\ +\cos(\alpha) \cdot GrT/2 \cdot \Theta + \cos(\alpha) \cdot GrXW/2 \cdot \Phi \end{aligned}$$

Momentum equation Y-component:

$$\begin{aligned} U \partial V/\partial X + V \partial V/\partial Y = -\partial P/\partial Y + \partial^2 V/\partial X^2 + \partial^2 V/\partial Y^2 & \quad (2.22) \\ +\sin(\alpha) \cdot GrT/2 \cdot \Theta + \sin(\alpha) \cdot GrXW/2 \cdot \Phi \end{aligned}$$

Energy equation:

$$U \partial \Theta/\partial X + V \partial \Theta/\partial Y = 1/Pr (\partial^2 \Theta/\partial X^2 + \partial^2 \Theta/\partial Y^2) \quad (2.23)$$

Diffusion equation:

$$U \partial \Phi/\partial X + V \partial \Phi/\partial Y = 1/Sc (\partial^2 \Phi/\partial X^2 + \partial^2 \Phi/\partial Y^2) \quad (2.24)$$

Consequently, the boundary conditions in their dimensionless forms would be:

For $X=1.0$, $0.0 \leq Y \leq L$ Aspect ratio

$V=V2=0.0$ Dimensionless tangential velocity
at the cold wall

$U=U2$ Dimensionless normal velocity
at the cold wall

$\theta=-1.0$ Dimensionless temperature
at the cold wall

$\phi=-1.0$ Dimensionless mass fraction
at the cold wall

For $Y=0.0$ and $Y=L$, $0.0 \leq X \leq 1.0$

$U=V=0.0$

$\partial\theta/\partial Y = \partial\phi/\partial Y = 0.0$

For $X=0.0$, $0.0 \leq Y \leq L$

Case 1:

$V=V1=0.0$

$U=U1$

$\theta=1.0$

$\phi=1.0$

Case 2:

$V=V1 \neq 0.0$

$U=U1$

$\theta=1.0$

$\phi=1.0$

The dimensionless parameters appear in the normalized equations and the boundary conditions are defined as:

$Pr = C_p \nu_0 / K$ Prandtl number

$Sc = \nu_0 / D_{GV}$ Schmidt number

$Gr_T = d^3 g \beta_0 (T_1 - T_2) / (\nu_0^2)$ Grashof number for heat transfer

$Gr_{XW} = d^3 g \delta_0 (XW_1 - XW_2) / (\nu_0^2)$ Grashof number for mass transfer

$$L=1/d = \text{Asp}$$

Aspect ratio

Having normalized the equations, the solution of the problem can be obtained by solving either the dimensionless equations or the original ones. The former gives dimensionless results directly while the latter provides actual values which eventually have to be normalised.

A computer program which solves the finite difference equations based on the original equations (such as equations (2.1)-(2.5)) is easier to work with than one based on dimensionless equations (such as (2.20)-(2.24)), since any changes in the original equations, due to changing the assumptions, can be easily absorbed in the computer program without going through a normalization procedure. However, normalization must proceed separately to define dimensionless variables and parameters so that the generality of the solution and correlations are guaranteed.

subscripts i, j, k, l and m . All the scalar variables are stored at their grid nodes while the velocity components are stored at the points which are located mid-way between the grid intersections. Around the location of the variables control volumes are set up. Therefore there are three kinds of control volumes or cells, namely: scalar, u - and v -control volume. Figure 3.1 also shows a typical example of each of them.

This grid system with arbitrary spacing has the advantage that instead of employing needlessly expensive fine and uniform grids, fine meshes are employed only near the wall sides where great changes in the values of variables occur. The mesh grid, mostly 19×15 , with

3. METHOD OF SOLUTION

For solving Set 1 or Set 2 of the equations of change (given in the previous chapter), a finite difference method which has been devised recently by Spalding and others [16] for treating convective, steady, low speed and recirculating flows is used in this work. The application of the method to the present problem is as follows.

3.1 GRID

The first step in deriving the finite difference equations is the establishment of a suitable grid and storage location for the variables. The grid employed is regular and rectangular with arbitrary spacing and is depicted in Figure 3.1. In this figure, the intersections of the solid lines make the grid nodes. A considered grid node and its immediate neighbours are denoted by the subscripts P, W, E, S and N. All the scalar variables are stored at these grid nodes while the velocity components are stored at the points which are located mid-way between the grid intersections. Around the location of the variables control volumes are set up. Therefore there are three kinds of control volumes or cells, namely: scalar-, u- and v-control volume. Figure 3.1 also shows a typical example of each of them.

This grid system with arbitrary spacing has the advantage that instead of employing needlessly expensive fine and uniform grids, fine spaces are employed only near the wall sides where great changes in the values of variables occur. The mesh grid, mostly 17X16, with

concentrated nodes near the walls was satisfactory for this work, as higher numbers of nodes were not producing more accurate results.

3.2 FINITE DIFFERENCE EQUATION OF ENERGY

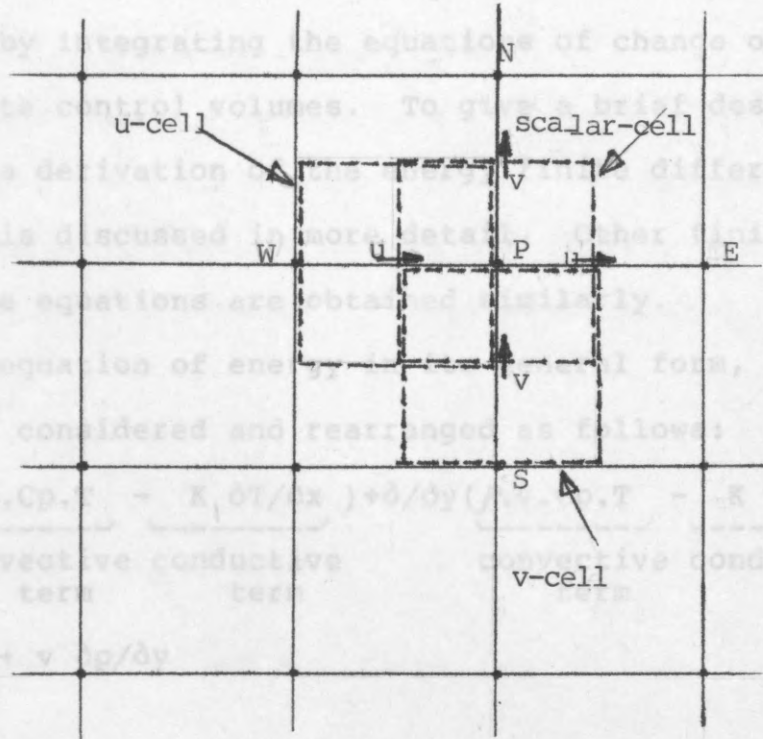
In general, the finite difference equations are obtained by integrating the equations of change over appropriate control volumes. To give a brief description of this, a derivation of the energy finite difference equation is discussed in more detail. Other finite difference equations are obtained similarly.

The equation of energy in differential form, Equation (2.4), is considered and rearranged as follows:

$$\frac{\partial}{\partial x} (\rho u C_p T - K \frac{\partial T}{\partial x}) + \frac{\partial}{\partial y} (\rho v C_p T - K \frac{\partial T}{\partial y}) = S$$

convective term
convective term

$$u \frac{\partial p}{\partial x} + v \frac{\partial p}{\partial y} \quad (3.1)$$



It can be seen that the left hand side of the equation represents the variation of the total flux (convective + conduction) in the directions of x and y respectively.

Integrating Figure 3.1 The grid and different types of control volumes as in Figure 3.2, gives:

$$\int_{V} \frac{\partial}{\partial x} (\rho u C_p T - K \frac{\partial T}{\partial x}) dx + \int_{V} \frac{\partial}{\partial y} (\rho v C_p T - K \frac{\partial T}{\partial y}) dy = \int_{V} S dV \quad (3.2)$$

or:

$$(q_w - q_e) + (q_s - q_n) = \int_{V} S dV \quad (3.3)$$

where:

$\int_{V} S dV$ represents the integration of \dot{q} over the control volume.

concentrated nodes near the walls was satisfactory for this work, as higher numbers of nodes were not producing more accurate results.

3.2 FINITE DIFFERENCE EQUATION OF ENERGY

In general, the finite difference equations are obtained by integrating the equations of change over appropriate control volumes. To give a brief description of this, a derivation of the energy finite difference equation is discussed in more detail. Other finite difference equations are obtained similarly.

The equation of energy in its general form, Equation (2.4), is considered and rearranged as follows:

$$\underbrace{\partial/\partial x (\rho \cdot u \cdot C_p \cdot T)}_{\text{convective term}} - \underbrace{K \partial T / \partial x}_{\text{conductive term}} + \underbrace{\partial/\partial y (\rho \cdot v \cdot C_p \cdot T)}_{\text{convective term}} - \underbrace{K \partial T / \partial y}_{\text{conductive term}} = u \partial p / \partial x + v \partial p / \partial y \quad (3.1)$$

It can be seen that the left hand side of the equation represents the variation of the total flux (convective + conduction) in the directions of x and y respectively. Integration of this equation over a scalar control volume as in Figure 3.2, gives:

$$\int_w^e \partial/\partial x (\rho \cdot u \cdot C_p \cdot T - K \partial T / \partial x) dx + \int_s^n \partial/\partial y (\rho \cdot v \cdot C_p \cdot T - K \partial T / \partial y) dy = ST \quad (3.2)$$

or:

$$(q_e - q_w) + (q_s - q_n) = ST \quad (3.3)$$

Where:

ST represents the integration of $\vec{v} \cdot \nabla p$ over the control

volume;

w, e, s and n are the points on the faces of the control volume located midway between neighbouring grid nodes (see Figure 3.2);

q_e, q_w, q_s and q_n are the fluxes of energy crossing the boundaries of the control volume at e, w, s and n, respectively.

A hybrid formula, which is a combination of the central and upwind difference schemes, is employed to define each of the fluxes in Equation (3.3). The implication of the formula for expressing flux q_e is given below:

$$\text{For } -D_e < F_e < D_e : q_e = F_e (T_P + T_E) - D_e (T_E - T_P) \quad (3.4)$$

$$\text{For } F_e \geq D_e : q_e = F_e \cdot T_P \quad (3.5)$$

$$\text{For } F_e \leq -D_e : q_e = F_e \cdot T_E \quad (3.6)$$

Where:

$$F_e = \rho_e \cdot u_e \cdot C_{p_e} \cdot A_e / 2.0 \quad (3.7)$$

$$D_e = K_e \cdot A_e / \delta x_e \quad (3.8)$$

Where:

A_e stands for the cross-sectional area at point e;

δx_e is the distance between nodes P and E (see Figure 3.2);

Other parameters in Equations (3.7)-(3.8) are evaluated

at point e where q_e crosses the boundary of

the control volume.

In a similar way other q's are defined.

Substituting q_e, q_w, q_s and q_n in Equation (3.3) gives:

$$CT_P \cdot T_P - CT_W \cdot T_W - CT_E \cdot T_E - CT_S \cdot T_S - CT_N \cdot T_N = ST \quad (3.9)$$

where:

T_P, T_W, T_E, T_S and T_N are the temperatures at the locations P, W, E, S and N respectively;

CT_P, CT_W, CT_E, CT_S and CT_N are the corresponding coefficients.

where:

For $-D \frac{\partial T}{\partial x} = CT_P - P$ (3.10)

For $-D \frac{\partial T}{\partial x} = CT_P - P$ (3.11)

For $-D \frac{\partial T}{\partial x} = CT_P - P$ (3.12)

Other coefficients are defined in a similar way.

It can be shown that a relationship between the coefficients in Equation (3.9) can be written as:

$$CT_P = CT_W + CT_E + CT_S + CT_N \quad (3.13)$$

Equations (3.9)-(3.13) are applicable to all control volumes except those which are next to the evaporating and condensing walls, which need to be treated in another way. This will be dealt with in Section 3.5.

Figure 3.2 Notation for a scalar control volume

The procedure for deriving the finite difference equations of diffusion is the same as described in the previous section; conductive and convective terms are rearranged in the left hand side and other terms are grouped on the right hand side of the equations. Integration over the appropriate control volume will give the following equations:

For the diffusion equation:

$$CT_W \cdot T_W - CT_W \cdot T_P - CT_E \cdot T_P - CT_S \cdot T_P - CT_N \cdot T_P = \dot{Q}_v \quad (3.14)$$

where:

T_P, T_W, T_E, T_S and T_N are the temperatures at the locations P, W, E, S and N respectively;

CT_P, CT_W, CT_E, CT_S and CT_N are the corresponding coefficients.

where:

$$\text{For } -D_e < F_e < D_e \quad : \quad CT_E = D_e - F_e \quad (3.10)$$

$$\text{For } F_e > D_e \quad : \quad CT_E = 0.0 \quad (3.11)$$

$$\text{For } F_e > -D_e \quad : \quad CT_E = -2 F_e \quad (3.12)$$

Other coefficients are defined in a similar way.

It can be shown that a relationship between the coefficients in Equation (3.9) can be written as:

$$CT_P = CT_W + CT_E + CT_S + CT_N \quad (3.13)$$

Equations (3.10)-(3.13) are applicable to all control volumes except those which are next to the evaporating and condensing walls, which need to be treated in another way. This will be dealt with in Section 3.5.

3.3 FINITE DIFFERENCE EQUATIONS OF MOMENTUM AND DIFFUSION

The procedure for deriving the finite difference equations of diffusion and momentum is the same as described in the previous section; conductive and convective terms are rearranged in the left hand side and other terms are grouped in the right hand side of the equations. Integration of them over the appropriate control volumes will give the following equations:

For the diffusion equation:

$$CW_P \cdot W_P - CW_W \cdot W_W - CW_E \cdot W_E - CW_S \cdot W_S - CW_N \cdot W_N = SW \quad (3.14)$$

For the x-component of the momentum equation:

$$Cu_P \cdot u_P - Cu_W \cdot u_W - Cu_E \cdot u_E - Cu_S \cdot u_S - Cu_N \cdot u_N = Su \quad (3.15)$$

For the y-component of the momentum equation:

$$Cv_P \cdot v_P - Cv_W \cdot v_W - Cv_E \cdot v_E - Cv_S \cdot v_S - Cv_N \cdot v_N = Sv \quad (3.16)$$

where SW , Su and Sv introduce the integration of the terms other than convective-conductive ones over the control volumes. In the above equations coefficients are shown in the form of CW , Cu and Cv (with subscripts P , W , E , S and N). These are similar to those introduced in Equations (3.10)-(3.12) but they differ in the method of calculation of 'F' and 'D' implicit in the hybrid formula. As an example F_e and D_e for the calculation of CW_E , Cu_E and Cv_E are given.

Other values are similarly obtained.

For use in calculation of CW_E :

$$F_e = \rho_e u_e A_e / 2.0 \quad (3.17)$$

$$D_e = D_{GV} A_e / \delta x_e \quad (3.18)$$

For use in calculation Cu_E :

$$F_{eu} = \rho_{eu} u_{eu} A_{eu} / 2.0 \quad (3.19)$$

$$D_{eu} = \rho_{eu} A_{eu} / \delta x_{eu} \quad (3.20)$$

For use in calculation of Cv_E :

$$F_{ev} = \rho_{ev} u_{ev} A_{ev} / 2.0 \quad (3.21)$$

$$D_{ev} = \rho_{ev} A_{ev} / \delta x_{ev} \quad (3.22)$$

In the above equations subscripts eu and ev designate the locations and the types of the control volumes for which the parameters are defined. By referring to Figures 3.3 and 3.4 these are: eu for the right hand boundary of a

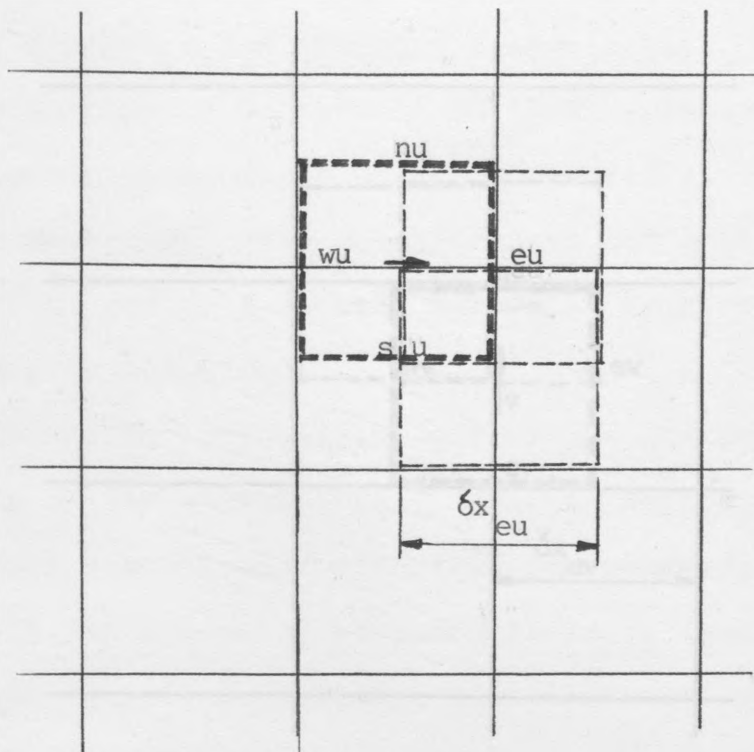


Figure 3.3 Notation for a u-control volume

of control volume and e_v for the right hand boundary of a control volume.

3.4 FINITE DIFFERENCE EQUATION OF CONTINUITY

As has been shown, the variables T , W , u and v (all except p) can be obtained from finite difference equations of energy, diffusion and momentum respectively. The

variable remaining to be calculated is the pressure term. The only remaining equation to be satisfied is the continuity equation. This equation does not contain the pressure term, and so a special method is required to obtain the pressure field. The algorithm used is called SIMPLER (Semi-Implicit Method for Pressure-Linked Equations) algorithm. It proceeds in two steps: first, an estimated pressure field is inserted in the continuity equation to obtain an initial velocity field; then, the appropriate corrections to the pressure field are calculated so that the resulting velocity field will satisfy the continuity equation. The full description of the algorithm is given by Patankar and Gosman [31-33].

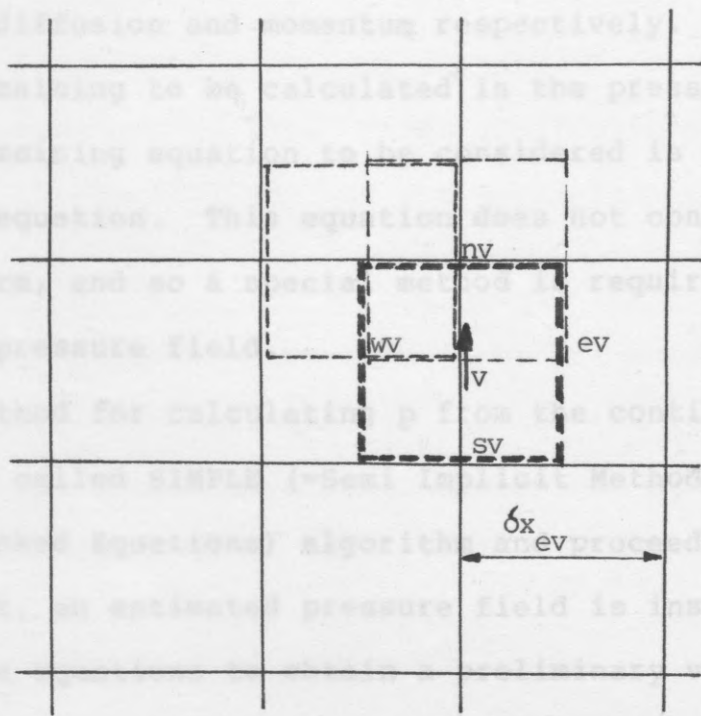


Figure 3.4 Notation for a v-control volume

By applying the SIMPLER algorithm to the continuity equation the 'pressure correction' equation results:

$$a_p \hat{p}_p - a_w \hat{p}_w - a_e \hat{p}_e - a_s \hat{p}_s - a_n \hat{p}_n = b \quad (3.23)$$

where:

$\hat{p}_p, \hat{p}_w, \hat{p}_e, \hat{p}_s$ and \hat{p}_n are the pressure correction values at locations P, W, E, S and N respectively, see Figure 3.2;

u-control volume and e_v for the right hand boundary of a v-control volume.

3.4 FINITE DIFFERENCE EQUATION OF CONTINUITY

As has been shown, the variables T , W , u and v (all except p) can be obtained from finite difference equations of energy, diffusion and momentum respectively. The variable remaining to be calculated is the pressure term. The only remaining equation to be considered is the continuity equation. This equation does not contain the pressure term, and so a special method is required to obtain the pressure field.

The method for calculating p from the continuity equation is called SIMPLE (=Semi Implicit Method for Pressure Linked Equations) algorithm and proceeds in two steps: first, an estimated pressure field is inserted in the momentum equations to obtain a preliminary velocity field; then, the appropriate corrections to the pressure field are calculated so that the resulting velocity field will satisfy the continuity equation. The full description of the procedure can be found in some of the articles published by Spalding, Patankar and Gosman [31-33].

By applying the SIMPLE algorithm to the continuity equation the 'pressure correction' equation results:

$$C'_P \cdot p'_P - C'_W \cdot p'_W - C'_E \cdot p'_E - C'_S \cdot p'_S - C'_N \cdot p'_N = 0.0 \quad (3.23)$$

where:

p'_P , p'_W , p'_E , p'_S and p'_N are the pressure correction values at locations P , W , E , S and N respectively, see Figure 3.2;

C'_{p_P} , C'_{p_W} , C'_{p_E} , C'_{p_S} and C'_{p_N} are the coefficients of the pressure correction terms and with reference to Figure 3.2 are specified as follows:

$$C'_{p_W} = \rho_w \cdot A_w / C_{u_P} \quad (3.24)$$

where ρ_w and A_w are density and cross-sectional area at location w respectively and C_{u_P} is taken from an equation similar to Equation (3.13). Other coefficients are calculated in the same way and are inter-related by:

$$C'_{p_P} = C'_{p_W} + C'_{p_E} + C'_{p_S} + C'_{p_N} \quad (3.25)$$

When the pressure correction terms are known from Equation (3.23), they are used to correct the velocity field which has been initially obtained from Equations (3.15)-(3.16), so:

$$u = u_{old} + A_w / C_{u_P} \cdot (p'_P - p'_W) \quad (3.26)$$

$$v = v_{old} + A_s / C_{v_P} \cdot (p'_P - p'_S) \quad (3.27)$$

The situation can be perceived from Figure 3.1 where:

u_{old} and v_{old} are velocity components calculated from equations (3.15) and (3.16) respectively;

u and v are corrected values of u_{old} and v_{old} respectively;

A_w and A_s are cross-sectional areas at locations w and s respectively;

C_{u_P} and C_{v_P} are obtained from equations similar to that of (3.13).

As can be seen from Equations (3.26) and (3.27) the difference between pressure correction values at any two neighbouring nodes is used as a drive force for removing

excess from (or adding deficiency to) the velocity values obtained from the momentum equations.

Preliminary pressures, initially inserted in the momentum equations, are also modified;

$$p = p_{old} + \dot{p} \quad (3.28)$$

where:

p_{old} is the preliminary pressure field;

\dot{p} is the correction value for the pressure at a given mesh node;

p is the corrected value of the pressure.

3.5 BOUNDARY CONDITIONS

At the boundaries of the calculation domain, the general finite difference scheme is not applicable. Hence special measures are required for integration of the equation of change over the control volumes next to the walls. In order that the resulting algebraic equations should be in harmony with the other difference equations which have been derived so far, and also that minimum complexity be added to the computer program based on them, some care should be taken. To satisfy this Gosman [34] has suggested a method, namely 'false source', for insertion of the boundary conditions into the difference equations. His method is easy to use but in certain conditions, such as the present one with transferring mass at the evaporating and condensing walls, leads to a slight error in the result. To remove error from the results two alternative methods have been devised and are satisfactory as shown by comparison with the method of false source of Gosman. These methods and their derivations are given in Appendix [1].

The application of one of the methods given in Appendix [1], which is easiest to use, is given below. In this method there is no need to produce new finite difference equations for the control volumes next to the walls. The previously described equations can be used and necessary modifications are only made in determination of the coefficients in these equations:

- a) For $x=0.0$ and $0 \leq y \leq 1$ (control volumes next to the hot wall, see Figure 2.1)

In the energy equation, Equation (3.9), CT_W is re-evaluated as:

$$CT_W = 2 D_W + 2 F_W \quad (3.29)$$

In the diffusion equation, Equation (3.14), CW_W is re-evaluated as:

$$CW_W = 2 D_W + 2 F_W \quad (3.30)$$

In the x-component of the momentum equation, Equation (3.15), Cu_W remains as before;

In the y-component of the momentum equation, Equation (3.16), Cv_W re-evaluated as:

$$Cv_W = 2 D_{wv} + 2 F_{wv} \quad (3.31)$$

- b) For $x=d$ and $0.0 \leq y \leq 1$ (control volumes next to the cold wall, see the same figure)

In the energy equation:

$$CT_E = 2 D_e + 2 F_e \quad (3.32)$$

In the diffusion equation:

$$CW_E = 2 D_e + 2 F_e \quad (3.33)$$

In the x-component of the momentum equation no change is needed;

In the y-component of the momentum equation:

$$Cv_E = 2 D_{ev} + 2 F_{ev} \quad (3.34)$$

For the pressure correction Equation (3.23), the above boundary conditions are automatically inserted and no further adjustment is needed.

3.6 SOLUTION PROCEDURE

When all of the finite difference equations are prepared, their solution proceeds by the cyclic repetition of the following steps:

- 1) Initial estimates of the values of all the variables are provided;
- 2) The momentum Equations (3.15) and (3.16) are solved to provide a preliminary velocity field;
- 3) The pressure correction Equation (3.23) is solved and in its result the corrected pressures, Equation (3.28), and velocities, Equations (3.26) and (3.27), are obtained;
- 4) The improved values of velocities are used in the energy and the diffusion equations. These are then solved to give the temperature field and the mass fraction field;
- 5) The new values of the variables are regarded as improved estimates and are used to start a new cycle. Steps 1-5 are repeated until convergence is achieved.

It must be added that in solving each of the individual equations in steps 2, 3 and 4, a line-by-line iteration method is used [14]. Since the coefficients in these equations have to be recalculated in each cycle

usually 5 to 10 internal iterations are found to be sufficient.

The computer program, given in Appendix [2], was prepared to carry out the mathematical calculations involved. In most cases convergent results are obtained in approximately 100 iterations. At this stage heat transfer and mass transfer rates at the evaporating and condensing films together with the corresponding coefficients, Nusselt and Sherwood numbers respectively, are calculated.

4. HEAT TRANSFER IN AN INCLINED RECTANGULAR CAVITY

The procedure described in the previous chapters for solving the problems concerned with simultaneous heat and mass transfer can be tested through its application to a comparatively simple situation. That is, the process of pure heat transfer in an inclined cavity, $\alpha = 0.0$ to 90.0 degrees. The physical model is shown in Figure 4.1, where the hot and the cold faces are dry and no mass transfer is involved in the overall energy transfer in the cavity.

4.1 EQUATIONS TO BE SOLVED

For the pure heat transfer case, the equations to be solved are simplified versions of those which describe a combined transfer of heat and mass: Among the equations of change the diffusion equation is eliminated and the density dependence of the mole fraction of the water vapour (which appeared in the form of $\rho_0/\beta_0(XW-XW_0)$ in the momentum equations), is removed. These changes can be easily implemented in the computer program by inserting $XW1$ and $XW2$ equal to zero at the boundaries and removing the solution of the diffusion equation from the program. This causes no damage to the structure of the program itself. Furthermore, the angle of inclination, α , is inserted in the momentum equations.

In the following sections, the equations are solved, first for the case of a vertical cavity ($\alpha=90.0$) and then for other angles of inclination (from 0.0 to 90.0 degrees with 10.0 degree intervals).

RESULTS AND COMPARISONS FOR THE CASE OF A VERTICAL CAVITY

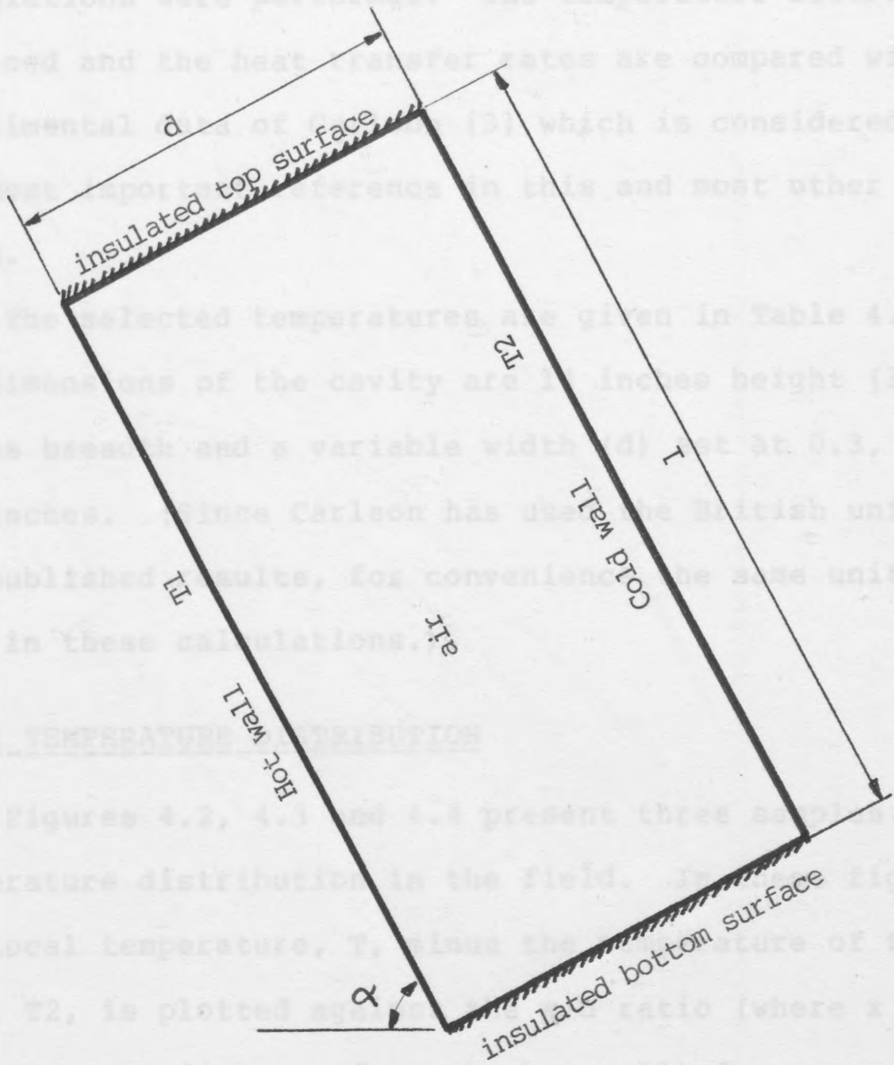
For a number of different combinations of wall temperatures and width to height ratios of the cavity, calculations were performed. The temperature distributions obtained and the heat transfer rates are compared with the experimental results of Carlson (3) which is considered to be the most authoritative reference in this and most other related work.

The selected temperatures are given in Table 4.1 and the dimensions of the cavity are 1.0 inches height (1), 1/8 inches breadth and a variable width (d) set at 0.3, 0.7 or 1.4 inches. Since Carlson has used the British units in his published results, for convenience the same units are used in these calculations.

4.1.1 TEMPERATURE DISTRIBUTION

Figures 4.2, 4.3 and 4.4 present three samples of the temperature distribution in the field. In these figures, the local temperature, T , along the surface of the hot face, T_1 , is plotted against the distance from the cold face, T_2 , is plotted against the distance from the hot face (where x indicates the distance from the hot wall) for several values of the height in the cavity. The solid curves are given by the present calculation. The temperature scale on the ordinate relates to one of the temperature profiles; the others are shifted in the vertical direction.

Figure 4.1 Physical model of heat transfer in an inclined rectangular cavity



The temperature scale on the ordinate relates to one of the temperature profiles; the others are shifted in the vertical direction.

Figure 4.2 shows the temperature distribution for a situation in which the temperature difference between the

4.2 RESULTS AND COMPARISONS FOR THE CASE OF A VERTICAL CAVITY

For a number of different combinations of wall temperatures and width to height ratios of the cavity, calculations were performed. The temperature distributions obtained and the heat transfer rates are compared with the experimental data of Carlson [3] which is considered to be the most important reference in this and most other related works.

The selected temperatures are given in Table 4.1 and the dimensions of the cavity are 14 inches height (l), 16 inches breadth and a variable width (d) set at 0.3, 0.7 or 1.4 inches. (Since Carlson has used the British units in his published results, for convenience the same units are used in these calculations.).

4.2.1 TEMPERATURE DISTRIBUTION

Figures 4.2, 4.3 and 4.4 present three samples of the temperature distribution in the field. In these figures, the local temperature, T , minus the temperature of the cold face, T_2 , is plotted against the x/d ratio (where x indicates the distance from the hot wall) for several values of the height in the cavity. The solid curves are given by Carlson and were obtained by an "interferometric method" whereas the points are given by the present calculation. The temperature scale on the ordinate relates to one of the temperature profiles; the others are shifted in the vertical direction.

Figure 4.2 shows the temperature distribution for a situation in which the temperature difference between the

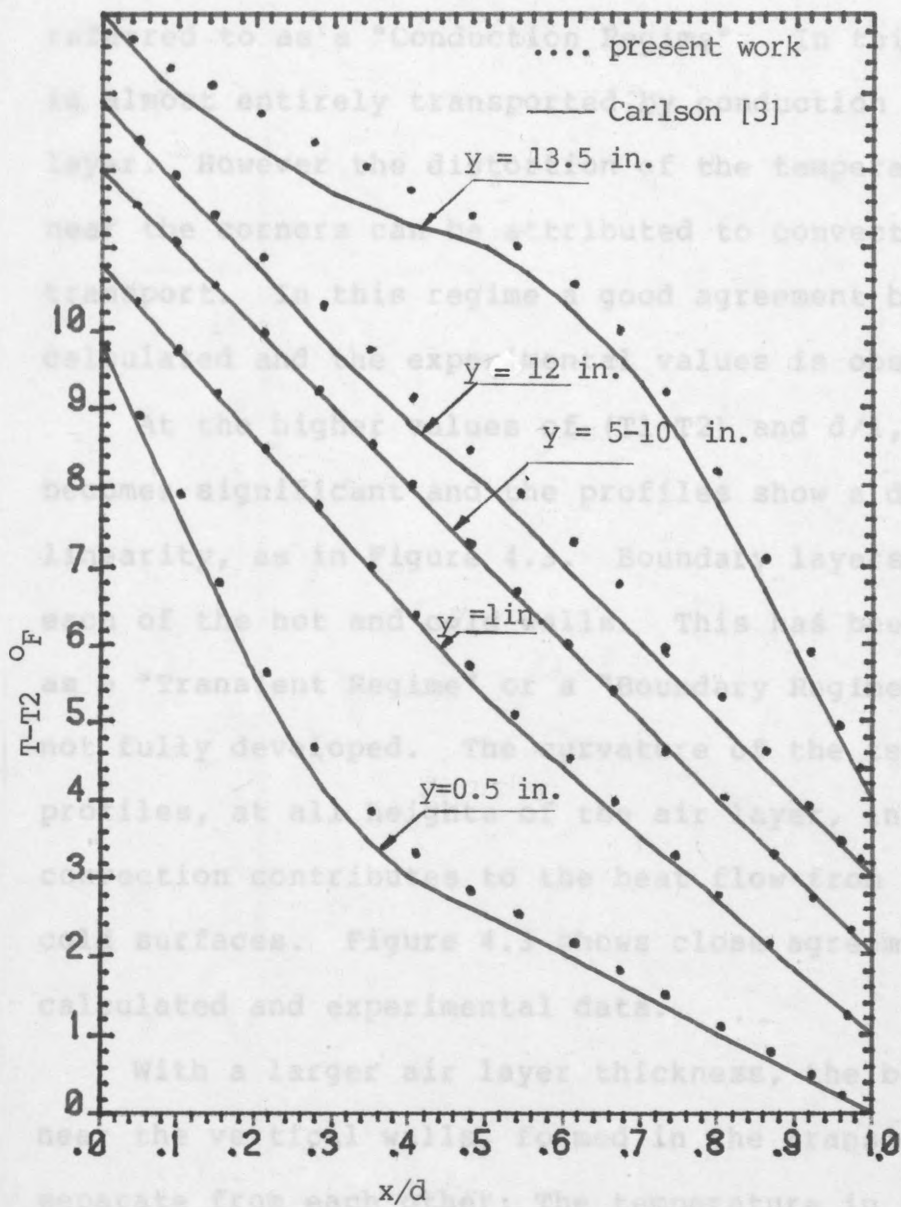


Figure 4.2 Temperature profiles in Conduction regime of flow in a vertical cavity (Width=0.7 in.; Height=14.0 in.)

hot and the cold walls, T_1-T_2 , and d/l ratio are relatively small. The temperature profiles are linear at the central portion and slightly curved at the upper and lower corners. Following Eckert and Carlson [35], this has been referred to as a "Conduction Regime". In this regime heat is almost entirely transported by conduction across the air layer. However the distortion of the temperature field near the corners can be attributed to convective energy transport. In this regime a good agreement between the calculated and the experimental values is observed.

At the higher values of (T_1-T_2) and d/l , convection becomes significant and the profiles show a departure from linearity, as in Figure 4.3. Boundary layers are formed on each of the hot and cold walls. This has been referred to as a "Transient Regime" or a "Boundary Regime" though it is not fully developed. The curvature of the temperature profiles, at all heights of the air layer, indicates that convection contributes to the heat flow from the hot to the cold surfaces. Figure 4.3 shows close agreement between calculated and experimental data.

With a larger air layer thickness, the boundary layers near the vertical walls, formed in the transient regime, separate from each other: The temperature in the central portion of the cavity becomes constant and the temperature gradients are concentrated in the layers adjacent to the hot and the cold surfaces, as shown in Figure 4.4. This is a fully developed Boundary Regime. In this regime the recirculating natural convective flow within the cavity mainly takes place near the walls. The air in the central portion remains at a stand still. This, together with the

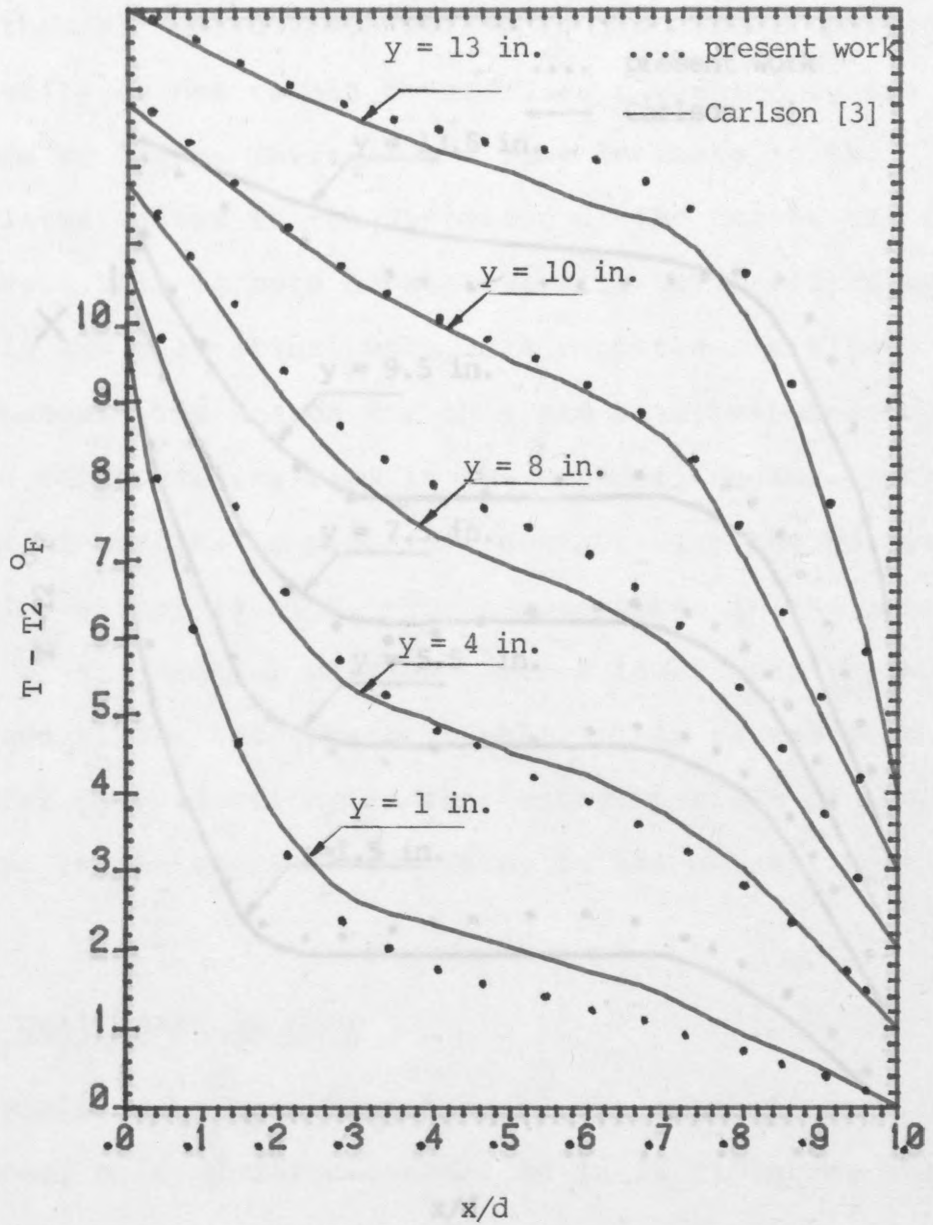
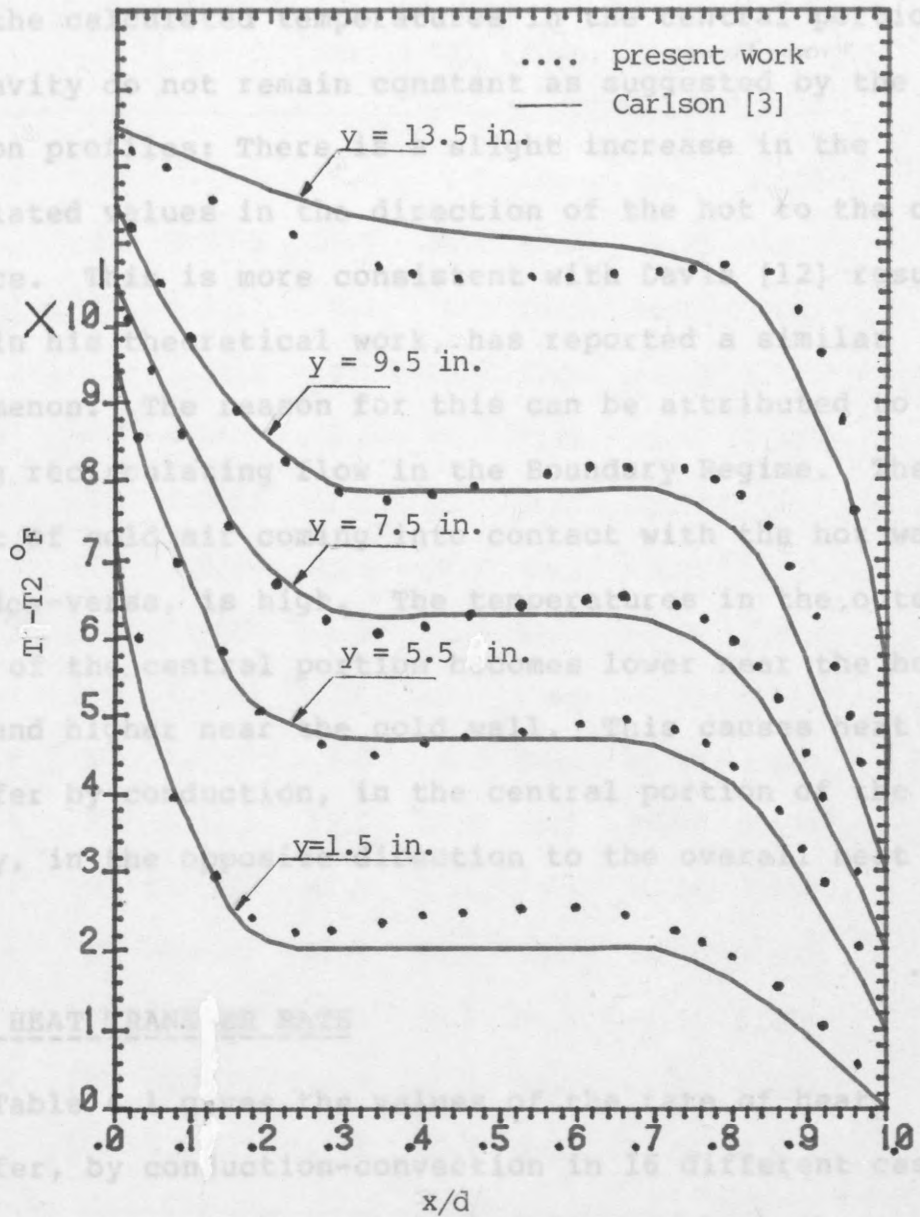


Figure 4.3 Temperature profiles in Transient regime of flow in a vertical cavity (Width=1.4 in.; Height=14.0 in.)

constant temperatures, implies that no heat is transferred by convection or conduction through this portion of the field.

Looking more carefully at Figure 4.4, it can be seen that the calculated values in the direction of the hot to the cold surface. This is more consistent with [12] results who, in his theoretical work, has reported a similar phenomenon. The reason for this can be attributed to the strong recirculating flow in the boundary regime. The amount of contact with a hot wall, and vice versa, is high. The temperature in the outer edges of the central portion becomes lower for the hot wall and higher near the cold wall. This causes a transfer of production, in the central portion of the cavity, in the direction to the over-cold flow.



4.2.2 HEAT TRANSFER RATES

Table 4.1 provides a summary of the heat transfer, by conduction-convection in 16 different cases. Among them, Run numbers 3, 10 and 13 are those whose temperature fields are given in Figures 4.2, 4.3 and 4.4 respectively.

Figure 4.4 Temperature profiles in Boundary regime of flow in a vertical cavity (Width=1.4 in.; Height=14.0 in.)

values of Grashof Numbers varying from 1.4×10^4 to 5.3×10^5 and therefore provides all possible flow regimes. As it can be seen from the last column in Table 4.1, for the conduction regimes, the calculated Nusselt numbers are

constant temperatures, implies that no heat is transferred by convection or conduction through this portion of the field.

Looking more carefully at Figure 4.4, it can be seen that the calculated temperatures in the central portion of the cavity do not remain constant as suggested by the Carlson profiles: There is a slight increase in the calculated values in the direction of the hot to the cold surface. This is more consistent with Davis [12] results who, in his theoretical work, has reported a similar phenomenon. The reason for this can be attributed to the strong recirculating flow in the Boundary Regime. The amount of cold air coming into contact with the hot wall, and vice-versa, is high. The temperatures in the outer edges of the central portion becomes lower near the hot wall and higher near the cold wall. This causes heat transfer by conduction, in the central portion of the cavity, in the opposite direction to the overall heat flow.

4.2.2 HEAT TRANSFER RATE

Table 4.1 gives the values of the rate of heat transfer, by conduction-convection in 16 different cases. Among them, Run numbers 3, 10 and 13 are those whose temperature fields are given in Figures 4.2, 4.3 and 4.4 respectively. A wide range of $(T_1 - T_2)$ and d , width, gives values of Grashof Numbers varying from $1.4 \text{ E } 04$ to $5.3 \text{ E } 05$ and therefore provides all possible flow regimes. As it can be seen from the last column in Table 4.1, for the conduction regimes, the calculated Nusselt numbers are

1	2	3	4	5	6	7	8	9
Run No.	Width Inch	T1-T2 °F	Gr $\cdot 10^{-4}$	Heat Transfer		Regime of flow	Devit. %	Nusselt No.
				expt.	cal.			
1	0.3	10	0.0178	9.6	9.7	Cond.	+0.7	1.000
2	0.3	85	0.2018	90.7	86.2	Cond.	-5.25	1.011
3	0.7	10	0.3627	4.3	4.5	Cond.	+4.23	1.083
4	0.7	35	1.4140	18.2	19.6	Tran.	+7.10	1.377
5	0.7	60	1.6410	38.8	37.9	Tran.	-2.40	1.441
6	0.7	85	2.5630	61.3	60.0	Tran.	-2.10	1.642
7	0.7	110	3.6700	85.6	84.7	Tran.	-1.05	1.827
8	0.7	135	5.0020	114.1	111.6	Tran.	-2.89	2.001
9	0.7	160	6.6100	143.8	140.0	Tran.	-2.71	2.162
10	1.4	10	1.8180	3.8	4.2	Tran.	+8.65	1.800
11	1.4	35	6.9710	19.5	20.8	Boun.	+6.80	2.670
12	1.4	60	13.1320	41.3	41.2	Boun.	-0.26	3.130
13	1.4	85	20.5100	61.3	64.0	Boun.	+4.21	3.500
14	1.4	110	29.3640	84.6	88.5	Boun.	+4.44	3.820
15	1.4	135	40.0190	110.7	115.2	Boun.	+3.90	4.130
16	1.4	160	52.8820	141.9	143.4	Boun.	+1.04	4.420

Average Deviation = ±1.1

Table 4.1 Predicted and reported heat transfer rates in a vertical rectangular cavity

nearly 1.0, as would be expected. These values increase as the Grashof Numbers increase and the convection grows in the flow. Excellent agreement, in most cases, between the heat transfer rates from the present solution and the experimental values is observed.

4.3 RESULTS AND COMPARISONS FOR THE CASE OF INCLINED CAVITIES

For an inclined cavity with the angle of inclination ranging from 0.0 to 90.0 degrees, calculations were performed for a number of cases. The results are given in Table 4.2 where the experimental data of Schinkel et al [36] are also given for comparison. (Schinkel's data was chosen because it compares consistently well with the small number of other pertinent works.). The range of Rayleigh numbers is 1.4×10^4 to 1.4×10^6 and of aspect ratios is 6 to 27. A good agreement between the results is observed.

4.4 CONCLUSIONS

Close agreement between the data produced by the present calculations, in this chapter, and those obtained from the experiments by Carlson [3], indicates that:

- a) The equations describing a pure heat transfer in an enclosure (equations (2.13)-(2.16) in chapter 2), have been stated correctly;
- b) The solution to these equations (through the procedure described in chapter 3), has been successfully done.

Angle	Ra=1.4 E 04			Ra=1.1 E 05			Ra=1.4 E 06			
	Nu		Deviation	Nu		Deviation	Nu		Deviation	
	cal.	expt.		cal.	expt.		cal.	expt.		
0.0	2.41	2.50	3.6%	3.69	3.60	-2.50%	9.60	9.85	2.53%	
10.0	2.40	2.53	5.14%	3.61	3.54	1.98%	9.01	9.22	2.27%	
20.0	2.26	2.40	5.83%	3.43	3.54	3.10%	8.33	8.59	3.00%	
30.0	2.17	2.27	4.82%	3.36	3.54	5.08%	8.19	8.34	1.75%	
40.0	2.02	2.15	6.05%	3.61	3.54	-1.98%	7.68	8.08	5.01%	
50.0	2.12	2.02	-4.95%	3.60	3.54	-1.69%	8.28	8.08	-2.24%	
60.0	1.73	1.82	4.94%	3.11	3.31	6.04%	7.71	7.83	1.54%	
70.0	1.81	1.77	-2.26%	3.14	3.31	5.13%	7.32	7.71	5.01%	
80.0	1.47	1.57	6.37%	3.25	3.06	-6.21%	7.05	7.35	4.08%	
90.0	1.58	1.52	-3.95%	2.81	2.90	3.10%	7.14	7.07	-0.99%	
Average deviation=			-2.60%	=			0.80%	= 2.18%		

Table 4.2 Predicted and reported Nusselt Numbers for an inclined rectangular cavity

5. WATER DISTILLATION IN A VERTICAL RECTANGULAR CAVITY

In this chapter the problem of pure heat transfer, considered in the previous chapter, is extended to a more complicated problem. That is the process of water distillation in a vertical cavity. The physical model is similar to Figure 2.1 except that the vertical cavity ($\alpha=90.0$ degrees) is filled with air and the liquid films are the saline water on the hot wall and the distilled water on the cold wall.

5.2 PREPARATION OF THE COMPUTER PROGRAM

5.1 NATURE OF THE PROCESS

The process of water distillation in the cavity is essentially caused by the temperature inequality at the walls: The mole fraction of the water vapour contained in the humid air, within the cavity, is a function of the local total pressure and the local temperature. At the hot and the cold walls, since $T_1 > T_2$, it can be concluded that $X_{W1} > X_{W2}$ (The variation of the total pressure in the cavity is usually very small and its effect on the mole fraction is negligible compared with that of temperature variation.). The difference between X_{W1} and X_{W2} causes, according to Fick's first law, a diffusion of water vapour from the region of high concentration (the hot film) to the region of lower concentration (the cold film). This mechanism of mass transfer by diffusion is accompanied by an analogous mechanism of heat transfer by conduction from the hot wall to the cold wall.

The transfer of heat and mass by conduction-diffusion is aided by a natural convection recirculating flow when

(T1-T2), (XW1-XW2) and the width of the cavity are high enough. In this situation the hot humid air, with a high water vapour concentration, travels from the hot wall around the cavity and comes in contact with the cold wall. Consequently some heat and mass is delivered to the cold film.

Thus, the process of distillation in a cavity is a combined mechanism of conduction, diffusion and convection. Their contribution to the process can be deduced from the flow behaviour in the cavity.

5.2 PREPARATION OF THE COMPUTER PROGRAM

The computer program devised in chapter 3 for solving the equations of change was adapted as follows to solve the problem at hand:

- a) The equations of change, (2.13)-(2.17), which have been derived under assumptions (1-8) in chapter 2, were considered;
- b) The boundary conditions of Case 1 (introduced in Chapter 2), was applied to the boundaries of the cavity;
- c) The angle of inclination, α , was put equal to 90.0 degrees and inserted in the momentum Equations (2.14) and (2.15);
- d) The various cavity dimensions were introduced into the program;
- e) The physical properties of the humid air K , C_p , μ , and D_{AW} were also inserted into the program. The physical properties are evaluated in Appendix [3].

5.3 CASES UNDER CONSIDERATION

For the numerical calculation the cases considered resemble those situations investigated experimentally by

Davis [1]: The height and the breadth of the cavity are taken as constant and equal to 6 inches (15.24 cm) and 24 inches (60.96 cm) respectively. The width of the cavity changes from 0.25 inches (0.6 cm) to 2.0 inches with intervals of 0.25 inches (0.6 cm). The temperatures at the hot and the cold walls vary from 87.5°F (30.8°C) to 134.5°F (56.9°C), providing a wide range of temperature difference between the hot and the cold walls from 4°F (2.2°C) to 34.4°F (19.1°C). Table 5.1 gives the different situations. The run numbers given in Table 5.1 and other subsequent tables are the same numbers assigned by Davis in his experimental program.)

5.4 RESULTS AND COMPARISONS

The primary solution of the equations of change (2.13)-(2.17), Set 2, produced results for the velocity-, pressure-, water vapour mass fraction- and temperature-field. The rates of heat and mass transfer and their relevant coefficients, Nusselt and Sherwood Numbers respectively, were also calculated.

The available experimental data are the rates of heat and mass transfer and the temperature field; Hence comparisons can be made only in respect to these. In the following sections the rate of heat and mass transfer are compared with the corresponding experimental data and the necessary modifications are made to the present solution. Temperature fields are compared when the final solution is achieved.

5.4.1 MASS TRANSFER

Before dealing with the heat and mass transfer rates,

Run NO.	Width of the Cavity		Hot Side Temperature		Cold Side Temperature	
	In	Cm	°F	°C	°F	°C
28	0.50	1.27	104.9	40.5	95.1	35.0
29	0.50	1.27	91.4	33.0	87.4	30.7
30	0.50	1.27	93.3	34.1	87.4	30.7
31	0.50	1.27	107.7	42.1	91.9	33.3
33	2.00	5.08	93.4	34.1	86.9	30.5
34	2.00	5.08	94.8	34.9	85.3	29.6
35	2.00	5.08	97.5	36.4	83.3	28.5
36	2.00	5.08	101.3	38.5	79.8	26.6
38	2.00	5.08	106.0	41.1	74.7	23.7
45	1.50	3.81	105.2	40.7	94.4	34.7
46	1.50	3.81	104.9	40.5	70.6	21.4
48	1.50	3.81	101.9	38.8	77.2	25.1
49	1.50	3.81	87.5	30.8	71.8	22.1
51	1.75	4.44	87.5	30.8	71.9	22.2
56	1.75	4.44	107.2	41.8	73.6	23.1
58	1.75	4.44	108.0	42.2	90.6	32.6
62	1.25	3.17	106.0	41.1	74.8	23.8
63	1.00	2.54	106.0	41.1	74.6	23.7
67	0.75	1.91	115.7	46.5	104.6	40.3
68	0.75	1.91	102.0	38.9	96.8	36.0
69	0.75	1.91	100.4	38.0	80.0	26.7

Height of the cavity = 6.00 Inches (15.24 Cm)

Table 5.1 Cases under consideration

it is advantageous to examine the regimes of flow in the cavity. This would help for a better understanding of the kind of results obtained.

From the calculated results of the mass fraction-, temperature- and velocity-field, three regimes of flow, similar to those existing in a pure heat transfer case, were observed. Typical examples of these regimes are given in the form of mass fraction distribution (mid-height of the cavity) in Figures 5.1, 5.2 and 5.3 and the velocity distribution (at different heights in the cavity) in Figure 5.4.

Figure 5.1 shows a linear distribution of the mass fraction at midheight of the cavity, which indicates the existence of a conduction-diffusion regime of flow, i.e., the heat and mass are predominately transported by conduction and diffusion respectively.

Figure 5.2 and 5.3 are the mass fraction distribution obtained from Run-62 and Run-63 for transient and boundary flow regimes. (See Table 5.1 for the parameters of Run-62 and Run-63.). Both figures indicate the presence of mass transfer by convection as well as that by diffusion. In Figure 5.3 the flat part of the curve in the central region of the cavity suggests a fully developed boundary regime in Run-62. This can also be depicted from the corresponding vertical velocity profiles in Figure 5.4; The humid air in the central region remains at a stand still and no mass is transferred by diffusion or by convection in this region.

The regimes of flow described above are in agreement with the findings of Davis [1] and Hu [2].

Tables 5.2, 5.3 and 5.4 give the rates of mass

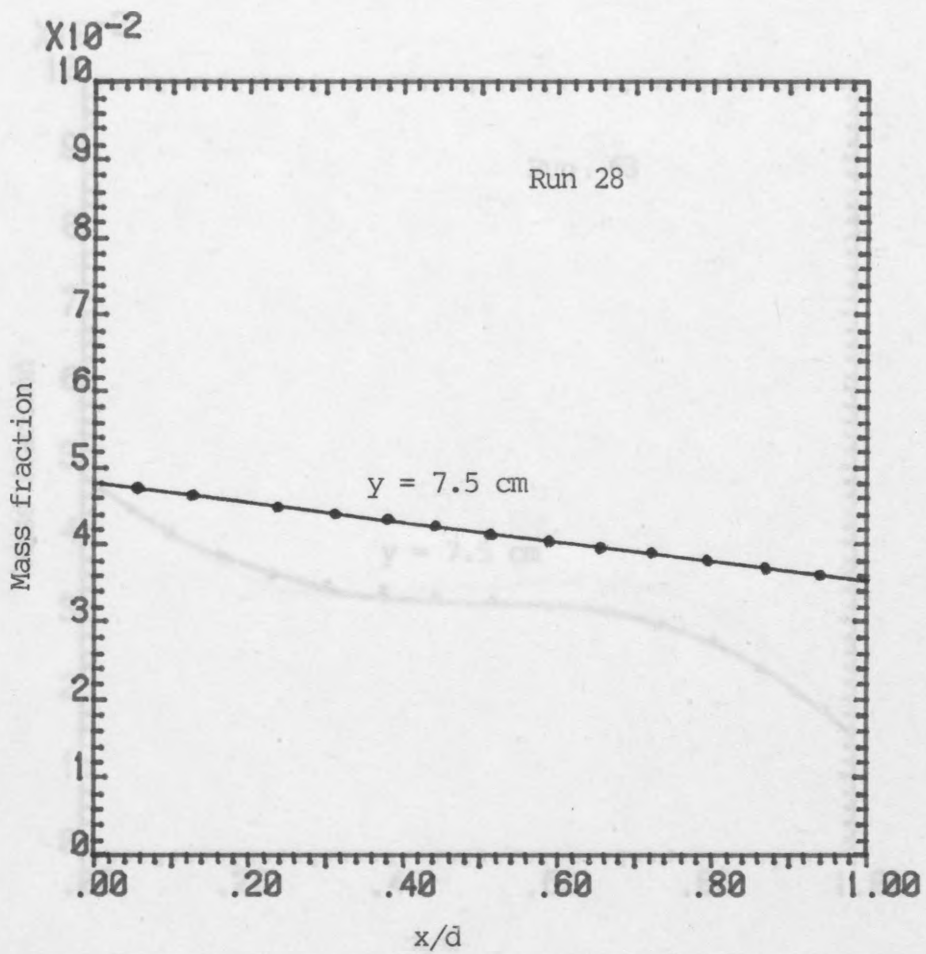


Figure 5.2 Mass fraction distribution at mid-height across a vertical cavity in

Figure 5.1 Mass fraction distribution at mid-height across a vertical cavity in Conduction-Diffusion regime of flow

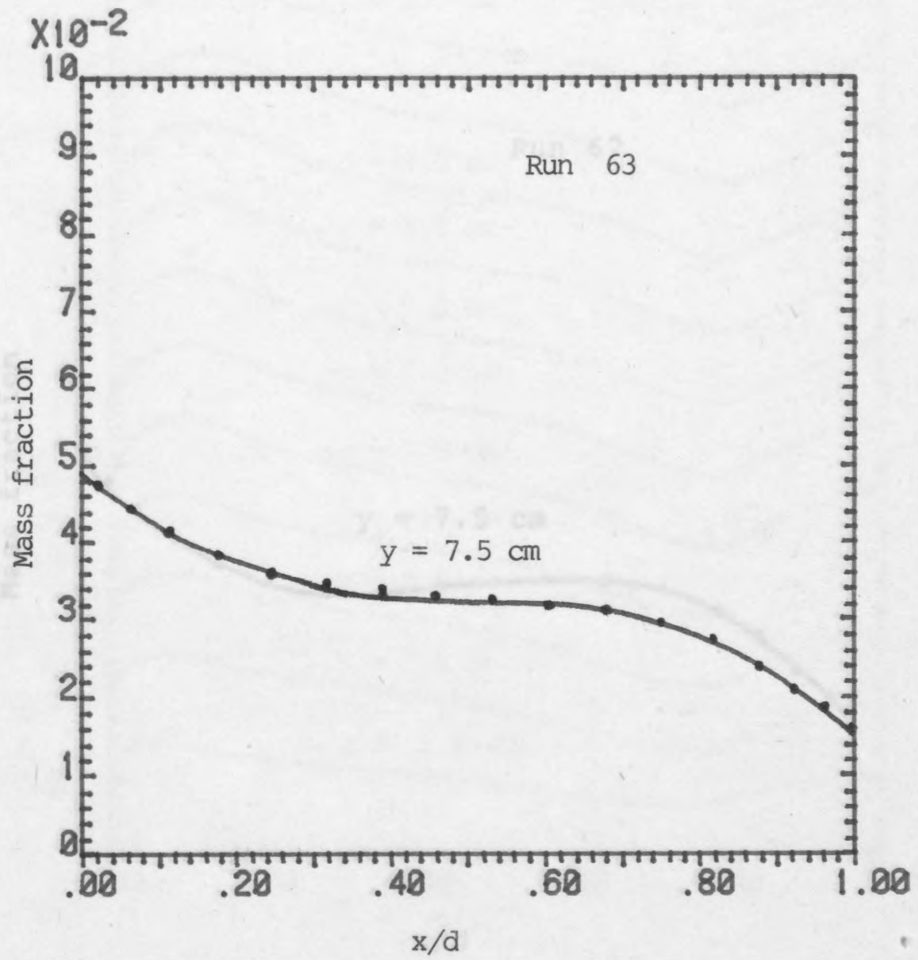


Figure 5.2 Mass fraction distribution at mid-height across a vertical cavity in Transient regime of flow

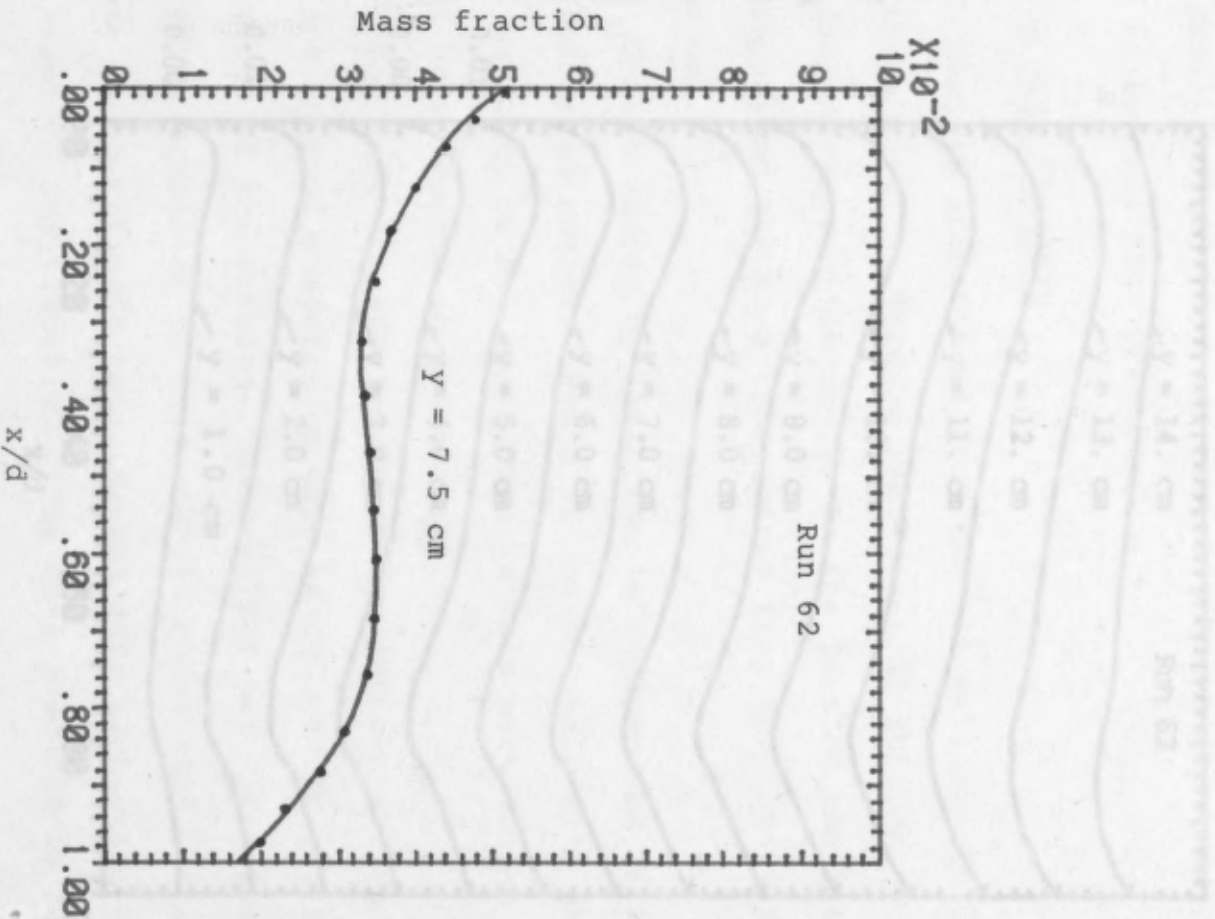


Figure 5.3 Mass fraction distribution at mid-height across a vertical cavity in Boundary regime of flow

transfer for some cases in each of the flow regimes of Conduction-Diffusion, Transient and Boundary, respectively. In these tables distillation rates obtained from the present calculations, column (1), and as reported by Davis,

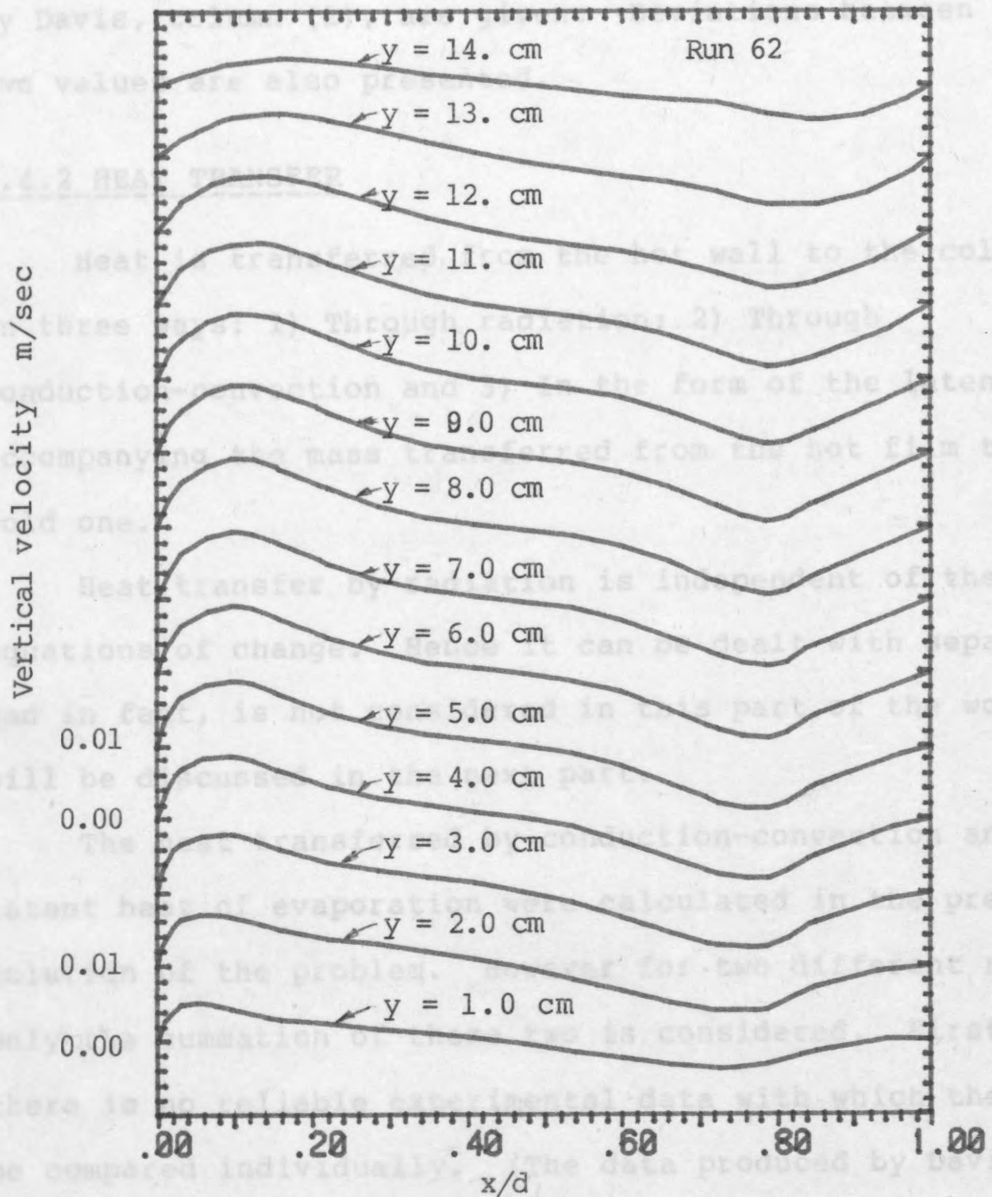


Figure 5.4 Normal velocity distribution at different heights across a vertical cavity in Boundary regime of flow

transfer for some cases in each of the flow regimes of Conduction-Diffusion, Transient and Boundary, respectively. In these tables distillation rates obtained from the present calculations, column (1), and as reported by Davis, column (2), are given. Deviations between the two values are also presented.

5.4.2 HEAT TRANSFER

Heat is transferred from the hot wall to the cold wall in three ways: 1) Through radiation; 2) Through conduction-convection and 3) In the form of the latent heat accompanying the mass transferred from the hot film to the cold one.

Heat transfer by radiation is independent of the equations of change. Hence it can be dealt with separately and in fact, is not considered in this part of the work but will be discussed in the next part.

The heat transferred by conduction-convection and the latent heat of evaporation were calculated in the present solution of the problem. However for two different reasons only the summation of these two is considered. First, there is no reliable experimental data with which they can be compared individually. (The data produced by Davis [1] is in the form of "total heat transfer". He reported a great deal of uncertainty when the components were separated from each other.). Secondly; for convenience the correlation of heat transfer for use in the next part of this work is based on the summation of the components 2) and 3). Consequently, in the corresponding tables all data of heat transferred is the sum of the heat transferred by

Run	(1) Distillation Calculated Gr/hr	(2) Distillation Expt. [1] Gr/hr	(2)-(1) ----- (1) %
28	11.07	11.00	-0.63
29	3.17	3.28	3.33
30	4.86	4.83	-0.62
31	18.54	17.00	-9.00
68	4.26	4.18	-1.91
			Average Deviation=-1.76%

Table 5.2 Predicted mass transfer rates; vertical
cavity; Conduction-Diffusion regime

Run	(1) Distillation Calculated Gr/hr	(2) Distillation Expt. [1] Gr/hr	(2)-(1) ----- (1) %
63	32.96	26.30	-25.32
67	14.57	12.24	-19.04
69	17.71	14.02	-26.32
			Average Deviation=-23.56%

Table 5.3 Predicted mass transfer rates; vertical
cavity; Transient regime

production-convection and the heat conveyed by mass transfer.

Tables 5.5, 5.6 and 5.7 are similar to Tables 5.2, 5.3 and 5.4 respectively, except that here the heat transfer is considered.

Run	(1) Distillation Calculated Gr/hr	(2) Distillation Expt. [1] Gr/hr	(2)-(1) ----- (1) %
33	4.31	3.17	-35.96
36	20.13	16.54	-21.17
38	33.00	25.38	-30.02
46	34.27	27.02	-26.83
48	23.48	18.51	-26.85
56	36.11	28.26	-27.77
62	32.84	26.56	-23.32

Average Deviation=-27.42%

is within acceptable limits.

However, in the transient and boundary regimes, due to the complexity of the fluid flow (especially when $(X_1 - X_2)$ and $(X_{W1} - X_{W2})$ are relatively high), greater deviation

Table 5.4 Predicted mass transfer rates; vertical cavity; Boundary regime

average deviation of -27.42% in Tables 5.3 and 5.4 for heat transfer, and -11.67% and -16.37% in Tables 5.5 and 5.7 for mass transfer.

It is clear that this method produces resultant data uniformly higher than that reported through experiment. This has also been reported by Lu [2] who theoretically examined the problem of water distillation in a vertical rectangular cavity.

5.3 IMPROVEMENT OF THE SOLUTION

The large deviations between the calculated and

conduction-convection and the heat conveyed by mass transfer.

Tables 5.5, 5.6 and 5.7 are similar to Tables 5.2, 5.3 and 5.4 respectively, except that here the heat transfer is considered.

5.4.3 DISCUSSION OF THE RESULTS

The close agreement between predicted and experimental rates of mass and heat transfer given in Tables 5.2 and 5.5 respectively, seems to be due to the simplicity of the fluid flow in the conduction-diffusion regime. Linear distribution of the temperature and the mass fraction in this regime makes it easy to be modelled and described mathematically. An average deviation of -1.73% for the mass transfer rates and -4.96% for the heat transfer rates is within acceptable limits.

However, in the transient and boundary regimes, due to the complexity of the fluid flow (especially when (T_1-T_2) and $(X_{W1}-X_{W2})$ are relatively high), greater deviation between calculated and experimental data is observed; an average deviation of -23.56% and -27.42% in Tables 5.3 and 5.4 for heat transfer, and -13.66% and -16.37% in Tables 5.6 and 5.7 for mass transfer.

It is clear that this method produces resultant data uniformly higher than that reported through experiment. This has also been reported by Hu [2] who theoretically examined the problem of water distillation in a vertical rectangular cavity.

5.5 IMPROVEMENT OF THE SOLUTION

The large deviations between the calculated and

Run	(1) Heat Transfer Calculated Kj/hr	(2) Heat Transfer Expt. [1] Kj/hr	(2)-(1) ----- (1) %
28	30.90	29.24	-5.6
29	9.29	8.47	-9.6
30	14.18	13.53	-4.8
31	51.91	50.64	-2.5
68	11.97	11.69	-2.3

Average Deviation=-4.96%

Table 5.5 Predicted heat transfer rates; vertical
cavity; Conduction-Diffusion regime

Run	(1) Heat Transfer Calculated Kj/hr	(2) Heat Transfer Expt. [1] Kj/hr	(2)-(1) ----- (1) %
63	97.28	84.05	-15.74
67	39.44	35.56	-10.91
69	52.46	45.88	-14.34

Average Deviation=-13.66%

Table 5.6 Predicted heat transfer rates; vertical
cavity; Transient regime

experimental heat and mass transfer rates in the boundary flow regime is undesirable. One source of the

disagreement may be due to discrepancy in the experimental data. Up to a deviation of 10% in the experimental data, the deviation would be accepted. However, the deviations reported at present are too high. This indicates that the calculations derived under assumptions

(1)-(4) and the boundary condition of Case 1 (in section 2.7 of chapter 2), are not sufficiently accurate in describing the process of distillation in the cavity. Therefore, the following attempts were made in order to find out ways of improving the solution.

2.5. ESTIMATION OF TANGENTIAL VELOCITY AT THE BOUNDARY

Law and Davis [1] studied the velocity profile in a vertical cavity. He [2] argued that failure to consider this velocity would lead to prediction of greater distillation rates than the actual value. Hence to obtain this, the boundary condition of Case 2 (introduced in section 2.7),

Table 5.7 Predicted heat transfer rates; vertical cavity; Boundary regime

For a velocity of the evaporating film, Table 5.6 provided the calculated distillation rates for Run 62 as an example. (Note that the magnitudes of these tangential velocities are particularly related to the experiments done by Davis [1] in his work.). As can be seen the distillation rates decrease as velocity increases, so that for a velocity of 0.1 m/sec the deviation from the experimental data is diminished. However, the actual velocity for Run-62 (and approximately for other runs) is

Run	(1) Heat Transfer Calculated Kj/hr	(2) Heat Transfer Expt. [1] Kj/hr	(2)-(1) ----- (1) %
33	12.74	9.66	-31.88
36	59.44	49.83	-19.28
38	97.40	82.97	-17.39
46	102.49	92.85	-10.38
48	69.61	59.74	-16.52
56	106.51	94.32	-12.92
62	96.83	91.14	-6.24

Average Deviation=-16.37%

experimental heat and mass transfer rates in the boundary flow regime is undesirable. One source of the disagreements may be due to discrepancy inherited in the experimental works. Up to 10% deviation could be accepted. However the deviations resulted at present are too high. This indicates that the equations derived under assumptions (1)-(8) and the boundary condition of Case 1 (in section 2.2 of chapter 2), are not sufficiently accurate in describing the process of distillation in the cavity. Therefore, the following attempts were made in order to find out ways of improving the solution.

5.5.1 EFFECT OF TANGENTIAL VELOCITY AT THE HOT BOUNDARY

The film of the saline water coming down the hot wall has a velocity. The air in contact with the moving film has the same tangential velocity in the same direction, i.e. downward. Hu [2] argued that failure to consider this velocity would lead to prediction of greater distillation rates than the actual values. Hence to examine this, the boundary conditions of Case 2 (introduced in section 2.2), were introduced into the program.

For a range of tangential velocity of the evaporating film, Table 5.8 provides the calculated distillation rates for Run 62 as an example. (Note that the magnitudes of these tangential velocities are particularly related to the experiments done by Davis [1] in his work.). As can be seen the distillation rates decrease as velocity increases, so that for a velocity of -0.1 m/sec the deviation from the experimental data is diminished. However the actual velocity for Run-62 (and approximately for other runs), is

(are) about -0.03 m/sec. Therefore, the improvement, in this particular example, would be a reduction in deviation from -23.32% (for $v_1=0.0$ in Table 5.4) to -16.71% (for $v_1=-0.03$ m/sec in Table 5.8), i.e. an improvement of 6.61% has been achieved.

5.5.2 EFFECT OF VARIABLE PROPERTIES

In a theoretical investigation dealing with the equations of change, usually the physical properties are assumed to be constant and only the effect of buoyancy force is taken into account as in assumptions (7)-(8) in section 2.2. These assumptions simplify the equations while producing little effect on the results.

However, since the present method of solution employed in this work is capable of dealing with the variable properties, the validity of these assumptions were examined. By eliminating assumptions (7)-(8) the equations of change become Equation (2.1)-(2.5) i.e. Set 1. Then, setting the computer program for solving these equations, results were obtained for a few cases.

Table 5.9 gives a typical example in which distillation rates for Run-62, resulting from equations Set 1 and Set 2, are presented. A little difference is observed suggesting that the usual assumptions (7)-(8) for the process of natural convection in a hot box are justified.

5.5.3 PHASE CHANGE

As was shown, from assumptions (1)-(8), (7) and (8) are well justified and little or no improvement is gained by eliminating them. Now, in this section assumption (3)

Tangential Velocity m /sec	Distillation Rate Gr /hr	Deviation from Expt %
0.000	32.82	-23.32
-0.001	32.78	-23.00
-0.010	32.18	-20.75
-0.030	31.00	-16.71
-0.060	30.02	-12.64
-0.100	26.77	- 0.45

Table 5.8 Effect of tangential velocity on mass transfer rates (Run 62)

Set of equations	Distillation Rate Gr/hr
(1)	32.82
(2)	32.72

Table 5.9 Effect of variable physical and transport properties on mass transfer rate (Run 62)

is reconsidered. According to this assumption no phase change is taking place in the process of distillation in the cavity. However, when the calculated mass fraction field was compared with the saturated values at the prevailing temperatures, it was noticed that in almost every case the former is higher than the latter, i.e. $W > W_{sat}$. This apparent oversaturation is a product of faulty mathematical modelling and does not represent the actual case.

In the actual process of distillation it seems likely that the water vapour in reaching the relatively cold regions, becomes saturated. Furthermore, if the regions are cold enough, condensation would also take place. Therefore in writing the diffusion equation, any possibility of phase change must also be considered. The diffusion equation which appeared in Set 1 and Set 2 is not capable of predicting the mass fraction field of water vapour since this equation is based on "no phase change". Consequently, the complete form of the diffusion equation is stated as follows [29]:

$$\text{div} (\rho \cdot \vec{V} \cdot W_g) - \text{div} (\rho \cdot D_{AW} \cdot \text{grad} (W_g)) = -R \quad (5.1)$$

In the above equation $W_g \leq W_{sat}$, where:

W_g is the mass fraction of the vapour;

W_{sat} is the mass fraction of a saturated humid air at the same temperature and the same pressure in a given locality in the cavity;

R is the rate of phase change, and is positive when the state is changing from vapour to liquid and negative

otherwise.

In Equation (5.1) both R and Wg are unknown and have to be determined; An additional equation is required to relate one (or both) of the unknown(s) to some known values. One possible way of doing so is to assume that the whole mixture is saturated, hence:

$$Wg = Wsat \quad (5.2)$$

Substituting (5.2) in (5.1) gives:

$$\text{div} (\rho \cdot \vec{V} \cdot Wsat) - \text{div} (\rho \cdot D_{AW} \cdot \text{grad} (Wsat)) = -R \quad (5.3)$$

The assumption of saturated humid air within the cavity, in the case of phase change, is not unrealistic, since;

- a) If condensation takes place in a particular region in the cavity, some liquid water molecules will be present;
- b) Due to the recirculating motion of the fluid, it is very likely that these molecules of liquid water are transported throughout the cavity;
- c) In the unsaturated regions (with a local mass fraction less than the corresponding saturated mass fractions), some of the molecules of liquid water would re-evaporate.

In this way the whole mixture would be saturated.

In Equation (5.2) Wsat is calculated as follows:

$$Wsat = \frac{M_{H2O} \cdot XWsat}{M_{H2O} \cdot XWsat + (1.0 - XWsat) \cdot M_{Air}} \quad (5.4)$$

where:

$$XWsat = \frac{P_{H2O}}{p} \quad (5.5)$$

where,

M_{H_2O} and M_{Air} are molar mass of Water and Air respectively; p and p_{H_2O} are total pressure and partial pressure of the water at the local temperature, respectively.

p_{H_2O} is a function of temperature and can be obtained from the empirical equation given by Lange- [37]:

$$p_{H_2O} = [10.0^{(8.10765-1750.286/(235.+T))}] / 750.0 \text{ bar} \quad (5.6)$$

By substituting Equations (5.6), (5.5) and (5.4) in Equation (5.3), R can be obtained.

R can be negative or positive. This means that condensation and evaporation are both allowed to take place in appropriate regions in the field. The latent heat of evaporation or condensation is then removed from the mixture or is given to the mixture, respectively. Consequently the equation of energy, (2.17), is modified to account for this heat exchange as below:

$$\tilde{C}_p (\rho u \partial T / \partial x + \rho v \partial T / \partial y) = K (\partial^2 T / \partial x^2 + \partial^2 T / \partial y^2) + R \cdot h_{vap} \quad (5.7)$$

Substituting R from Equation (5.1) in the above equation gives:

$$\tilde{C}_p (\rho u \partial T / \partial x + \rho v \partial T / \partial y) = K \partial^2 T / \partial x^2 - h_{vap} \cdot [(\rho u \partial w_{sat} / \partial x + \rho v \partial w_{sat} / \partial y) - D_{AW} (\partial^2 w_{sat} / \partial x^2 + \partial^2 w_{sat} / \partial y^2)] \quad (5.8)$$

where h_{vap} is the latent heat of evaporation of water.

It is assumed that the phase change has no effect on the momentum and the continuity equations and they remain as they were in Set 1 and Set 2.

5.6 FINAL SOLUTION

Equations (2.13), (2.14), (2.15) and (5.8) form Set-3 of the equations of change describing water distillation in a rectangular cavity. These equations are, in fact, derived under assumptions (1)-(8) excluding assumption (3) for phase change. To solve them, appropriate changes to the computer program were made (see Appendix [4]). The results obtained are given in this section.

5.6.1 RESULTS AND COMPARISONS

a) Heat and mass transfer

Tables 5.10 and 5.11 give some of the results of the heat transfer and mass transfer rates respectively. Both boundary conditions of Case 1 (with tangential velocity $v_1=0.0$) and Case 2 ($v_1=-0.03$ m/sec) have been considered in the calculations. The corresponding results are given in the columns under (1) and (2) respectively. Deviations of (1) and (2) from the experimental results are also given.

The cases in both Tables 5.10 and 5.11 belong to the convective flow regimes. (Transient and Boundary regimes are regarded as Convective flow regimes.). For the Conduction-Diffusion regime, the application of the final set of equations of change to the cases belonging to this regime produce almost identical results to those of Tables 5.2 and 5.5 for mass and heat transfer rates, respectively.

b) Temperature field

Figure 5.5 gives an example of the temperature distribution across the cavity for three different heights of 0.5 inches (1.27 cm), 3.0 inches (7.62 cm) and 5.5

Run No.	(1) (V1=0.0) Mass Rate Gr/hr	(2) (V1=-0.03) Mass Rate Gr/hr	Expt.-(1) ----- Expt. %	Expt.-(2) ----- Expt. %
33	4.31	3.82	-35.90	-20.0
36	18.80	17.31	-13.60	- 4.60
38	29.27	27.14	-15.30	- 6.90
46	30.26	28.32	-11.99	- 4.81
48	18.51	20.37	-17.99	-10.04
56	32.15	29.92	-13.76	- 5.87
62	30.01	28.09	-12.50	- 5.40
63	30.39	28.24	-15.55	- 7.37
67	13.85	13.18	-13.20	- 7.68
69	16.47	15.01	-17.47	- 6.99

Average=-16.72% , =-7.97%

Table 5.10 Mass transfer rates obtained from
Set 3 of the equations of change

Run No.	(1)	(2)	Expt.-(1)	Expt.-(2)
	(V1=0.0) Heat Rate Kj/hr	(V1=-0.03) Heat Rate Kj/hr	----- Expt. %	----- Expt. %
33	12.00	11.33	-24.22	-17.28
36	57.81	53.52	-16.01	-7.40
38	92.79	86.78	-11.83	-4.59
46	99.02	93.59	- 6.64	-0.79
48	68.31	64.11	-14.34	-7.31
56	101.63	96.54	- 7.75	-2.35
62	95.25	89.97	- 4.51	-1.28
63	96.68	90.60	-15.02	-7.79
67	39.00	35.96	- 9.67	-1.12
69	52.06	49.01	-13.47	-6.80

Average=-12.34% , =-5.67%

Table 5.11 Heat transfer rates obtained from
Set 3 of the equations of change

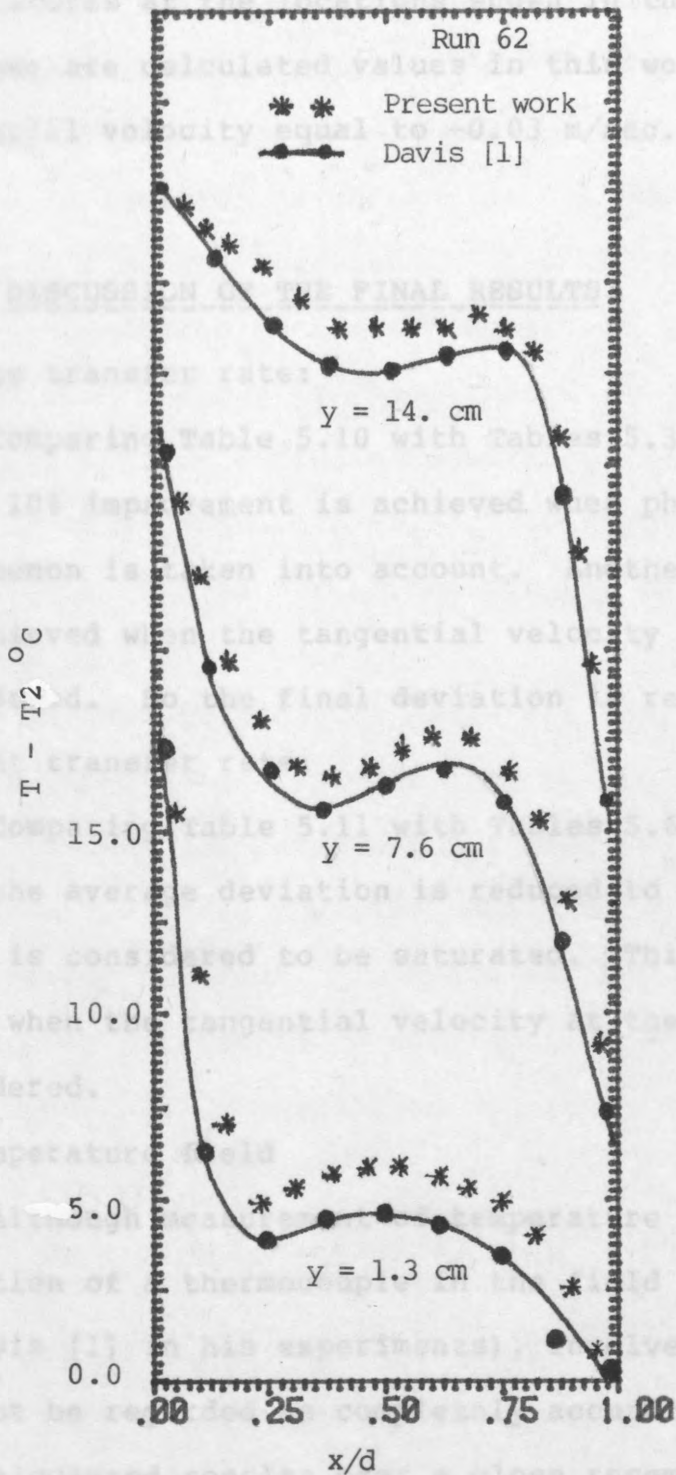


Figure 5.5 Temperature profiles at different heights

inches (13.97 cm). The solid curves and the circles have been produced by Davis [1] in a direct measurement of the temperatures at the locations shown in the figure. The asterisks are calculated values in this work with a boundary tangential velocity equal to -0.03 m/sec.

5.6.2 DISCUSSION OF THE FINAL RESULTS

a) Mass transfer rate:

Comparing Table 5.10 with Tables 5.3 - 5.4 shows that up to 10% improvement is achieved when phase change phenomenon is taken into account. Another 9% improvement is achieved when the tangential velocity is also considered. So the final deviation is reduced to -7.97% .

b) Heat transfer rate:

Comparing Table 5.11 with Tables 5.6 and 5.7 shows that the average deviation is reduced to 12.34% when the fluid is considered to be saturated. This reduces to only 5.67% when the tangential velocity at the hot film is also considered.

c) Temperature field

Although measurement of temperature using direct insertion of a thermocouple in the field (as has been done by Davis [1] in his experiments), involves some error and can not be regarded as completely accurate, experimental and calculated results bear a close resemblance, as can be seen in Figure 5.5.

5.7 HEAT AND MASS TRANSFER CORRELATIONS

5.7.1 NORMALIZATION OF THE EQUATIONS OF CHANGE

As was previously mentioned, the parameters which affect the heat and mass transfer, would be indicated by the normalization of the analytical model. In section 2.3, for Set 2 of the equations of change ((2.13)-(2.17)) this was done and the normalized Equations (2.20)-(2.24) were obtained. But due to phase change the energy equation, (2.16), and the diffusion equation, (2.17), were modified to the single Equation (5.8). Consequently, normalization has to be carried out on the new set of equations of change.

In the equations of Set-3 the continuity and the momentum equations are the same as those in Set-2. Hence their normalized forms are the same as those given in section 2.3. The equation remaining to be normalized is the energy equation. In doing so, the dimensionless variables introduced in section 2.3 are inserted in Equation (5.8), the resultant equation would be as below:

$$U \frac{\partial \theta}{\partial X} + V \frac{\partial \theta}{\partial Y} = 1/Pr (\partial^2 \theta / \partial X^2 + \partial^2 \theta / \partial Y^2) \quad (5.9)$$
$$- Bz [(U \frac{\partial \phi}{\partial X} + V \frac{\partial \phi}{\partial Y}) - 1/Sc. (\partial^2 \phi / \partial X^2 + \partial^2 \phi / \partial Y^2)]$$

In the above equation, Bz is a newly introduced dimensionless group which represents the phase change phenomena in the equation of energy. Bz is determined as:

$$Bz = h_{vap}/Cp (W1-W2)/(T1-T2) \quad (5.10)$$

or equally:

$$Bz = h_{vap}/Cp (GrXW/GrT) \quad (5.11)$$

When all the dimensionless groups are known, then the relationships between them and the dependent dimensionless parameters of heat and mass transfer (Nusselt numbers and Sherwood numbers respectively) can be assumed as follows:

$$Nu = f(Gr_T, Gr_{XW}, Pr, Sc, Bz, L, \dots) \quad (5.12)$$

$$Sh = f(Gr_T, Gr_{XW}, Pr, Sc, Bz, L, \dots) \quad (5.13)$$

In these relationships, Nu and Sh are defined in Appendix- [5].

5.7.2 MODELS OF CORRELATIONS

5.7.2.a TYPE 1

From theoretical work dealing with simultaneous heat and mass transfer for a vertical flat plate, the models of correlations are generally reported as follows:

For heat transfer:

$$(Nu_{\text{cond-conv}})_1 = a_1 (Gr_{\text{com}})_1^{n_1} \quad (5.14)$$

The index "cond-conv" indicates that Nusselt number is based on the heat transferred by the conduction-convection mechanism. Other components of "total heat transfer" (the latent heat of evaporation and the radiation), are not included.

For mass transfer:

$$(Sh)_1 = a_2 (Gr_{\text{com}})_1^{n_2} \quad (5.15)$$

where Gr_{com} is a combined Grashof number defined as follows:

For binary mixtures with $Sc > Pr$, e.g. n-heptane, air:

$$Gr_{\text{com}} = Gr_T + \sqrt{Pr/Sc} Gr_{XW} \quad (5.16)$$

For binary mixtures with $Pr > Sc$, e.g. water vapour, air:

$$Gr_{com} = Gr_{XW} + \sqrt{Sc/Pr} Gr_T \quad (5.17)$$

Note that in (5.14) and (5.15), the index "1" indicates that the corresponding dimensionless groups are based on the height of the cavity.

This type of correlation model was used in the analytical part of the work by Davis [1]. However, in the experimental part, models (5.14) and (5.15) were not working satisfactorily. An additional term, though not explained analytically, had to be added in order to fit the experimental data to the models. The new models suggested by Davis were in the form:

$$(Nu_{cond-conv,lat})_1 = a_1 Gr_{com}^{n1} (Gr_{XW}/Gr_T)_1^{m1} \quad (5.18)$$

$$Sh_1 = a_2 Gr_{com}^{n2} (Gr_{XW}/Gr_T)_1^{m2} \quad (5.19)$$

The appearance of the additional term in models (5.18) and (5.19) can be explained by the normalized energy equation, (5.9), suggested in the present work for the case of phase change in the field; where the term Gr_{XW}/Gr_T is implicit in Bz number, (5.11).

Correlation models (5.18) and (5.19) can be given in the following forms when the dimensionless groups are based on the width of the cavity. (In this case no index is used instead of 1.).

$$Nu_{cond-conv,lat} = a_1 Gr_{com}^{n1} (Gr_{XW}/Gr_T)^{m1} L^{k1} \quad (5.20)$$

and, formulae (5.22)-(5.25), have to be determined.

This should be done by fitting the predicted data into the models. The method involves the following steps in the next

$$Sh = a_2 Gr_{com}^{n_2} (Gr_{XW}/Gr_T)^{m_2} L^{k_2} \quad (5.21)$$

where "L" is the aspect ratio, l/d.

Further, correlation models (5.20) and (5.21) can be expressed in term of Bz:

$$Nu_{cond-conv, lat} = a_1 Gr_{com}^{n_1} Bz^{m_1} L^{k_1} \quad (5.22)$$

and,

$$Sh = a_2 Gr_{com}^{n_1} Bz^{m_1} L^{k_1} \quad (5.23)$$

Note that the constants in correlation models (5.22) and (5.23) are not necessarily of the same magnitude as similar ones in other equations.

5.7.2.b TYPE 2

An alternative form of correlation model can be represented in the form:

$$Nu_{cond-conv, lat} = a_1 Gr_T^{n_1} Gr_{XW}^{m_1} L^{k_1} \quad (5.24)$$

$$Sh = a_2 Gr_T^{n_2} Gr_{XW}^{m_2} L^{k_2} \quad (5.25)$$

In these formulae, Pr and Sc, appearing in correlations Type-1, are absent since they are almost constant in the considered range of T1 to T2 and XW1 to XW2. Also the term of h_{vap}/C_p contained in Bz can be assumed constant in this range. The other two components contained in Bz (Gr_T and Gr_{XW} , see Equation (5.11)), are already present in the formulae. Hence, Bz itself is not included.

The constants appearing in both types of correlation

models, formulae (5.22)-(5.25), have to be determined. This should be done by fitting the predicted data into the models. The method involved is dealt with in the next section.

5.7.3 METHOD OF CORRELATION

Consider the correlation formula expressed in the form

$$y = a \cdot x_1^{n_1} \cdot x_2^{n_2} \cdot x_3^{n_3} \dots \quad (5.26)$$

where n different sets of y , x_1 , x_2 , x_3 , ... are known from experiments or calculations. Then the usual method for evaluating the constants a , n_1 , n_2 , n_3 , ... is as follows:

- a) Against the values of one of the variables (when others are constant), y is plotted on a log-log scale. A linear curve is produced, the gradient of which constitutes the exponent of the corresponding variable, e.g. n_1 for x_1 ;
- b) The above is repeated for other variables until all of the exponents are known;
- c) The value of "a" can be found by taking an average from the following equation:

$$a = y / (x_1^{n_1} \cdot x_2^{n_2} \cdot x_3^{n_3} \dots) \quad (5.27)$$

However in the present situation the above procedure is not fully applicable because the dimensionless groups, x_1 , x_2 , x_3 ,, vary simultaneously. Hence a new method was employed to replace the usual graphical one.

The new method is essentially a combined average-least squares method and its main features are as below:

- a) For a set of exponents the average value of the coefficient

- a" is obtained;
- b) Using "a", estimated values of y are calculated;
- c) The Standard Error of Estimate, SEE, is calculated as:

$$SEE = \sqrt{\frac{\sum_{i=1}^{i=n} (y_{\text{calculated}} - y_{\text{estimated}})^2}{n}} \quad (5.28)$$

- d) For different sets of exponents steps a), b) and c) are taken. To avoid examining enormous numbers of the different possible sets of exponents, a "concentrated-scheme" was used.
- e) The best set of constants is that which produces the minimum SEE.

The calculations are executed by a program named "COR" given in Appendix [6].

5.7.4 RESULTS OF CORRELATION

Results presented in this section are those belonging to Boundary and Transient regimes. For Conduction Diffusion regimes, because of the linearity of the temperature and the mass fraction distribution across the cavity, Nusselt and Sherwood numbers are equal to unity.

5.7.4.a CORRELATIONS OF TYPE 1

To assess this type of correlation model, Figures 5.6 and 5.7 examine the variation of $Nu_{\text{cond-conv,lat}}$ and Sh against Gr_{com} , respectively. The data used in both graphs are obtained from the present calculations and different symbols designate the aspect ratios.

In Figure 5.6, points with $Bz=3.1$, $Bz=4.2$, $Bz=5.2$,

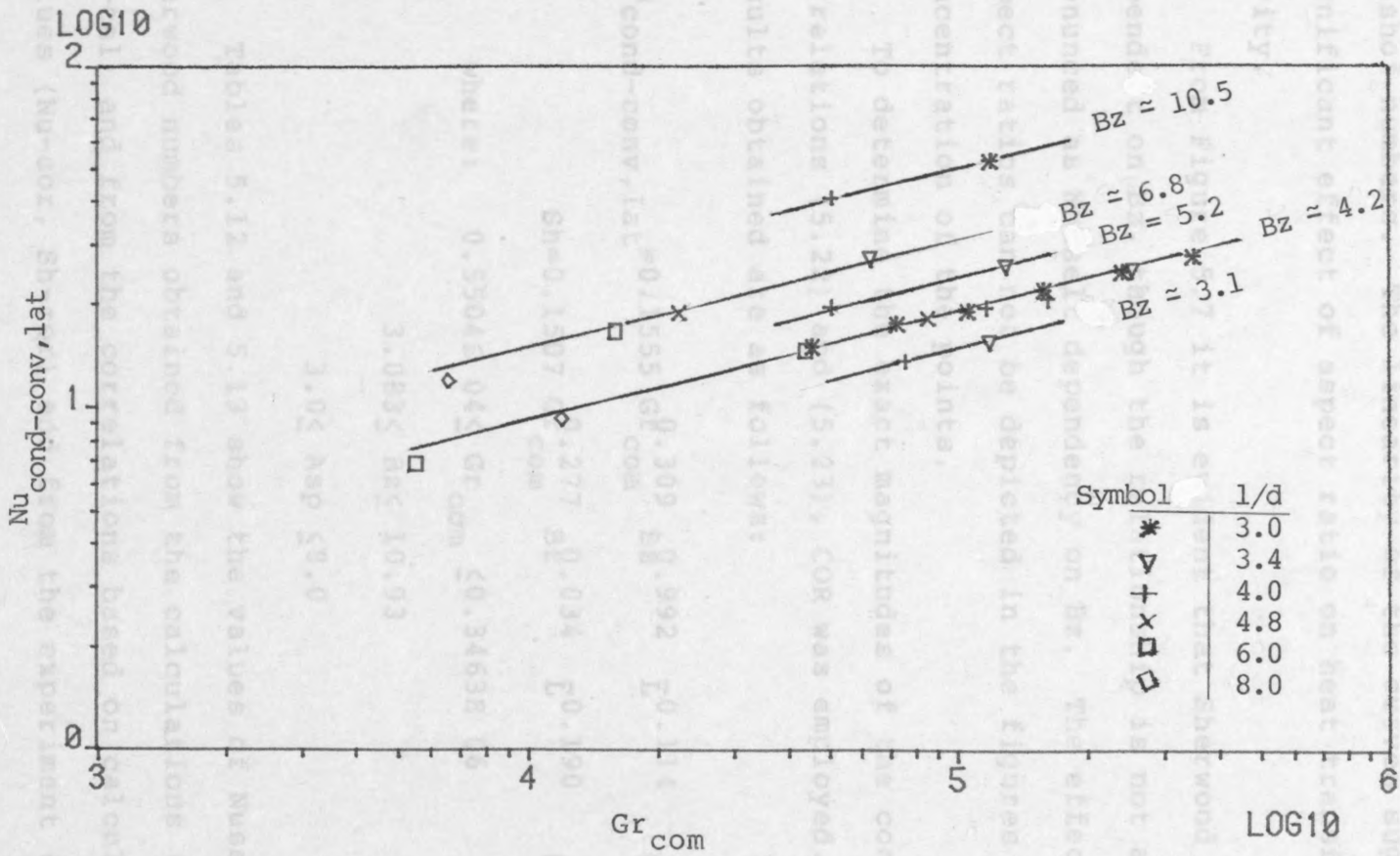


Figure 5.6 Variation of Nusselt number with combined Grashof number

Bz=6.8 and Bz=10.5 clearly form five parallel linear curves. This indicates that Nusselt numbers are strongly dependent on Bz numbers. The slopes of the curves show the degree to which Nusselt numbers are dependent on Combined Grashof numbers. The linearity of the curves suggests no significant effect of aspect ratio on heat transfer in the cavity.

From Figure 5.7 it is evident that Sherwood number is dependent on Bz, though the relationship is not as clearly pronounced as Nusselt dependency on Bz. The effect of the aspect ratios can not be depicted in the figures due to the concentration of the points.

To determine the exact magnitudes of the constants in correlations (5.22) and (5.23), COR was employed. The results obtained are as follows:

$$Nu_{\text{cond-conv, lat}} = 0.1555 Gr_{\text{com}}^{0.309} Bz^{0.992} \bar{L}^{-0.114} \quad (5.29)$$

$$Sh = 0.1507 Gr_{\text{com}}^{0.277} Bz^{0.034} \bar{L}^{-0.190} \quad (5.30)$$

where: $0.5504E 04 \leq Gr_{\text{com}} \leq 0.3463E 06$

$$3.083 \leq Bz \leq 10.93$$

$$3.0 \leq Asp \leq 8.0$$

Tables 5.12 and 5.13 show the values of Nusselt and Sherwood numbers obtained from the calculations (Nu-cal, Sh-cal) and from the correlations based on calculated values (Nu-cor, Sh-cor) and from the experiment (Nu-expt, Sh-expt), respectively. The correlated values are obtained from correlations (5.29) and (5.30). In both tables Nu-cor deviation from the calculated data, $((1)-(2))/(1)$, and from the experimental data, $((3)-(2))/(3)$, is given.

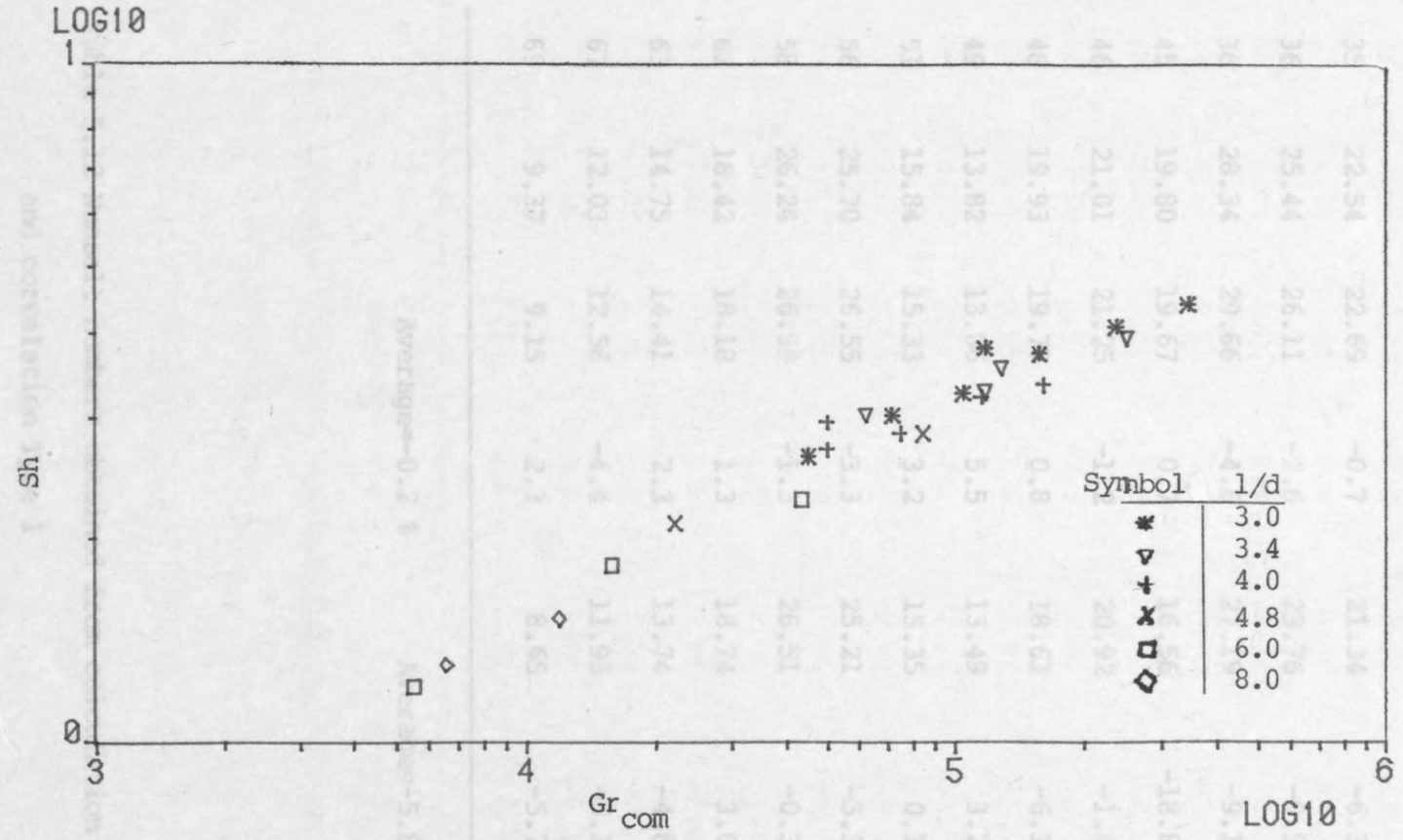


Figure 5.7 Variation of Sherwood number with combined Grashof number

Run	(1) Nu-cal	(2) Nu-cor	$\frac{(1)-(2)}{(1)}$ %	(3) Nu-expt	$\frac{(3)-(2)}{(3)}$ %
33	17.82	17.61	1.2	15.23	-15.6
34	19.28	19.79	-2.6	18.01	-9.9
35	22.54	22.69	-0.7	21.34	-6.3
36	25.44	26.11	-2.6	23.76	-9.9
38	28.34	29.66	-4.6	27.19	-9.1
45	19.80	19.67	0.7	16.56	-18.8
46	21.01	21.25	-1.2	20.92	-1.6
48	19.93	19.77	0.8	18.63	-6.1
49	13.82	13.06	5.5	13.49	3.2
51	15.84	15.33	3.2	15.35	0.1
56	25.70	26.55	-3.3	25.21	-5.3
58	26.24	26.59	-1.3	26.51	-0.3
62	18.42	18.18	1.3	18.74	3.0
63	14.75	14.41	2.3	13.74	-4.8
67	12.03	12.56	-4.4	11.95	-5.1
69	9.37	9.15	2.3	8.65	-5.7

Average=-0.2 %

Average=-5.8 %

Table 5.12 Nusselt numbers obtained from calculation
and correlation Type 1

Run	(1)	(2)	(1)-(2)	(3)	(3)-(2)
	Sh-Cal	Sh-Cor	(1) %	Sh-Expt	(3) %
33	2.86	2.82	1.5	2.43	-16.3
34	3.06	3.11	-1.4	2.74	-13.6
35	3.49	3.44	1.4	3.30	-4.2
36	3.80	3.83	-0.8	3.74	-2.3
38	4.03	4.21	-4.5	3.92	-7.6
45	2.48	2.41	3.0	2.22	-8.6
46	3.10	3.21	-3.4	3.07	-4.3
48	2.99	2.95	1.4	2.81	-5.1
49	2.72	2.61	4.1	2.29	-13.9
51	3.11	3.05	1.9	2.79	-9.4
56	3.61	3.74	-3.9	3.54	-5.9
58	3.24	3.18	1.8	2.86	-11.4
62	2.61	2.60	0.5	2.58	-1.0
63	2.09	2.07	0.8	2.03	-2.2
67	1.16	1.20	-3.1	1.13	-5.8
69	1.42	1.38	2.5	1.27	-8.8

Average= 0.1

Average=-7.5

Table 5.13 Sherwood numbers obtained from calculation and correlation Type 1

5.7.4.b CORRELATIONS OF TYPE 2

For correlations of Type 2, (5.24) and (5.25), the effect of GrXW or GrT on Nusselt and Sherwood numbers can not be deduced from graphs. The reason, as would be seen in Equations (5.31) and (5.32), is the relatively high exponents of aspect ratios in this type of correlation. The correlations are:

$$\text{Nu}_{\text{cond-conv, lat}} = 1.9572 \text{ GrT}^{0.309} \text{ GrXW}^{0.992} \text{ L}^{-0.114} \quad (5.31)$$

$$\text{Sh} = 0.1935 \text{ GrT}^{0.151} \text{ GrXW}^{0.126} \text{ L}^{-0.193} \quad (5.32)$$

$$\text{where: } 0.4368\text{E } 04 \leq \text{GrT} \leq 0.2755\text{E } 06$$

$$0.1418\text{E } 04 \leq \text{GrXW} \leq 0.9336\text{E } 05$$

$$3.0 \leq \text{Asp} \leq 8.0$$

The results obtained from (5.31)-(5.32) were compared with the corresponding data from calculations and experiments; Tables 5.14 and 5.15, similar to those of 5.12 and 5.13, give the comparisons.

5.7.5 DISCUSSION OF THE CORRELATIONS

Columns 4 in Tables 5.12 - 5.15 show the deviations of the correlated data from the calculated ones. (n.b. the former being based on the latter.). The maximum absolute deviations and the average deviations, given in the bottom of columns 4, are as follows:

For heat transfer correlations:

Type 1, from Table 5.12; Average=-0.2% , Max=5.5%

Type 2, from Table 5.14; Average=-0.2% , Max=5.8%

For mass transfer correlations:

Type 1, from Table 5.13; Average=0.1% , Max=4.5%

Run	(1)	(2)	$\frac{(1)-(2)}{(1)}$	(3)	$\frac{(3)-(2)}{(3)}$
	Nu-Cal	Nu-Cor	%	Nu-Expt	%
33	17.82	17.62	1.1	15.23	-15.7
34	19.28	19.81	-2.7	18.01	-10.0
35	22.54	22.73	-0.8	21.34	-6.5
36	25.44	26.13	-2.7	23.76	-10.0
38	28.34	29.60	-4.4	27.19	-8.8
45	19.80	19.73	0.4	16.56	-19.1
46	21.01	21.19	-0.8	20.92	-1.3
48	19.93	19.78	0.8	18.63	-6.2
49	13.82	13.01	5.8	13.49	3.5
51	15.84	15.27	3.6	15.35	0.5
56	25.70	26.47	-3.0	25.21	-5.0
58	26.24	26.64	-1.5	26.51	-0.5
62	18.42	18.20	1.2	18.74	2.9
63	14.75	14.41	2.3	13.74	-4.8
67	12.03	12.57	-4.5	11.95	-5.2
69	9.37	9.19	1.9	8.65	-6.2

Average= -0.2 Average= -5.8

Table 5.15 Sherwood numbers obtained from calculation
and correlation Type 1

Table 5.14 Nusselt numbers obtained from calculation
and correlation Type 2

Run	(1)	(2)	$\frac{(1)-(2)}{(1)}$	(3)	$\frac{(3)-(2)}{(3)}$
	Sh-Cal	Sh-Cor	%	Sh-Expt	%
33	2.86	2.82	1.6	2.43	-16.2
34	3.06	3.10	-1.2	2.74	-13.4
35	3.49	3.44	1.6	3.30	-4.0
36	3.80	3.82	-0.5	3.74	-2.0
38	4.03	4.20	-4.3	3.92	-7.3
45	2.48	2.39	3.5	2.22	-8.1
46	3.10	3.21	-3.5	3.07	-4.4
48	2.99	2.95	1.5	2.81	-5.0
49	2.72	2.63	3.2	2.29	-15.0
51	3.11	3.08	1.1	2.79	-10.2
56	3.61	3.74	-3.6	3.54	-5.6
58	3.24	3.16	2.3	2.86	-10.8
62	2.61	2.60	0.6	2.58	-0.9
63	2.09	2.07	0.8	2.03	-2.3
67	1.16	1.20	-2.9	1.13	-5.6
69	1.42	1.38	2.3	1.27	-9.0

Average = 0.2 , = -7.5

Table 5.15 Sherwood numbers obtained from calculation
and correlation Type 2

Type 2, from Table 5.15; Average=0.2% , Max=4.3%

These values generally give a high degree of accuracy for the correlations in two respects: Firstly, the correlations models are justified since the calculated dimensionless groups can be successfully fitted into them. Secondly, the method of correlation is efficient in producing such a fit.

Columns 6 in the same tables show the deviations of the correlated data (Nu-cor or Sh-cor) from the experimental ones (Nu-expt or Sh-expt) by Davis. These are: For heat transfer correlations:

Type 1, from Table 5.12, Average=-5.8% , Max=-18.8%

Type 2, from Table 5.14, Average=-5.8% , Max=-19.1%

For mass transfer correlations:

Type 1, from Table 5.13, Average=- 7.5%, Max=-16.3%

Type 2, from Table 5.15, Average=- 7.5%, Max=-16.2%

It is concluded that both types of correlation formula are useful.

The kind of results obtained in this chapter are unique; There are not any comparable data, either experimental or theoretical, in the pertinent literature (to the best knowledge of the author).

From these results those which are in the scope of the present study are presented.

6.1.1 HEAT AND MASS TRANSFER RATES

a) Conduction-Diffusion Flow regime

From the results obtained, it is known that the angle of inclination has no effect on the energy transport in this regime. For all angles of inclination the results

Tables 5.2 and 5.5 remained unchanged.

6. CORRELATION OF HEAT AND MASS TRANSFER IN AN INCLINED CAVITY

In the previous chapter the correlation of heat and mass transfer were obtained for a vertical cavity position. The object of this chapter is to extend those correlations to the more general situation of an inclined cavity. The cases considered (sets of T_1 , T_2 , d and l), are similar to those given in Table 5.1 but with addition of higher aspect ratios (l/d up to 18.0). The angle of inclination, α , alters from 0.0 to 90.0 degrees with 10.0 degrees intervals.

In each of the positions the same kind of result obtained for $\alpha=90.0$ degrees, was produced. From there, using COR, the correlations of heat and mass transfer (in Convective regimes), were provided.

6.1 RESULTS AND DISCUSSIONS

The kind of results obtained in this chapter are unique; There are not any comparable data, either experimental or theoretical, in the pertinent literature (to the best knowledge of the Author).

From these results those which are in the scope of the present study are presented.

6.1.1 HEAT AND MASS TRANSFER RATES

a) Conduction-Diffusion flow regime

From the results obtained, it is known that the angle of inclination has no effect on the energy transport in this regime. For all angles of inclination the results

Tables 5.2 and 5.5 remained unchanged.

b) Convective flow regimes

For some of the cases considered, the results of heat and mass transfer together with the corresponding coefficients ($Nu_{\text{cond-conv,lat}}$ and Sh respectively) are given in Appendix [7]. Table 6.1 is a typical example produced in Runs-62.

The effect of the angle on the rate of mass transfer, evident from Table 6.1 and other similar tables in Appendix [7], can be expressed in one diagram shown in Figure 6.1. In this figure the ratio of $Sh/Sh_{0.0}$ (where $Sh_{0.0}$ is Sherwood number at $\alpha=0.0$), is plotted against α for each of the cases. (No distinction is made between the individual cases and all points are marked by *; since only the variation of $Sh/Sh_{0.0}$ against α is in question.). As can be seen, the highest ratio attributes to $0.0 \leq \alpha \leq 10.0$, i.e., when the cavity is nearly horizontal with its hot side on the bottom and the cold side on the top. With the increase of α , Sh decreases to its minimum magnitude (at $\alpha=30.0$ degrees) and then increases and remains almost at a constant level (at $50.0 < \alpha < 90.0$). A similar diagram can be drawn for Nusselts ratios against α .

This is typical of the behaviour of the energy transport in the distillator cavity at different angles of inclination. It is conclusive that the highest productivity is obtained for $0.0 \leq \alpha \leq 10.0$.

6.1.2 CORRELATIONS OF HEAT AND MASS TRANSFER

The two types of correlation model, introduced in the previous chapter, were employed. The data for different

Run 62

Width =33.17 cm

T1=41.1 °C T2=23.8 °C

GrT=0.6703 E 05

GrXW=0.2279 E 06

Gr_{com}=0.8428 E 05 Bz=4.225

Angle of inclination	Distillation Gr/hr	Sh	Heat Transfer Kj/hr	Nu
0.0	35.145	3.63	112.524	23.04
10.0	29.727	3.01	95.220	19.50
20.0	28.750	2.91	94.684	19.39
30.0	25.945	2.63	83.128	17.02
40.0	27.091	2.74	86.787	17.77
50.0	27.796	2.81	89.030	18.23
60.0	28.264	2.86	90.528	18.54
70.0	28.455	2.88	91.135	18.66
80.0	28.404	2.88	90.971	18.63
90.0	28.091	2.84	89.976	18.42

Table 6.1 Predicted heat and mass transfer rates in an inclined rectangular cavity (Run 62)

angles of inclination were plotted into them and the constants of the correlations were found. Tables 6.2 and 6.3 give a Type 1 correlation of heat and mass transfer in convective film regimes. The range of dimensionless groups are also given. Tables 6.4 and 6.5 are similar to 6.2 and 6.3, respectively, and give a Type 2 correlation. The validity of the formulae are within the range of Gr, Gr_w and Re_w given in the tables.

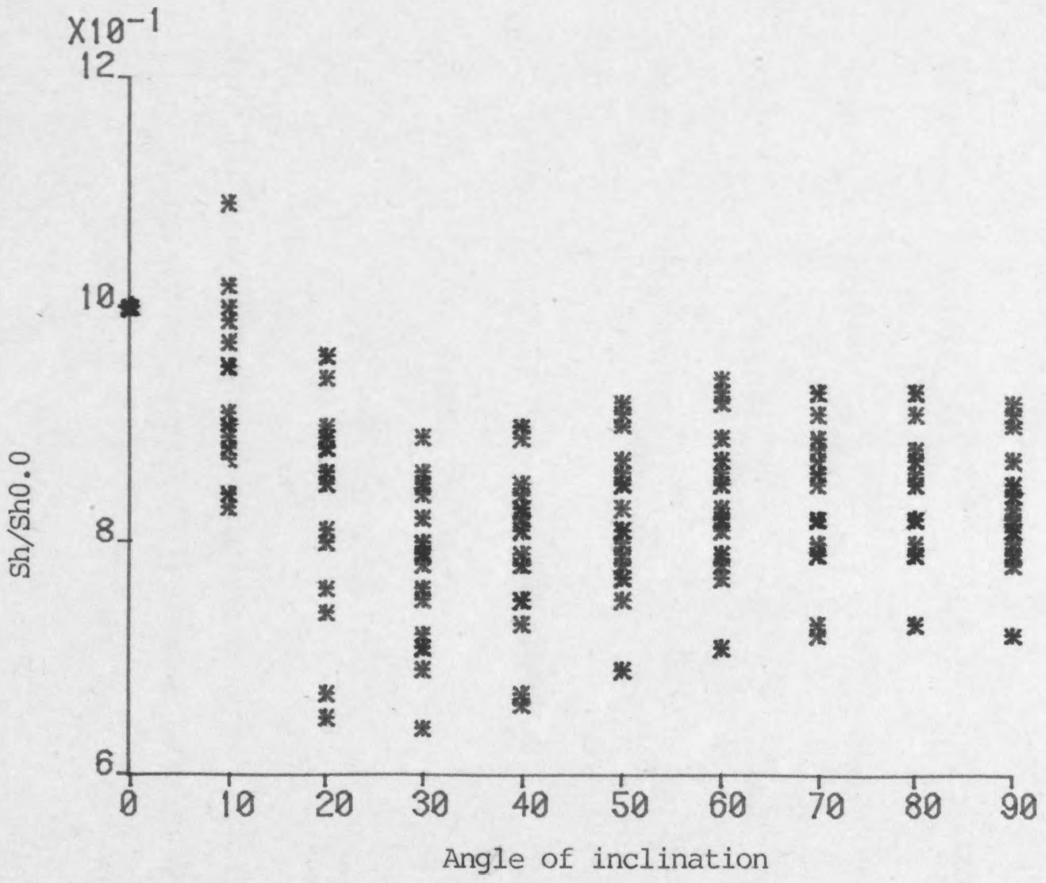


Figure 6.1 Variation of Sherwood number ratio with angle of inclination

angles of inclination were fitted into them and the constants of the correlations were found.

Tables 6.2 and 6.3 give a Type 1 correlation of heat and mass transfer in Convective flow regimes. The range of dimensionless groups are also given.

Tables 6.4 and 6.5 are similar to 6.2 and 6.3, respectively, and give a Type 2 correlations. The validity of the formulae are within the range of GrT, GrXW and Asp, given in the tables.

Angle of Inclination (°)	Gr _T	Gr _{XW}	Asp
40.0	0.1565	0.313	0.961
50.0	0.1389	0.324	0.972
60.0	0.1526	0.318	0.920
70.0	0.1446	0.322	0.924
80.0	0.1524	0.316	0.926
90.0	0.1505	0.308	0.922

Table 6.2 Heat transfer correlations in a rectangular cavity with different angles of inclination (Type 1)

Angle of Inclination	Nu _{cond-conv, lat}			
0.0	0.1623	Gr _{com} ^{0.303}	Bz ^{0.992}	Asp ^{0.043}
10.0	0.3042	Gr _{com} ^{0.249}	Bz ^{1.017}	Asp ^{-0.054}
20.0	0.5569	Gr _{com} ^{0.219}	Bz ^{1.056}	Asp ^{-0.359}
30.0	0.2823	Gr _{com} ^{0.279}	Bz ^{0.863}	Asp ^{-0.200}
40.0	0.1569	Gr _{com} ^{0.313}	Bz ^{0.961}	Asp ^{-0.138}
50.0	0.1389	Gr _{com} ^{0.324}	Bz ^{0.922}	Asp ^{-0.082}
60.0	0.1526	Gr _{com} ^{0.318}	Bz ^{0.920}	Asp ^{-0.089}
70.0	0.1446	Gr _{com} ^{0.320}	Bz ^{0.924}	Asp ^{-0.063}
80.0	0.1514	Gr _{com} ^{0.316}	Bz ^{0.926}	Asp ^{-0.065}
90.0	0.1555	Gr _{com} ^{0.309}	Bz ^{0.992}	Asp ^{-0.114}

where: $0.5504E 04 \leq Gr_{com} \leq 0.3463E 06$

$3.083 \leq Bz \leq 10.93$

$3.0 \leq Asp \leq 18.0$

Table 6.2 Heat transfer correlations in a rectangular cavity with different angles of inclination (Type 1)

Angle of Inclination	Sh			
0.0	0.1506	$Gr_{com}^{0.267}$	$Bz^{0.162}$	$Asp^{-0.072}$
10.0	0.3033	$Gr_{com}^{0.208}$	$Bz^{0.185}$	$Asp^{-0.181}$
20.0	0.5827	$Gr_{com}^{0.175}$	$Bz^{0.233}$	$Asp^{-0.502}$
30.0	0.2762	$Gr_{com}^{0.239}$	$Bz^{0.037}$	$Asp^{-0.326}$
40.0	0.1539	$Gr_{com}^{0.273}$	$Bz^{0.134}$	$Asp^{-0.264}$
50.0	0.1367	$Gr_{com}^{0.284}$	$Bz^{0.092}$	$Asp^{-0.206}$
60.0	0.1493	$Gr_{com}^{0.278}$	$Bz^{0.093}$	$Asp^{-0.214}$
70.0	0.1404	$Gr_{com}^{0.280}$	$Bz^{0.097}$	$Asp^{-0.185}$
80.0	0.1469	$Gr_{com}^{0.276}$	$Bz^{0.100}$	$Asp^{-0.190}$
90.0	0.1507	$Gr_{com}^{0.277}$	$Bz^{0.034}$	$Asp^{-0.190}$

where: $0.5504E 04 \leq Gr_{com} \leq 0.3463E 06$

$3.083 \leq Bz \leq 10.93$

$3.0 \leq Asp \leq 18.0$

Table 6.3 Mass transfer correlations in a rectangular cavity with different angles of inclination (Type 1)

Angle of Inclination	$Nu_{cond-conv, lat}$		
0.0	2.0410 $GrT^{-0.679}$	$GrXW^{0.984}$	$Asp^{0.049}$
10.0	3.9157 $GrT^{-0.740}$	$GrXW^{0.991}$	$Asp^{-0.046}$
20.0	7.5547 $GrT^{-0.795}$	$GrXW^{1.015}$	$Asp^{-0.352}$
30.0	2.5537 $GrT^{-0.580}$	$GrXW^{0.861}$	$Asp^{-0.193}$
40.0	1.8319 $GrT^{-0.645}$	$GrXW^{0.960}$	$Asp^{-0.131}$
50.0	1.4864 $GrT^{-0.602}$	$GrXW^{0.928}$	$Asp^{-0.075}$
60.0	1.6189 $GrT^{-0.604}$	$GrXW^{0.925}$	$Asp^{-0.081}$
70.0	1.5516 $GrT^{-0.607}$	$GrXW^{0.929}$	$Asp^{-0.055}$
80.0	1.6262 $GrT^{-0.611}$	$GrXW^{0.929}$	$Asp^{-0.058}$
90.0	1.9572 $GrT^{-0.676}$	$GrXW^{0.988}$	$Asp^{-0.105}$

where: $0.4368E 04 \leq GrT \leq 0.2755E 06$

$0.1418E 04 \leq GrXW \leq 0.9336E 05$

$3.0 \leq Asp \leq 18.0$

Table 6.4 Heat transfer correlations in a rectangular cavity with different angles of inclination (Type 2)

Angle of Inclination	Sh		
0.0	0.2621 GrT ^{0.042}	GrXW ^{0.223}	Asp ^{-0.074}
10.0	0.5369 GrT ^{-0.020}	GrXW ^{0.227}	Asp ^{-0.182}
20.0	1.1450 GrT ^{-0.087}	GrXW ^{0.260}	Asp ^{-0.505}
30.0	0.3493 GrT ^{0.135}	GrXW ^{0.103}	Asp ^{-0.328}
40.0	0.2497 GrT ^{0.071}	GrXW ^{0.200}	Asp ^{-0.266}
50.0	0.2020 GrT ^{0.117}	GrXW ^{0.166}	Asp ^{-0.208}
60.0	0.2202 GrT ^{0.112}	GrXW ^{0.165}	Asp ^{-0.215}
70.0	0.2095 GrT ^{0.109}	GrXW ^{0.170}	Asp ^{-0.187}
80.0	0.2203 GrT ^{0.104}	GrXW ^{0.171}	Asp ^{-0.192}
90.0	0.1935 GrT ^{0.151}	GrXW ^{0.126}	Asp ^{-0.193}

where: $0.4368E 04 \leq GrT \leq 0.2755E 06$

$0.1418E 04 \leq GrXW \leq 0.9336E 05$

$3.0 \leq Asp \leq 18.0$

Table 6.5 Mass transfer correlations in a rectangular cavity with different angles of inclination (Type 2)

7. SOLAR STILLS

7.1 BASIC OPERATION

Basically a solar still is a "transparent cover-absorber liner" system in which the sun's radiation is transmitted through the cover and absorbed in the liner. The energy absorbed is then consumed for heating the saline water or sea water (which stays above and next to the liner) to a temperature above that of the cover. Due to the temperature difference between the water and the cover, water molecules evaporate from the surface of the water, diffuse through the humid air layer and condense on the glass. Simultaneously some heat is also transferred in the same direction.

The aforementioned process can be performed in many different geometrical situations. Some of the most popular kinds of solar stills are as follows.

7.2 ROOF-TYPE STILLS

This type of still is historically the oldest type of still and has been in use for a very long time [38]. It consists of a tightly closed transparent cover in the form of a roof, made generally of glass. Sea water or saline water is contained in a black surfaced horizontal basin or tray. Figure 7.1 shows a cross-sectional view of one of the latest Australian design [68] of this type of still.

The conventional roof type still has the advantages of simplicity, reliability and absence of power requirement, but has the disadvantages of a large area requirement per

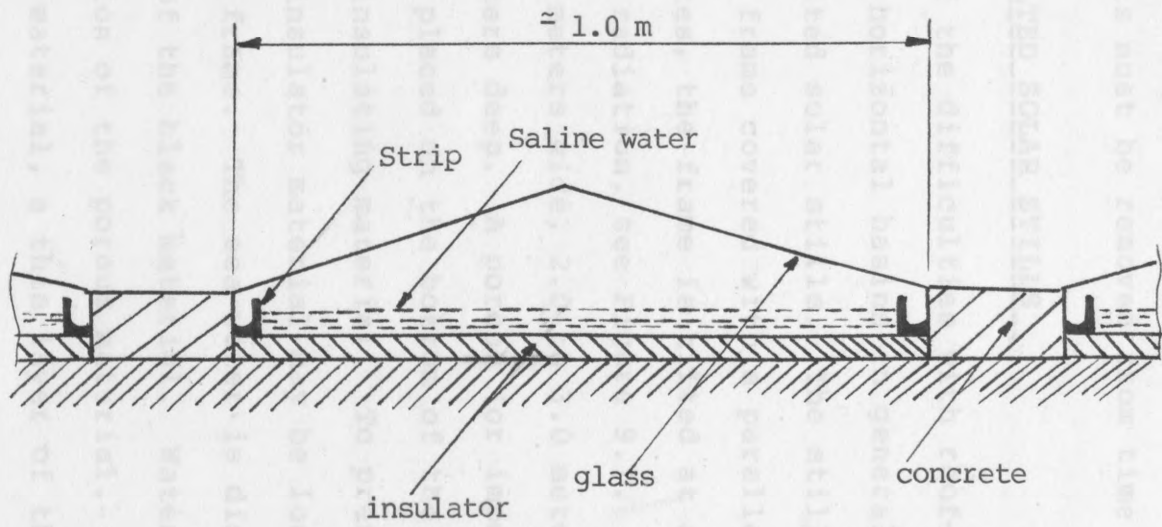


Figure 7.1 Cross section of a roof type solar still mounted on the ground

unit of water distilled and a relatively high capital cost. A serious difficulty in operating them appears to be the problem of deposits of light colored precipitate which change the black color of the liner to grey or even white [39]. This causes a considerable decrease in water yield. Such deposits must be removed from time to time.

7.3 FLAT TILTED SOLAR STILLS

Most of the difficulties with roof-type stills, and stills with horizontal basins in general, are avoided in the flat tilted solar stills. The still consists of a rigid, flat frame covered with a parallel glass. As its name indicates, the frame is tilted at an angle to receive the maximum radiation, see Figure 9.1. The frame may be 1.0 to 1.30 meters wide, 2.0 to 3.0 meters long and 5.0 to 7.5 centimeters deep. A porous (or impermeable), black material is placed on the bottom of the still over a waterproof insulating material. To prevent heat loss, an additional insulator material may be located outside and beneath the frame. The sea water is distributed at the upper edge of the black material. Water is fed by the wicking action of the porous material. (In the case of an impermeable material, a thin layer of the saline water can be adjusted to flow over the black surface.).

Due to the advantages of higher productivity and lower capital cost, compared with roof-type, the flat tilted still has been under more attention in recent time. One of the important features of the flat tilted still is its flexibility, i.e., it can be extended to a "multiple-effect" still. Consequently this type of still

was chosen to be studied in this part of the present work. As it takes the shape of a rectangular cavity, the correlation of heat and mass transfer obtained in Part-1 can be applied to this study.

7.4 MULTIPLE EFFECT SOLAR STILLS

A multiple-effect solar still uses sunlight to provide the heat of evaporation in the first cell. Then the heat of condensation from the first cell is used to provide the heat of evaporation in the second cell, and so on. The condenser of the last cell can be cooled with water or air.

A few experiments dealing with multiple effect solar stills, (Telkes [40-43] and Dunkle[18]), show that there are no advantages to this type of still unless the costs associated with each succeeding effect are less than the cost of an equivalent area of a single effect solar still. Therefore it is necessary that theoretical work is done in order to assess the process for any possible improvements. However, this can be done only after a successful theoretical investigation into a single effect solar still.

The total solar energy incidence at a given locality

8. SOLAR RADIATION

Solar energy is the driving force of solar stills and the first subject to be considered is the availability of this energy. The object of this section therefore, is to examine the amount of radiation received by a tilted panel with different angles of inclination and orientation, in different hours of a day and in different days of a year.

8.1 SOLAR RADIATION REACHING THE EARTH

The average solar radiation on a surface outside the atmosphere and perpendicular to the sun's rays (Extraterrestrial Radiation) is about 1350 W/M². While passing through the atmosphere, this radiation can be:

- a) absorbed in the atmosphere;
- b) scattered and returned back in to space;
- c) scattered but reaching the earth;
- d) unchanged and reaching the earth.

Absorption is due to the upper atmospheric zone and water vapour near the surface, while radiation scattering is due to interception by air molecules, water molecules and dust particles.

The total amount of radiation, averaged over the whole solar spectrum, for the earth is about 23% of the extraterrestrial radiation [44]. This is only an approximation. The actual amount which reaches a particular location on the surface is dependent on many factors: latitude, time, local atmospheric differences (clouds and dust) etc.. Moon [45] has presented an analysis of some of these.

8.2 DIRECT AND DIFFUSE RADIATION

The total solar energy incidence at a given locality can be considered to be made up of direct and diffuse radiation. The direct radiation is received solely along the Sun-Earth direction whilst the diffuse radiation, which is the result of scattering, comes from the entire sky dome. Direct and diffuse radiation have quite distinctive features (e.g. different angles of incidence) and it is often necessary to determine the proportion of each of them in the total amount of radiation received by a horizontal surface during a period of time. The ratio of direct to diffuse radiation varies with prevailing conditions but is typically high for clear atmospheric conditions and low for overcast skies, high humidity and atmospheric pollution.

One of the pioneering investigations which produced empirical correlations of total and diffuse radiation on a horizontal surface is the work of Liu and Jordan[46]. Their work has been the basis of most other investigations since 1960. Liu and Jordan produced a number of graphs which give (on an hourly, daily and monthly basis) the ratio of diffuse to total radiation against the ratio of total to extraterrestrial radiation. A three part formula which resulted from a study of these graphs (undertaken in the present work) may be expressed as follows:

$$\text{for } 0.05 < Q_t/Q_e < 0.28: \quad Q_d/Q_t = -0.87(Q_t/Q_e) + 1.04 \quad (8.1)$$

$$\text{for } 0.28 < Q_t/Q_e < 0.75: \quad Q_d/Q_t = -1.32(Q_t/Q_e) + 1.17 \quad (8.2)$$

$$\text{for } 0.75 < Q_t/Q_e < 1.00: \quad Q_d/Q_t = 0.18 \quad (8.3)$$

where;

Q_e = daily extraterrestrial radiation on a horizontal

surface

Q_t = daily total radiation on a horizontal surface

Q_d = daily diffuse radiation on a horizontal surface

For an hourly basis case the correlation presented by Liu and Jordan is more applicable to clear days; it gives increasingly uncertain results as total daily radiation decreases. However, more recently, Bugler [47] has suggested some empirical correlations of more general use. These correlations, which will be used in the present work, are as follows:

$$\text{for } 0.0 < H_t/H_{cl} < 0.4 : H_d/H_t = 0.94 \quad (8.4)$$

$$\text{for } 0.4 < H_t/H_{cl} < 1.0 : H_d/H_t = [1.29 - 1.19(H_t/H_{cl})] / [1.0 - 0.334(H_t/H_{cl})] \quad (8.5)$$

where:

H_t = hourly total radiation on a horizontal surface

H_{cl} = hourly total radiation on a horizontal surface for clear sky condition

H_d = hourly diffuse radiation on a horizontal surface

8.3 GEOMETRY OF DIRECT AND DIFFUSE RADIATION

As the amount of energy received by a tilted surface is a strong function of the angle of incidence of radiation, the geometry of the direct and diffuse radiation has to be studied in more detail.

8.3.1 DIRECT RADIATION

The angle of incidence of the direct radiation on a plane of any particular orientation relative to the earth at any time can be determined in terms of several angles.

These angles are [48]:

Φ = latitude (north positive);

δ = declination (i.e., the angular position of the sun at solar noon with respect to the plane of the equator);

α = the angle between the horizontal and the plane (positive towards south);

δ = the surface azimuth angle, that is, the deviation of the normal to the surface from the local meridian (the zero point being due south, east positive and west negative);

ω = hour angle, solar noon being zero, and each hour equaling 15 degrees of longitude with morning positive and afternoons negative;

θ = the angle of incidence of direct radiation, with the respect to the normal to the plane.

The declination, δ , can be found from the approximate equation of Cooper [49]:

$$\delta = 23.45 \sin[360(284+n)/365] \quad (8.6)$$

where n is the day of the year. A more accurate calculation given by the author (Appendix [8]) gives:

$$\delta = \sin^{-1} [\sin(23.45) \cdot \sin(360(284+n)/365)] \quad (8.7)$$

The relationship between θ and the other angles is given:

$$\begin{aligned} \cos\theta = & \sin\delta \sin\phi \cos\alpha - \sin\delta \cos\phi \sin\alpha \cos\delta \\ & + \cos\delta \cos\phi \cos\alpha \cos\omega \\ & + \cos\delta \sin\phi \sin\alpha \cos\delta \cos\omega \\ & + \cos\delta \sin\alpha \sin\delta \sin\omega \end{aligned} \quad (8.8)$$

For a horizontal surface, $\cos\theta_h$, is obtained by inserting $\theta=0.0$ in the above equation:

$$\cos\theta_h = \sin\delta \sin\phi + \cos\delta \cos\phi \cos\omega \quad (8.9)$$

8.3.2 DIFFUSE RADIATION

Although direct radiation and its geometry is well

understood there is no completely satisfactory analysis of diffuse radiation, especially with respect to its apparent angle of incidence on a surface. For overcast skies, the diffuse radiation received is substantially independent of the angular position of the sun as would be intuitively expected. An "isotropic" assumption is satisfactory under these conditions, i.e., a uniform intensity of the diffuse radiation distributed over the sky dome.

On clear days the apparent direction of diffuse radiation is weighted towards the position of the sun, hence the assumption of isotropic distribution is not accurate. However, for practical use the isotropic assumption can be employed without serious errors as Norris [50] has proved in his investigation.

For an inclined surface, assuming isotropic diffuse radiation, Cooper [26] suggested:

$$\phi = \cos[45(1.0 + \cos\alpha)/(180.0 - \alpha)] \quad (8.10)$$

where:

ϕ = the apparent angle of incidence

8.4 RADIATION ON A HORIZONTAL AND ON A TILTED SURFACE

It is evident that the solar energy received at a given location will change with the inclination and orientation of the irradiated surface. However it would not be practical to measure the amount of insolation for all possible inclinations and orientations. For this reason measurements (or estimations) are only taken on a horizontal surface. Data for other positions of the surface are, therefore, calculated by conversion of the data for the horizontal surface.

Converting the data obtained for a horizontal position to that of a tilted position is mainly a practice of geometrical conversion of the corresponding angle of incidence. For this purpose it is necessary to consider a short period of time during which the angle of incidence, as well as the amount of radiation components (direct and diffuse), remains constant (or, to be more accurate, can be assumed to be constant.). Usually a period of one hour is taken.

The procedure for conversion of radiation data on a horizontal surface to that of an inclined surface can be stated as follows:

- 1) Daily total radiation on a horizontal surface is estimated;
- 2) Hourly total radiation on a horizontal surface is derived from total daily data.;
- 3) Components of hourly radiation, namely direct and diffuse radiation, are determined and are separately converted to values related to the tilted surface.
- 4) Daily, monthly and annual insolation on a tilted surface is obtained by integration of tilted hourly data over the period in question.

The above procedure will be applied in the following sections.

8.5 ESTIMATION OF DAILY TOTAL RADIATION ON A HORIZONTAL SURFACE

For purposes of design and evaluation of solar stills, it is often necessary to predict the availability of solar energy on a horizontal surface. Such predictions can be based on measurements of radiation from the location in

question or related meteorological data.

If radiation data are available, they can be used in several ways. One is to use the past daily data in their original forms, estimate the performance of a solar still under those past conditions, and on this basis project future performance. Alternatively the radiation data can be reduced to a more manageable form by statistical methods. The resulting time distribution is then used in the calculations. This method is especially suitable when the sequential characteristics of daily radiation is intended to be accounted for in the calculations. (e.g. the statistical method of modelling the insolation sequences by Brinkworth [54].).

Previously recorded radiation data is the best source of information for predicting daily radiation figures. But these values are generally not available for remote areas and many places in under developed countries. For such places empirical correlations can be used to estimate daily global insolation from related meteorological data such as measured hours of daily sunshine. The empirical correlation which is used in the present work is in the form [51]:

$$Q_t = Q_e [a + b (t_s/T_s)] \quad (8.11)$$

where:

a, b = constants;

t_s = actual daily duration of sunshine;

T_s = maximum possible daily duration of sunshine in the same day.

Values of Q_e, a, b, t_s, T_s are obtained as follows.

8.5.1 DAILY EXTRATERRESTRIAL RADIATION

In Equation (8.11), Daily extraterrestrial radiation, Q_e , is a function of latitude and time of year. It can be obtained for any day during a year from the following equation [52]:

$$Q_e = I_{sc} \frac{24}{\pi} [(1.0 + 0.033 \cos(360 n/365)) \cdot (\cos\phi \cos\delta \sin\omega + 2 \pi w / 360 \sin\phi \sin\delta)] \quad (8.12)$$

where I_{sc} = solar constant per hour, and w = sunrise hour angle. Other variables are the same angles defined in section 8.2 (see also list of Nomenclatures).

8.5.2 SUNSHINE HOURS AS PERCENTAGE OF MAXIMUM

Data of daily sunshine, t_s , is usually attainable more easily than that of direct measurements of daily radiation. For most places where direct measurement is not taken, t_s is recorded instead. However, for places where even this is not done, there is always a similar location to the place of interest, whose recorded data can be used instead of genuine data. In doing so, some cares must be taken in selecting similar places, i.e., with respect to the type of climates and vegetations as well as latitude.

When the actual duration of sunshine is known, determination of maximum possible duration in the same day can be easily obtained from the calculation. The following equation [52]: can do this task:

$$T_s = 2/15 \cos^{-1}(-\tan\phi \tan\delta) \quad (8.13)$$

The sunshine hours as possible percentage, t_s/T_s , is found by dividing the two values.

8.5.3 CONSTANTS 'a' AND 'b'

The type of climate and vegetation is the main factor for evaluating constants, a and b , for the use in Equation (8.11). Löff et al [53] has developed a set of values for a and b , related to the type of climate and vegetation. To use these constants, one needs to find the most similar type of the climate and vegetation to that of the place in question, from those stated by Löff et al. Then the corresponding values of a and b will be known.

Table 8.1 gives some of the values of a and b for different types of climates and vegetation, derived from the table produced by Löff et al. The symbols in columns 1 and 2 indicate the type of climate [69] and vegetation [52], respectively, where: Climate types are:

BS -- Steppe or semiarid climate;

BW -- Desert or arid climate;

Vegetation types are:

E -- Needleleaf evergreen trees;

GDsp-- Grass and other herbaceous plants; broadleaf deciduous, shrubforms, minimum height 1 meter, growth singly or in groups or patches;

Dsi -- Broadleaf deciduous, shrubform, minimum height 1 meter plants sufficiently far apart that they frequently do not touch;

Bzi -- Broadleaf evergreen, shrubform, minimum height 1 meter, growth singly or in groups or patches;

Dsp -- Broadleaf deciduous, shrubform, minimum height 1 meter, growth singly or in groups or patches.

8.5 HOURLY RADIATION ON A HORIZONTAL SURFACE

Location	Climate	Veg.	Sunshine hours in Percentage of Possible		a	b
			Range	Ave.		
Albuquerque, New Mexico	BS-BW	E	68-85	78	.41	.37
Brownsville, Texas	BS	GDsp	47-80	62	.35	.31
El paso, Texas	BW	Dsi	78-88	84	.54	.20
Ely, Nevada	BW	Bzi	61-89	77	.54	.18
Tamanrasset, Algeria	BW	Dsp	76-88	83	.30	.43

Table 8.1 Climate Constants for use in Equation (8.11)

An illustration of Equation (8.14) for an intermittency factor of $V=0.1$ is shown in Figure 8.11. The profile of a clear sky condition is also given for the same day. (c) about 2170.0 KJ/m²-day.

8.6 HOURLY RADIATION ON A HORIZONTAL SURFACE

It is normally assumed that an analogue for total solar radiation on a horizontal surface is given by a sine function with modification for the effect of clouds. The function, given by Close [25], is described as follow:

$$H_t = Q_t \pi / (2.T_s) \sin(\pi.t/T_s) + \quad (8.14) \\ Q_t \pi / (2.T_s) \sin(\pi.t/T_s) \cos(V.\pi.t/T_s)$$

where:

t is the time and designates hours after sunrise;
the factor V is to simulate the effect of intermittent cloud cover. (Other variables are the same given in section 8.2).

The first term in the right hand side of the equation is a sine distribution of total daily radiation, Q_t , so that:

$$Q_t = \int_{t=0.0}^{t=T_s} Q_t \pi / (2.T_s) \sin(\pi.t/T_s) \quad (8.15)$$

The second term in the right hand side is a symmetric variable which introduces some fluctuations in the hourly radiation. However, its integration over the whole day is zero:

$$\int_{t=0.0}^{t=T_s} Q_t \pi / (2.T_s) \sin(\pi.t/T_s) \cos(V.\pi.t/T_s) = 0.0 \quad (8.16)$$

(for $V=2n_i+1$; where n_i is an integer value and: $n_i \geq 1$)

An illustration of Equation (8.14) for an intermittency factor of $V=31$, a 12 hour day and a total radiation of 7640.0 KJ/m²-day is shown in Figure 8.1. The profile of a clear sky condition is also given for the same day. (Q_{cl} about 9170.0 KJ/m²-day).

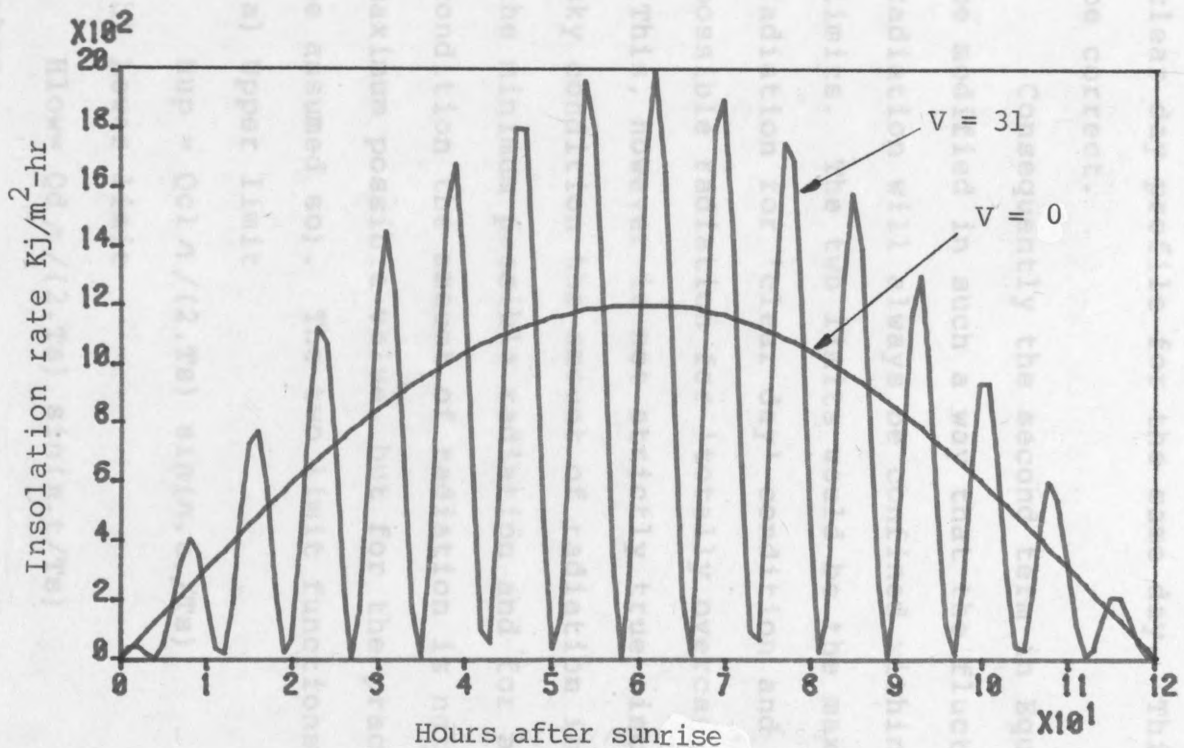


Figure 8.1 Insolation profile for the intermittency function with V equal to 0 and 31 (Equation 8.14)

One of the disadvantages of the aforementioned formula is, as can be seen from Figure 8.1, it gives a minimum radiation equal to zero for a number of times during a day (a number equal to V). It is evident that the insolation should not fall to zero as this implies zero diffuse radiation. Another difficulty with Equation (8.14) is that it gives a peak radiation value about twice that for a clear day profile for the same day. This, again, can not be correct.

Consequently the second term in Equation (8.14) has to be modified in such a way that the fluctuation of hourly radiation will always be confined within two appropriate limits. The two limits would be the maximum possible radiation for 'clear day' condition and the minimum possible radiation for 'totally overcast' condition. (This, however is not strictly true since for an overcast sky condition the amount of radiation is not necessarily the minimum possible radiation and for a clear sky condition the amount of radiation is not necessarily the maximum possible value, but for the practical use this can be assumed so). The two limit functions are given as:

a) Upper limit

$$H_{up} = Q_{cl} \pi / (2.T_s) \sin(\pi.t./T_s) \quad (8.17)$$

b) Lower limit

$$H_{low} = Q_d \pi / (2.T_s) \sin(\pi.t./T_s) \quad (8.18)$$

where:

H_{up} and H_{low} are upper and lower hourly limits respectively;

Q_d is the minimum amount of daily diffuse radiation and can be taken from equations (8.1)-(8.3);

Q_{cl} is the daily total radiation for a clear sky condition and can be obtained from Equation (8.11) by inserting a value of $t_s/T_s=1.0$ in that equation.

The defined limits can then be applied to Equation (8.14) in two different alternative ways:

$$H_t = Q_t \cdot \pi / (2 \cdot T_s) \sin(\pi \cdot t / T_s) + [Q_{cl} \cdot \pi / (2 \cdot T_s) - Q_t \cdot \pi / (2 \cdot T_s)] \sin(\pi \cdot t / T_s) \cos(\pi \cdot t \cdot V / T_s) \quad (8.19)$$

$$H_t = Q_t \cdot \pi / (2 \cdot T_s) \sin(\pi \cdot t / T_s) + [Q_t \cdot \pi / (2 \cdot T_s) - Q_d \cdot \pi / (2 \cdot T_s)] \sin(\pi \cdot t / T_s) \cos(\pi \cdot t \cdot V / T_s) \quad (8.20)$$

The difference between Equations (8.19) and (8.20) is in the amplitude of the fluctuation terms (the second terms in the right hand sides). In Equation (8.9) the amplitude is $[Q_{cl} \cdot \pi / (2 \cdot T_s) - Q_t \cdot \pi / (2 \cdot T_s)]$ whereas in Equation (8.20) it is: $[Q_t \cdot \pi / (2 \cdot T_s) - Q_d \cdot \pi / (2 \cdot T_s)]$. The application of these equations depends on the 'day cloudiness condition', i.e. Q_t/Q_{cl} . In the days with light clouds (high Q_t/Q_{cl}) the possibility of clear sky periods is greater than totally overcast periods and, hence, Equation (8.19) is applied. Whereas for densely clouded days (low Q_t/Q_{cl}) the Equation (8.20) is applied.

Figures 8.2 and 8.3 show the applications of Equations (8.19) and (8.20) respectively. In Figure 8.2 the ratio of Q_t/Q_{cl} is high ($Q_{cl}=9167.0$ KJ/m²-day, $Q_t=7640.0$ KJ/m²-day and $Q_t/Q_{cl}=0.83$) and hence, as would be expected, the profile is weighted toward the upper limit curve. With low ratio of Q_t/Q_{cl} ($Q_{cl}=9167.0$ KJ/m²-day, $Q_t=3055.0$ KJ/m²-day and $Q_t/Q_{cl}=0.33$), the opposite behaviour is shown in Figure 8.3, as the profile is nearer to the lower limit.

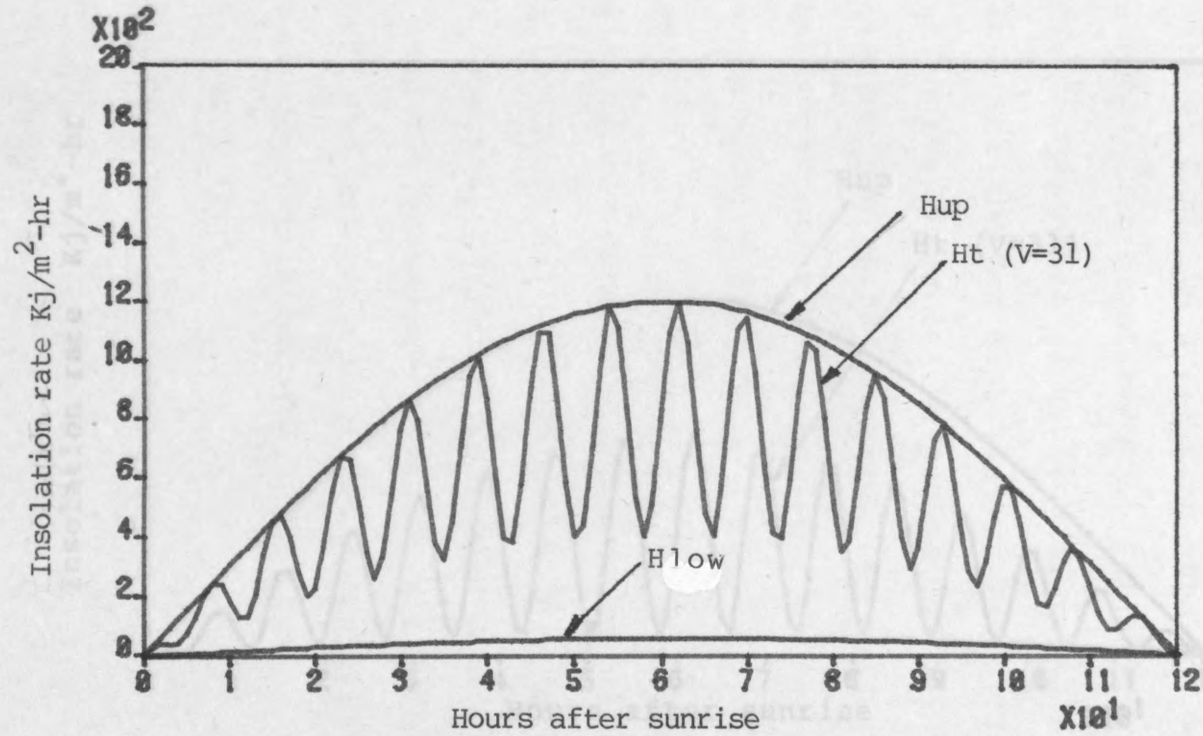


Figure 8.2 Insolation profile for a day with light cloud ($Q_t/Q_{cl}=0.83$; Equ. 8.19)

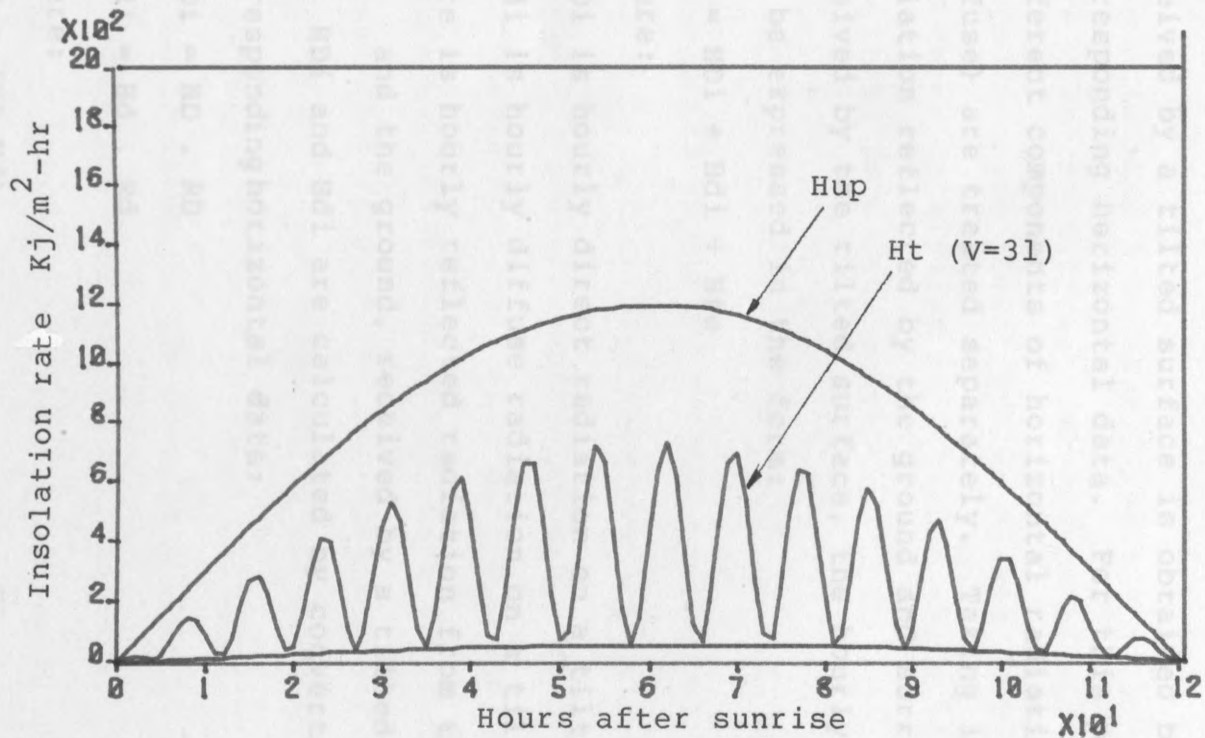


Figure 8.3 Insolation profile for a densely clouded day ($Q_t/Q_{cl}=0.33$; Equ. 8.20)

Comparing Figure 8.2 with 8.1 shows the improvement achieved by applying the equations suggested in the present work (8.19 or 8.20) in place of Equation (8.14) suggested by Close [54].

8.7 HOURLY RADIATION ON A TILTED SURFACE

As was noted (section 8.4) the hourly radiation received by a tilted surface is obtained by converting the corresponding horizontal data. For this purpose the two different components of horizontal radiation (direct and diffuse) are treated separately. Taking into account the radiation reflected by the ground and surroundings and received by the tilted surface, the hourly tilted radiation can be expressed in the form:

$$H_i = H_{Di} + H_{di} + H_{re} \quad (8.21)$$

where:

H_{Di} is hourly direct radiation on a tilted surface;

H_{di} is hourly diffuse radiation on a tilted surface;

H_{re} is hourly reflected radiation from the surroundings and the ground, received by a tilted surface.

H_{Di} and H_{di} are calculated by converting the corresponding horizontal data:

$$H_{Di} = H_D \cdot R_D \quad (8.22)$$

$$H_{di} = H_d \cdot R_d \quad (8.23)$$

where:

$$H_D = (H_t - H_d) \quad (8.24)$$

$$R_D = \cos\theta / \cos\theta_h \quad (8.25)$$

where:

H_t is defined in Section 8.2 and can be obtained by either direct measurement or from correlations

(8.19)-(8.20);

H_d can be obtained from correlations (8.4)-(8.5);

$\cos\theta$ and $\cos\theta_h$ are defined in section 8.3.1 and

can be calculated from Equations (8.8) and (8.9)

respectively.

H_{re} , in Equation (8.21), is given by Liu and Jordan-
[55]:

$$H_{re} = (H_D + H_d)(1.0 - \cos\alpha) \xi / 2.0 \quad (8.26)$$

where ξ is the diffuse reflectance of the ground and surroundings are "seen" by the tilted surface. Usually [52] ξ is taken at a value of 0.2 when there is no snow and 0.7 when there is a snow cover.

8.8 MONTHLY AND ANNUAL RADIATION ON A TILTED SURFACE

Figures of daily, monthly and annual insolation received by a tilted surface are obtained by following the procedure explained in section 8.4. That is, taking the steps presented in sections 8.5, 8.6 and 8.7 and integrating the tilted hourly data (obtained by application of section 8.7) over the periods in question. A program, named 'SOLAR', was prepared to do the calculations involved (see Appendix[9] for the SOLAR print-out.).

As an example, the program SOLAR was used to predict the insolation received by a tilted surface with different angles of inclination from 0.0 degree to 90.0 degrees with intervals of 10.0 degrees. The orientation angle of the surface is taken to be zero (i.e. towards the south) to receive maximum possible radiation. The locality is near the Persian Gulf and has the following characteristics:

- a) Latitude = 26.0 North;

- b) Climate and Vegetation similar to those indicated by the symbols 'BW' and 'Bzi' in Table 8.1, respectively, i.e., an arid climate with broadleaf evergreen, plants. (Hence the constants are: $a=0.54$ and $b=0.18$);
- c) Sunshine hours in percentage of possible in a range of 76% - 88%. (The figures produced by 'Solar Energy Organization' [56].).

Table 8.2 gives the monthly results as well as the annual figures. It can be seen that the maximum annual radiation belongs to a surface with 10.0 degrees inclination for this particular location.

Unfortunately measured radiation figures from the Persian Gulf are not available and hence the data predicted in Table 8.2 cannot be compared with actual data. Nevertheless the reliability of program SOLAR can be verified by applying it for a nearby place, i.e., Tehran (latitude=35.6 degrees north, $a=0.35$ and $b=0.28$). For Tehran daily radiation data (given clear sky conditions) for a 35.0 degrees tilted surface is available. The measurements were carried out in 1975 [56] and the results are given in Figure 8.4, where the data predicted by SOLAR is also given. A close agreement is observed.

8.9 TRANSMISSION AND ABSORPTION

Radiation received by the transparent cover of a solar still can not be completely utilized as some of the radiation impinging on the cover is reflected, some is absorbed within the cover itself and some transmits through it and enters the still. The latter is the fraction of

Angle of Inclination	0.0	10.0	20.0	30.0	40.0	50.0	60.0	70.0	80.0	90.0
Jan	99.6	115.8	128.6	137.4	142.0	142.4	138.5	130.4	118.3	102.7
Feb	105.7	117.9	126.6	131.4	132.3	129.1	122.1	111.3	97.2	80.2
Mar	146.1	154.9	159.1	158.5	153.0	142.9	128.5	110.2	88.6	64.3
Apr	182.1	183.2	178.8	169.0	154.0	134.4	110.8	83.9	54.9	25.3
May	204.7	197.8	185.0	166.6	143.4	116.3	86.3	55.1	24.7	1.4
Jun	208.7	197.8	180.8	158.5	132.0	102.3	70.9	39.5	11.6	0.2
Jul	214.4	204.8	188.9	167.4	141.3	111.6	79.6	47.1	17.0	0.2
Aug	209.1	206.5	197.7	182.8	162.5	137.3	108.3	76.6	43.7	12.9
Sep	188.8	195.9	197.1	192.3	181.7	165.6	144.4	118.8	89.7	57.8
Oct	157.6	172.6	182.3	186.4	184.9	177.8	165.4	147.9	125.9	100.1
Nov	119.5	137.3	151.0	160.2	164.5	163.8	158.1	147.7	132.8	113.8
Dec	95.4	112.3	125.8	135.5	141.1	142.4	139.5	132.3	121.1	106.2
Annual	1931.7	1997.0	2001.7	1946.1	1832.7	1666.0	1452.3	1200.7	925.5	664.9

Table 8.2 Monthly incident radiation (Kw-hr/m²) on an inclined surface with different angles of inclination (Latitude=26.0 degrees north, Azimuth=0.0)

*

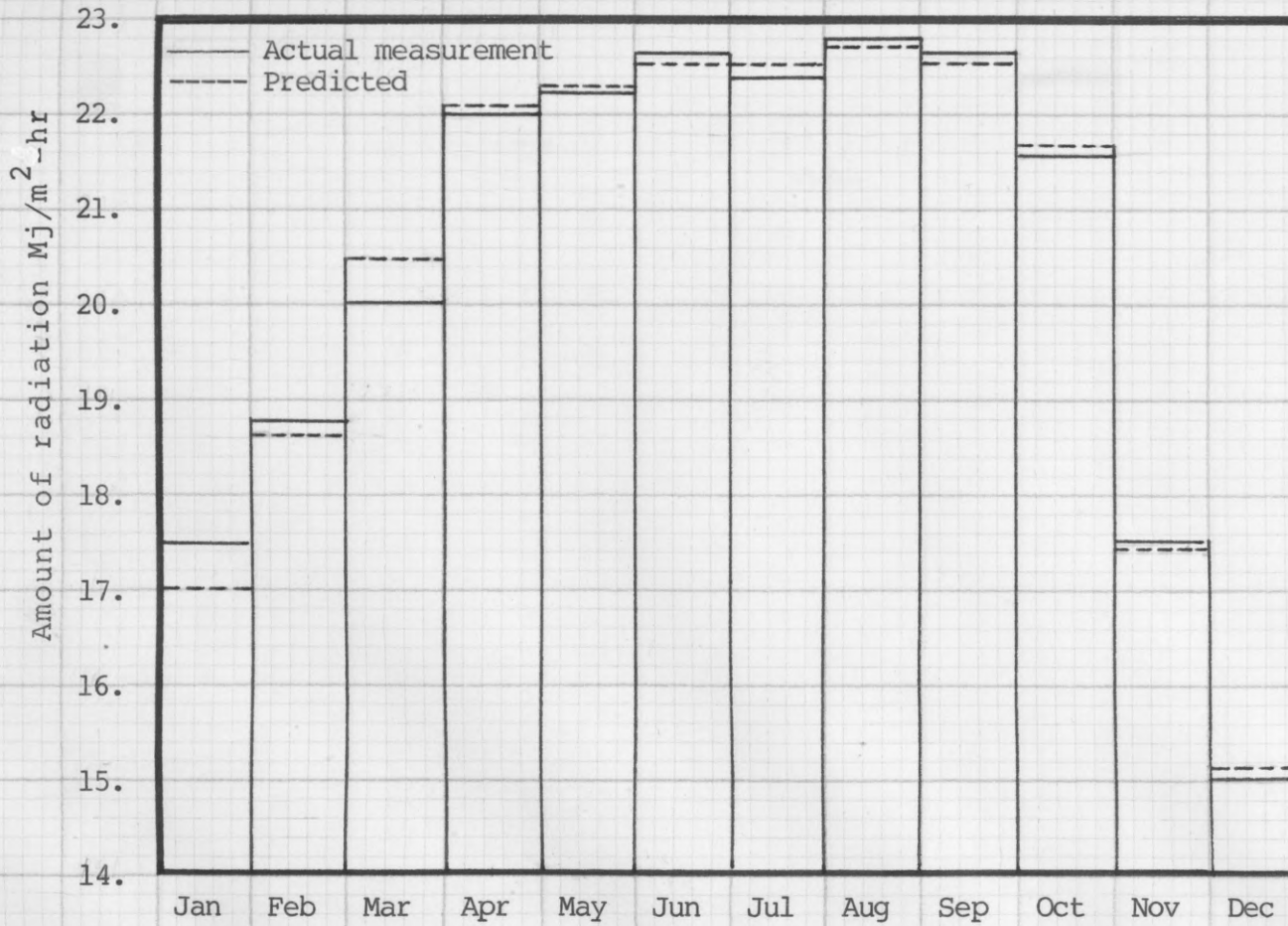


Figure 8.4 Monthly mean of daily radiation in Tehran on clear days (Latitude=35.6 N; Angle of inclination=35.0 deg.; Azimuth angle=0.0)

total incident radiation which actually takes part in the heat and mass transfer process and is of prime importance and must be evaluated. The small portion absorbed in the body of the cover affects the productivity, though indirectly, and therefore needs to be considered aswell.

One of the investigations to determine the aforementioned fractions can be found in Cooper [26] where, for a commercial window glass (usually used in solar stills), of low iron content (14% Fe₂O₃) and thickness of 2.8 mm, transmission and absorption of the radiation were plotted against the incidence angle of radiation, θ . The results derived from the related graphs produced by Cooper, are as follows:

a) Absorption:

$$\text{for } 0.0 \leq (\theta) \leq 80.0 \quad : \text{Abp} = 0.05 \quad (8.27)$$

$$\text{for } (\theta) > 80.0 \quad : \text{Abp} = 0.0 \quad (8.28)$$

b) Transmission:

$$\text{for } (\theta) \leq 40.0 \quad : \text{Trn} = 0.90 (\theta) \quad (8.29)$$

$$\text{for } 40.0 < (\theta) \leq 60.0 \quad : \text{Trn} = 1.00 - 0.0025 (\theta) \quad (8.30)$$

$$\text{for } 60.0 < (\theta) \leq 75.0 \quad : \text{Trn} = 1.45 - 0.01 (\theta) \quad (8.31)$$

$$\text{for } 75.0 < (\theta) \leq 90.0 \quad : \text{Trn} = 4.20 - 0.0466 (\theta) \quad (8.32)$$

where 'Abp' and 'Trn' indicate the percentages of the total radiation absorbed in the glass and transmitted through it, respectively. (Angles of θ are in degrees.).

Appropriate modifications, based on the above information, were made to SOLAR to enable it to predict figures for the insolation transmitted through a tilted glass. Table 8.3 gives the results obtained by reconsidering the example given in section 8.8 using a glass surface with different angles of inclination.

Angle of Inclination →	0.0	10.0	20.0	30.0	40.0	50.0	60.0	70.0	80.0	90.0
Jan	85.7	101.7	113.9	122.3	126.8	127.2	123.7	116.2	104.7	89.0
Feb	92.1	103.9	112.1	116.7	117.6	114.8	108.2	98.0	83.8	66.9
Mar	128.3	136.7	140.6	140.1	135.0	125.5	111.6	93.1	71.5	46.3
Apr	160.4	161.4	157.1	147.8	133.6	114.6	91.1	64.9	36.7	10.3
May	180.3	173.7	161.5	144.1	122.1	95.6	66.9	37.1	10.6	0.3
Jun	183.8	173.1	157.1	136.2	110.7	82.2	52.0	23.9	3.1	0.2
Jul	188.8	179.5	164.5	144.3	119.2	90.6	59.8	29.9	5.6	0.2
Aug	184.2	181.6	173.2	159.1	139.8	115.2	87.0	55.9	26.0	3.2
Sep	166.1	172.8	173.9	169.4	159.3	143.9	122.9	97.2	67.6	36.5
Oct	137.9	152.2	161.4	165.4	164.1	157.5	145.8	128.7	106.5	80.6
Nov	103.2	120.7	133.9	142.5	146.7	146.2	141.0	131.3	116.8	97.8
Dec	81.6	98.5	111.5	120.7	126.0	127.4	124.7	118.1	107.6	92.7
Annual	1692.4	1755.8	1760.6	1708.6	1600.8	1440.6	1234.8	994.6	740.6	523.8

Table 8.3 Monthly radiation (Kw-hr/m²) transmitted through a tilted transparent cover with different angles of inclination (Latitude=26.0 degrees north, Azimuth=0.0)

Comparison between Tables (8.2) and (8.3) shows that when transmitted through a glass a reduction in the total amount of insolation results. However the general distribution of energy with respect to the angle of inclination, is similar in both tables.

For this purpose the components of energy transfer are first introduced (by referring to Figure 3.1) and then related by writing the energy balances for different parts of the still. The equations obtained are then solved numerically for comparison with the reported experimental data.

3.1 ATTENUATION AND DISSIPATION OF SOLAR INCIDENT RADIATION

Solar radiation impinging on the transparent cover of the still suffers reflection at the air-cover interface and absorption within the cover material itself. This is only of the order of 10% (26). As the radiation enters the still, there is little or no absorption by the humid air, since the portion of the radiation vulnerable to water vapour would have been absorbed by the water molecules in the atmosphere before it reaches the ground. Most of the radiation reaching the bottom of the still is absorbed by the liner-drying water, the liner is made of some highly absorbent material.

From that portion of solar radiation which is reflected back by the bottom of the still, some is reflected back by the lower surface of the cover (and the condensed water beneath the cover) and a little escapes out of the still.

From the energy absorbed by the liner, some is

9. SIMULTANEOUS HEAT AND MASS TRANSFER IN A FLAT, TILTED SOLAR STILL

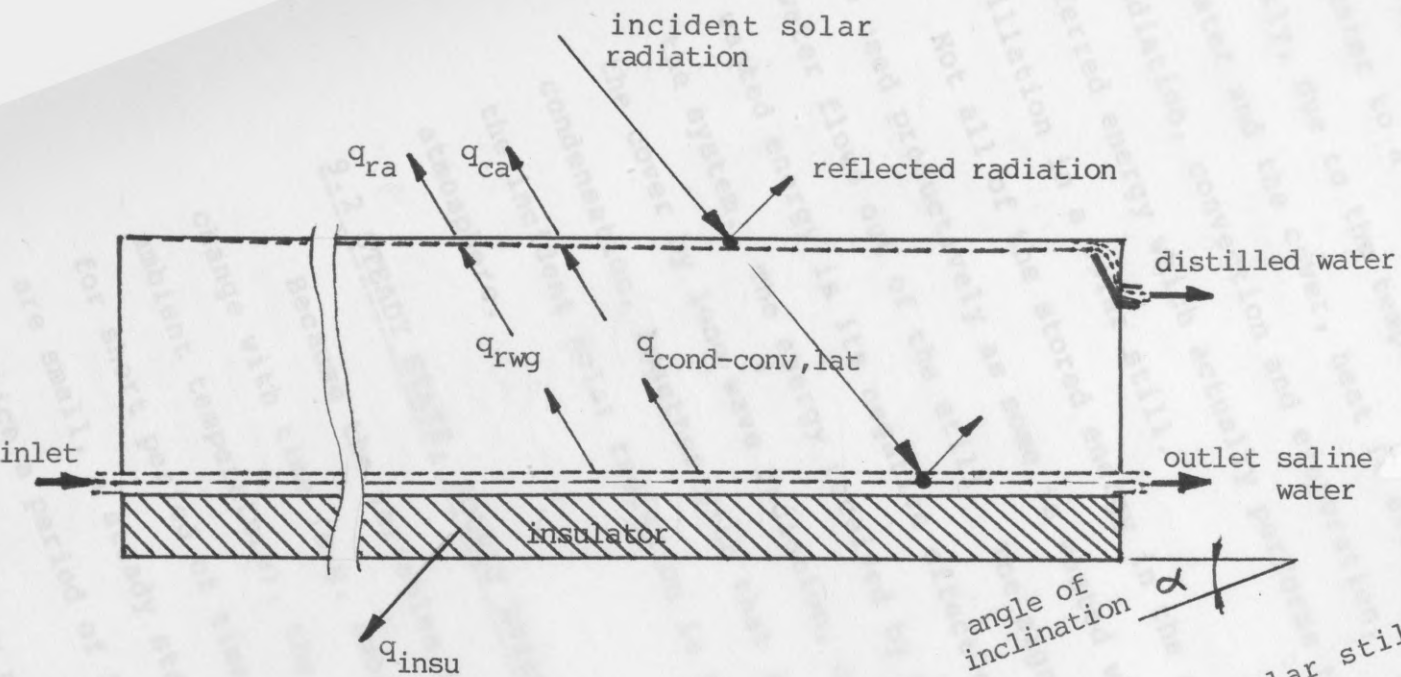
The aim of this chapter is to formulate the model of the process of solar distillation in a tilted solar still. For this purpose the components of energy transfer are first introduced (by referring to Figure 9.1) and then related by writing the energy balances for different parts of the still. The equations obtained are then solved numerically for comparison with the reported experimental data.

9.1 ATTENUATION AND DISSIPATION OF SOLAR INCIDENT RADIATION

Solar radiation impinging on the transparent cover of the still suffers reflection at the air-cover interface and absorption within the cover material itself. This is only of the order of 10% [26]. As the radiation enters the still, there is little or no absorption by the humid air, since the portion of the radiation vulnerable to water vapour would have been absorbed by the water molecules in the atmosphere before it reaches the ground. Most of the radiation reaching the bottom of the still is absorbed by the liner-saline water, (the liner is made of some highly absorbent material).

From that portion of solar radiation which is reflected back by the bottom of the still some is reflected back by the lower surface of the cover (and the condensed water beneath the cover) and a little escapes out of the still.

From the energy collected by the liner, some is



process in a flat tilted solar still

transferred to the saline water and the remainder is conducted out of the still through the bottom and the sides.

The energy transferred to the water, together with that initially absorbed from the incident solar radiation, heats the water to a temperature above that of the cover. Consequently, due to the temperature difference between the saline water and the cover, heat is exchanged through long wave radiation, convection and evaporation. This is the transferred energy which actually performs the process of distillation in a solar still.

Not all of the stored energy in the saline water can be used productively as some is wasted when the saline water flows out of the still. The significance of the wasted energy is its negative effect on the efficiency of the system. The energy received by the lower surface of the cover by long wave radiation, convection and condensation, together with that initially absorbed from the incident solar radiation is then dissipated into the atmosphere.

9.2 STEADY STATE, HOURLY ENERGY BALANCE

Because the variables involved in solar distillation change with time (e.g. amount of solar radiation and ambient temperature), the process is transient. However, for short period of time in which changes of the variables are small, a steady state process can be assumed. In practice a period of 1 hour is used.

9.2.1 COVER ENERGY BALANCE

By referring to Figure 9.1 conservation of energy for

the cover can be written as:

$$(q_{\text{cond-conv, lat}} + q_{\text{rwg}}) \cdot A_g + H_i \cdot \text{Abp} \cdot A_g = (q_{\text{ra}} + q_{\text{ca}}) \cdot A_g \quad (9.1)$$

where A_g is the area of glass.

The energy components appearing in the above equation are defined as follows:

- a) Simultaneous heat and mass exchange between cover and saline water, $q_{\text{cond-conv, lat}}$, is obtained as a function of cover temperature, water temperature and inclination angle of the still:

$$q_{\text{cond-conv, lat}} = A_g \cdot K_{\text{mix}} \cdot \text{Nu}_{\text{cond-conv, lat}} (T_g - T_w) / \text{Width} \quad (9.2)$$

where:

K_{mix} is the thermal conductivity of humid air within the still;

$\text{Nu}_{\text{cond-conv, lat}}$ is Nusselt number. The correlations presented in PART 1 provide the pertinent equations;

T_g and T_w are cover temperature and saline temperature, respectively;

'Width' is the distance between the cover and the bottom of the still.

- b) Heat exchange by long wave radiation between the cover and the bottom of the still, q_{rwg} , depends on the corresponding temperatures and the shape of still envelope:

$$q_{\text{rwg}} = F_{1-2} \cdot \sigma \cdot (T_w^4 - T_g^4) \quad (9.3)$$

Assuming a tilted flat still can be approximated as one gray surface enclosing another, the shape factor, F_{1-2} ,

for two parallel gray radiant sources connected by re-radiating side walls is defined as:

$$F_{1-2} = 1 / (1/e_g + 1/e_w - 1) \quad (9.4)$$

where in equations (9.3) and (9.4);

σ = Stefan-Boltzmann constant;

e_g = emissivity factor of the glass;

e_w = emissivity factor of the saline-liner.

c) Hourly total radiation and its absorption by the cover, $H_i.A_{bp}$, per unit area of the cover, can be obtained through application of program SOLAR.

d) Heat transfer from the transparent cover to the atmosphere by radiation, q_{ra} :

$$q_{ra} = \sigma \cdot e_g \cdot (T_g^4 - T_{sky}^4) \quad (9.5)$$

where T_{sky} is the apparent temperature of the sky.

T_{sky} can be assumed to be [52]:

$$T_{sky} = T_a - 10.0^\circ C \quad (9.6)$$

where T_a is the ambient temperature.

e) Heat transfer from the cover to the atmosphere by convection, q_{ca} , per unit area of the still, can be found as:

$$q_{ca} = h_{ca} \cdot (T_g - T_a) \quad (9.7)$$

where the heat transfer coefficient, h_{ca} , is a function of the angle of inclination of the cover and the wind velocity. An approximate value of h_{ca} , in $W/M^2-^\circ C$ for a flat plate with moderate inclination, can be found from the equation [52]:

$$h_{ca} = 5.7 + 3.8 V_w \quad (9.8)$$

where V_w is the wind velocity in M/Sec.

9.2.2 LINER-WATER ENERGY BALANCE

The energy balance over the system of liner-saline water for a short period of time, may be written as follows:

$$(q_{\text{cond-conv, lat}} + q_{\text{rwg}}) \cdot A_w + q_{\text{insu}} \cdot A_w + \text{Feed} \cdot C_{p_w} \cdot \Delta T + Q_{\text{loss}} = H_i \cdot \text{Trn} \cdot A_w \quad (9.9)$$

Components in the above equation are defined as follows.

a) q_{insu} = heat conduction from the liner to the atmosphere through the insulator beneath the still;

$$q_{\text{insu}} = A_1 \cdot K_{\text{insu}} \cdot (T_1 - T_{\text{insu}}) / \text{Thick} \quad (9.10)$$

This equation is coupled with another expressing heat dissipation from beneath of the insulator to the atmosphere, as:

$$q_{\text{insu}} = A_1 \cdot h_{\text{insu}} \cdot (T_{\text{insu}} - T_a) \quad (9.11)$$

In equations (9.10) and (9.11) variables are defined as follows:

K_{insu} is the thermal conductivity of the insulator;

T_{insu} is the temperature of the outer surface of the insulator;

'Thick' is the thickness of the insulator;

h_{insu} is the heat transfer coefficient for heat exchange between the outer surface of insulator (facing downward) and its environment. One equation [57] for calculating h_{insu} is in the form:

$$h_{\text{insu}} = 0.58 [(T_{\text{insu}} - T_a) / \text{Length}]^{0.25} \quad (9.12)$$

where 'Length' is the distance from the top edge to the lower edge of the still.

- b) The energy leaving the still with the outflowing saline water is proportional to the difference in temperature of saline water entering and leaving the still, ΔT , as well as to the rate of feed, 'Feed', and thermal capacity of water. The mathematical expression is the same as appeared in equation (9.9).
- c) Energy is lost in many different ways, there is leakage of humid air, heat rejection from the sides and loss in other ways. In a well designed still these are minimized.
- d) Energy absorbed by the liner-saline system, $H_i \cdot Trn \cdot A_w$, is evaluated by aid of SOLAR. It should be noticed that solar energy transmitted through the glass may not be entirely absorbed in the system, hence some allowance must be made. A credible factor for roof-type solar stills would be about 5% [58]. For a flat tilted still with a liner made of a porous material, this factor can be even less. However due to the relatively small space between the transparent cover and the bottom in a flat tilted solar still and hence a higher possibility for radiation to escape out, a value of 5% is assumed to be a good approximation.

9.3 METHOD OF SOLUTION

To test the reliability of program STILL, it is desired to use the program to predict distillation rates for a number of days and compare the results obtained with the experimental data. Unfortunately, in most cases the reported data does not include the environmental conditions (e.g. hourly radiation, ambient temperature, etc.) under which the measurements were taken. Using the data reported

- a) A temperature is guessed for the glass (initially equal to the ambient temperature);
- b) The set of equations (9.1)-(9.8) (expressing the energy

balance over the cover) are solved;

c) The results obtained in b) are checked by solving the set of equations (9.9)-(9.12) (expressing the energy balance over the saline water-liner);

d) A new temperature is assigned to the glass and above steps are repeated until consistent results are obtained from both sets of equations.

More details of the procedure together with the print-out of "STILL" (a computer program executing the calculations involved) are given in Appendix [10].

When the solution to the equations are made and the different temperatures (e.g. cover and water-liner temperatures) are known, the distillation rate can be calculated. GrT and GrXW are calculated and by referring to the correlations provided in PART 1 the relevant Sherwood Number is calculated. (For choosing the appropriate correlation, the angle of inclination is taken into account.). Thus:

$$\text{Distil} = \text{Sh} \cdot \text{Co} \cdot M_{\text{H}_2\text{O}} \cdot D_{\text{AW}} \cdot (XW_w - XW_g) / (\text{Width} \cdot (1 - XW_w)) \quad (9.13)$$

where Distil is the rate of the distillation per unit area and other variables are given above.

9.4 EXAMPLES OF NUMERICAL SOLUTIONS

To test the reliability of program STILL, it is desired to use the program to predict distillation rates for a number of days and compare the results obtained with the experimental data. Unfortunately, in most cases the reported data does not include the environmental conditions (e.g. hourly radiation, ambient temperature, etc.) under which the measurements were taken. Among the few reported

data with sufficient details are those reported by Telkes [60] which have been considered here. These data together with those predicted by the STILL program are compared in Table 9.1; good agreements are observed.

Input data to STILL are:

Width=5.0 cm

Length=50.0 cm

Wind velocity=0.0

Ambient temperature at solar noon=30.0 deg C

Tinlet= Ambient temperature at each hour

Feed rate=0.01 Kg/m²-sec

Daily solar energy (KJ/m ²)	Daily distilled water (liters/m ²)	
	calculated	reported [60]
11000	2.5	2.8
16500	4.9	4.8
22000	6.6	5.6

Table 9.1 Daily distillation rates for a

flat tilted solar still

19. PERFORMANCE OF A FLAT TILTED SOLAR STILL

In this chapter the application of program STILL (introduced in the previous chapter) is shown, and the factors most affecting the performance of a tilted solar still are evaluated. The results obtained will then be used to improve the program.

solar energy daily KJ/m ²	daily distilled liter/m ²	
	calculated	reported [60]
11000	2.6	2.8
16500	4.9	4.8
22000	6.6	6.6

Table 9.1 Daily distillation rates for a flat tilted solar still

- 1) solar radiation
- 2) ambient temperature
- 3) wind velocity.

For design variables:

- 4) aspect ratio of the still (the ratio of the distance between cover and the bottom to the length of the still);
- 5) angle of inclination.

For operational variables:

- 6) feed rate of saline water;
- 7) preheating.

Most of the above variables change with time, e.g., solar radiation and ambient temperature, producing a vast number of possible combinations. It is not practical to consider all of the possible situations. Hence in the present calculation four different values were assigned to each variable forming about 1200 combinations. By solving all of these cases the performance of a tilted solar still

can be simulated. Some of the results obtained are given in Appendix III.

10. PERFORMANCE OF A FLAT-TILTED SOLAR STILL

In this chapter the application of program STILL (introduced in the previous chapter) is shown, and the factors most affecting the performance of a tilted solar still are evaluated. The results obtained will then be used to improve the productivity of this type of still.

The variables involved in a solar still process can be categorised in three groups: atmospheric; design; and operational. In each group the more important variables are examined.

For atmospheric variables:

- 1) solar radiation;
- 2) ambient temperature;
- 3) wind velocity.

For design variables:

- 4) aspect ratio of the still (the ratio of the distance between cover and the bottom to the length of the still);
- 5) angle of inclination;

For operational variables:

- 6) feed rate of saline water;
- 7) preheating.

Most of the above variables change with time, e.g., solar radiation and ambient temperature, producing a vast number of possible combinations. It is not practical to consider all of the possible situations. Hence in the present calculations four different values were assigned to each variable forming about 1280 combinations. By solving all of these cases the performance of a tilted solar still

can be simulated. Some of the results obtained are given in Appendix [11].

10.1 EFFECT OF ATMOSPHERIC VARIABLES

10.1.1 SOLAR RADIATION

In general, the productivity of solar stills is primarily dependent upon the amount of solar radiation available. Other variables are of considerably less importance. For this reason, the performance of a tilted solar still is best demonstrated by plotting the water output of the still as a function of the amount of solar radiation available (on an hourly or daily basis per unit area of the still). Figure 10.1 shows such a plot, in which each point corresponds to a certain situation composed of a combination of different values of the variable involved.

The results presented in Figure 10.1, which is a linear relationship between productivity and solar energy, is in agreement with the performance of this type of still reported by some of the experimenters [59-60].

10.1.2 AMBIENT TEMPERATURE

The ambient temperature has two opposite effects on the productivity of a tilted solar still:

- a) As the ambient temperature increases the temperature difference between the surrounding and the cover, sides and the underside of the still decreases. Hence less energy will transfer out of the still. With a decrease in waste energy the saline water temperature rises and in result productivity increases;

b) With an increase of ambient temperature the heat loss from the cover decreases and consequently, its temperature increases. Therefore the difference between cover and liner temperature decreases leading to a lower productivity.

Figure 10.2 illustrates these two effects, as can be seen, with relatively lower insolation the kind of effect described in b) predominates over the other effect.

Therefore, the productivity is improved with an increase in ambient temperature. However, for higher amounts of radiation (>2000.0 KJ/hr-m²) the effect is opposite and productivity drops as ambient temperature increases (i.e. the effect described in a) predominates).

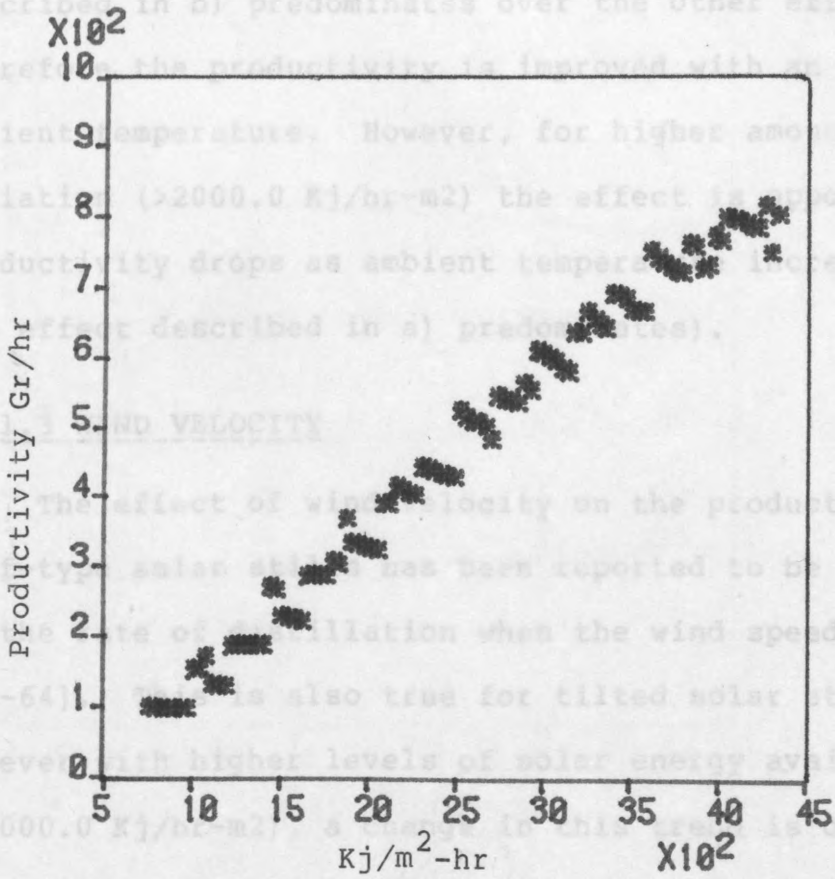


Figure 10.1 Effect of Insolation rate on productivity

The two different kinds of effect of the wind velocity on the productivity can be explained in the same way as that of ambient temperature: An increase in wind velocity cools the cover and, therefore, causes a higher energy loss as well as a higher temperature difference between the cover and the liner. The former can decrease the productivity whereas the latter can increase it. As was

b) With an increase of ambient temperature the heat loss from the cover decreases and consequently, its temperature increases. Therefore the difference between cover and liner temperature decreases leading to a lower productivity.

Figure 10.2 illustrates these two effects, as can be seen, with relatively lower insolation the kind of effect described in b) predominates over the other effect. Therefore the productivity is improved with an increase in ambient temperature. However, for higher amounts of radiation (>2000.0 KJ/hr- m^2) the effect is opposite and productivity drops as ambient temperature increases (i.e the effect described in a) predominates).

10.1.3 WIND VELOCITY

The effect of wind velocity on the productivity of roof-type solar stills has been reported to be a decrease on the rate of distillation when the wind speed increases [61-64]. This is also true for tilted solar stills. However with higher levels of solar energy available (>2000.0 KJ/hr- m^2), a change in this trend is observed. Figure 10.3 shows a slight increase in productivity with an increase in wind velocity.

The two different kinds of effect of the wind velocity on the productivity can be explained in the same way as that of ambient temperature: An increase in wind velocity cools the cover and, therefore, causes a higher energy loss as well as a higher temperature difference between the cover and the liner. The former can decrease the productivity whereas the latter can increase it. As was

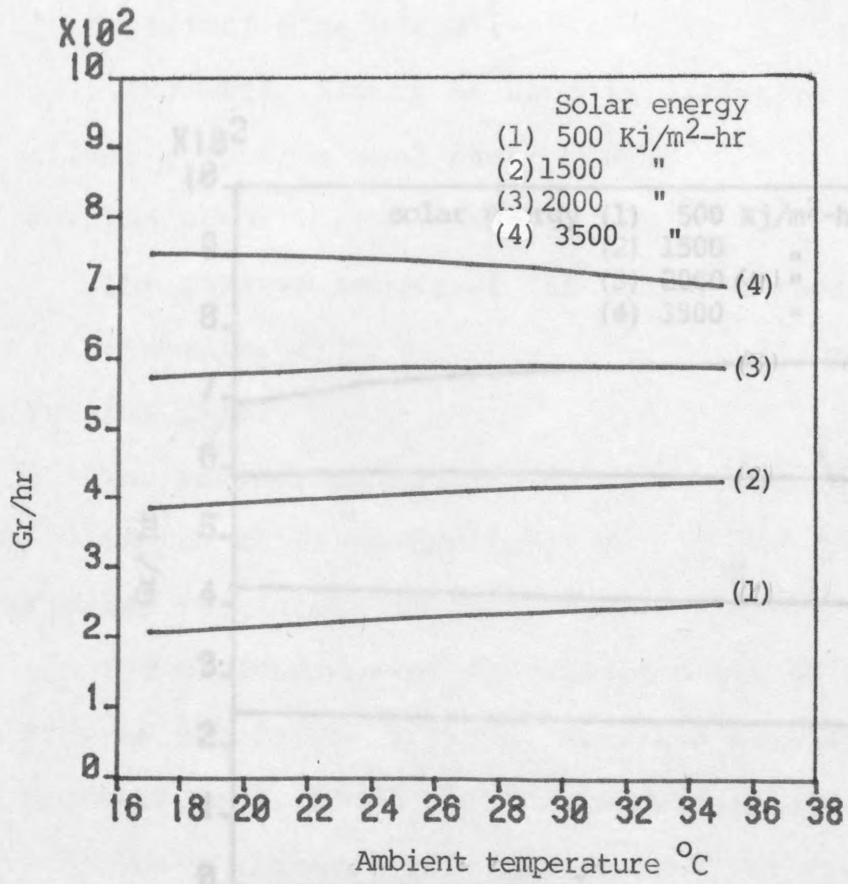


Figure 10.2 Effect of Ambient temperature on productivity

Figure 10.3 Effect of Wind velocity on productivity

mentioned, the amount of solar energy available is a decisive factor.

10.2 EFFECTS OF DESIGN FACTORS

The variables concerned in the design of tilted solar stills can be categorized in several groups. These mainly stem from the "choice of materials", "structure" and "geometrical dimensions".

The materials to be used in different parts of the still, should be such that:

For the cover:

solar energy	(1)	500	Kj/m ² -hr
	(2)	1500	"
	(3)	2000	"
	(4)	3500	"

The maximum amount of the radiation is transmitted;

For the insulator:

The maximum amount of radiation reaching the bottom of the still is absorbed;

For the evaporator:

The maximum energy is conducted out of the still.

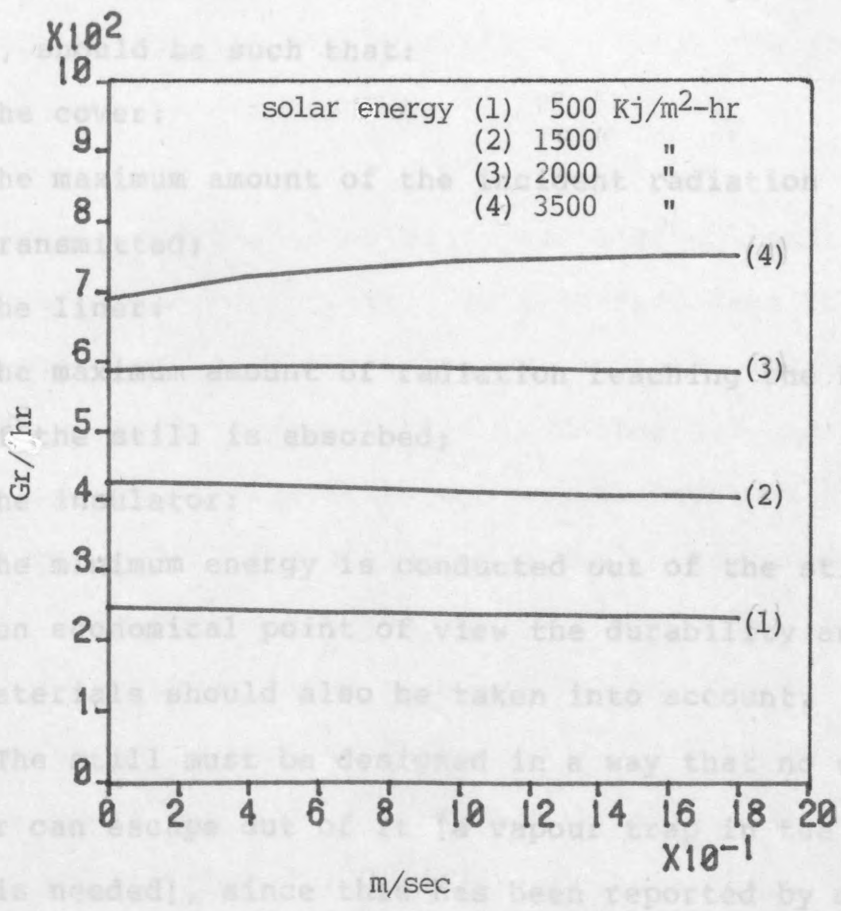
From an economical point of view the durability and cost of the materials should also be taken into account.

The still must be designed in a way that no water vapour can escape out of the still (if you cannot find a water exit is needed), since this has been reported by many experimenters to have a significant negative effect on the productivity.

Figure 10.3 Effect of Wind velocity on productivity

Maintenance are other important factors to be considered.

The problems corresponding to the choice of the materials and structural aspect have been well understood, and extensive investigations have been carried out by many experimenters. (For an excellent literature review see



mentioned, the amount of solar energy available is a decisive factor.

10.2 EFFECTS OF DESIGN FACTORS

The variables concerned in the design of tilted solar stills can be categorized in several groups. These mainly stem from the "choice of materials", "structure" and "geometrical dimensions".

The materials to be used in different parts of the still, should be such that:

For the cover:

1) The maximum amount of the incident radiation is transmitted;

For the liner:

2) The maximum amount of radiation reaching the bottom of the still is absorbed;

For the insulator:

3) The minimum energy is conducted out of the still.

From an economical point of view the durability and cost of the materials should also be taken into account.

The still must be designed in a way that no water vapour can escape out of it [a vapour trap in the water exit is needed], since this has been reported by many experimenters to have a significant negative effect on the productivity of the still. Ease of construction and maintainance are other important factors to be considered.

The problems corresponding to the choice of the materials and structural aspect have been well understood and extensive investigations have been carried out by many experimenters. [For an excellent literature review see

reference [65]]. However, less attention has been paid to the geometrical variables in experiments to date. These variables are essentially "angle of inclination" and "aspect ratio" which will be considered as follows.

10.2.1 ANGLE OF INCLINATION

The effects of the inclination on the productivity are twofold; a) the effect on collection of incident radiation, and b) the effect on internal simultaneous heat and mass transfer within the still envelope. These are explained respectively as follows.

a)

As was shown in chapter 8, for a given location the amount of incident radiation on a surface is a function of inclination angle (other variables being constant). One example of this is represented in Tables 8.2 and 8.3 in which the amount of monthly and annual insolation for different inclination angles is given. Because of the linear relationship between incident radiation and productivity in a tilted solar still (see figure 10.1), the results shown in tables similar to 8.2 can be directly attributed to the effect of the inclination angle on productivity. Thus for any particular location, the first task when designing a tilted solar still is to determine the best angle of inclination.

In the examples represented by Tables 8.2 and 8.3, the best angle of inclination lies between 0.0 and 20.0 degrees. The exact value should be decided upon when the effect of inclination on the distillation process has been taken into account.

b)

From Figure 6.1, presented in chapter 6, it was deduced that the rate of mass transfer in an inclined rectangular cavity is slightly affected by the position of the cavity. Thus with an angle of inclination between 0.0 and 20.0 degrees the highest rate of mass transfer will be obtained. Such an improvement on productivity together with that achieved by collecting the highest amount of radiation (and hence highest rate of distillation) provides a basis for choosing the appropriate angle of inclination for a tilted solar still.

10.2.2 ASPECT RATIO

In Part 1 it was concluded that for a constant temperature difference, between hot and cold faces in a rectangular cavity, the rate of simultaneous heat and mass transfer decreases as the thickness of the gas layer increases. However, in a tilted solar still, the temperatures of the cover and the saline water-liner do not remain constant and change with the rate of energy transfer. The interaction between the temperatures, the width (i.e. the gap between the cover and the bottom) and energy transfer can be expressed as follows:

- a) An increase of the width results in a decrease in energy transfer from the water surface to the cover;
- b) The decrease in the energy transfer cools the cover and, hence, the temperature difference between the cover and the saline water-liner, ΔT , increases;
- c) As ΔT increases, a further increase of energy transfer explained in a) is prevented.

The above has been illustrated in Figure 10.4; starting with a 1.0 cm width, the effect on productivity almost disappears with relatively greater width (> 3.0 cm). Further, different amounts of incident solar energy do not change the aforementioned trend.

10.3 EFFECTS OF OPERATIONAL VARIABLES

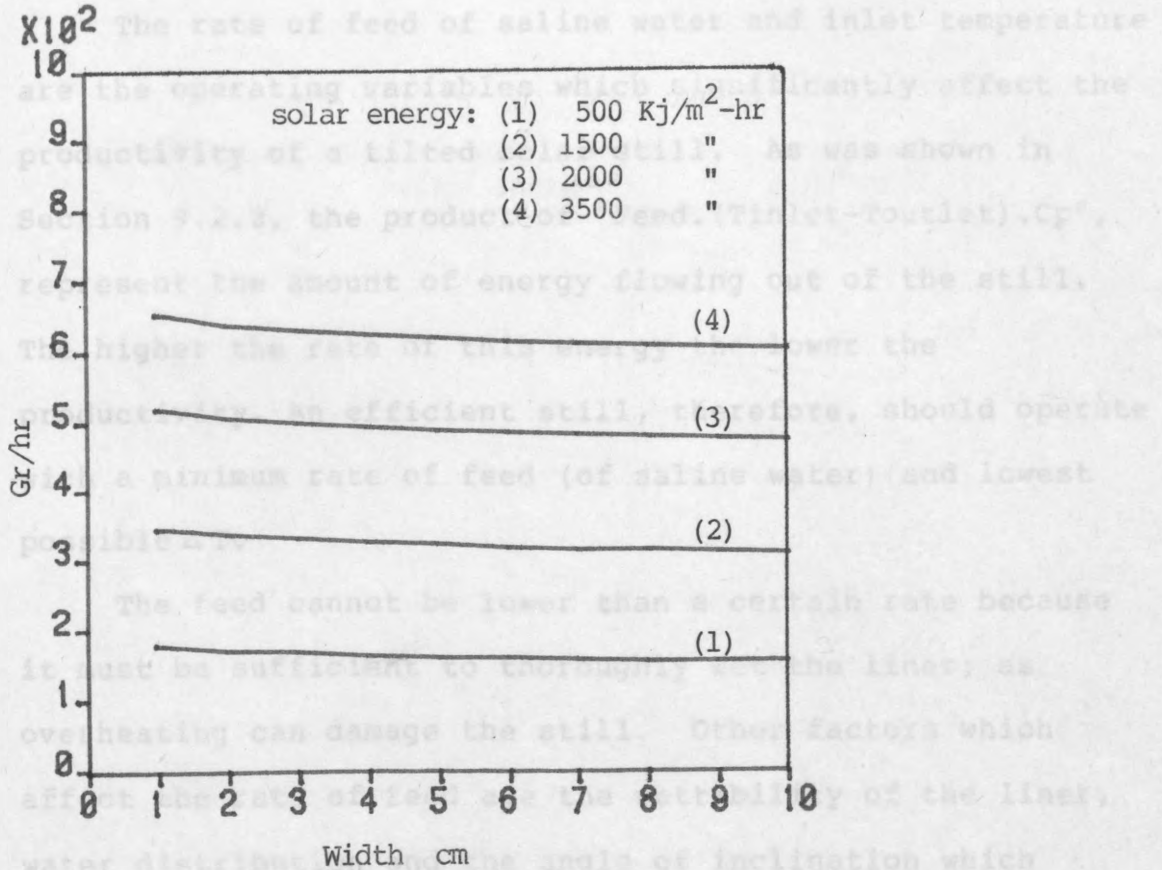


Figure 10.4 Effect of Width on productivity

The effects of wettability and water distribution on the rate of flow cannot be easily predicted. The optimized rate of flow should therefore be determined empirically. (The reported optimized rate, for such units, varies from 0.001 $\text{Kg/m}^2\text{-sec}$ to 0.01 $\text{Kg/m}^2\text{-sec}$ [67]).

The temperature difference between inlet and outlet saline water can be minimized only by increasing the inlet temperature (for a given rate of feed water). One way of

The above has been illustrated in Figure 10.4; starting with a 1.0 cm width, the effect on productivity almost disappears with relatively greater width (> 3.0 cm). Further, different amounts of incident solar energy do not change the aforementioned trend.

10.3 EFFECTS OF OPERATIONAL VARIABLES

The rate of feed of saline water and inlet temperature are the operating variables which significantly affect the productivity of a tilted solar still. As was shown in Section 9.2.2, the product of "Feed.(T_{inlet}-T_{outlet}).C_p", represent the amount of energy flowing out of the still. The higher the rate of this energy the lower the productivity. An efficient still, therefore, should operate with a minimum rate of feed (of saline water) and lowest possible ΔT .

The feed cannot be lower than a certain rate because it must be sufficient to thoroughly wet the liner; as overheating can damage the still. Other factors which affect the rate of feed are the wettability of the liner, water distribution and the angle of inclination which control the velocity of the flowing water.

The effects of wettability and water distribution on the rate of flow cannot be easily predicted. The optimized rate of flow should therefore be determined empirically. (The reported optimized rate, for such units, varies from 0.001 Kg/m²-sec to 0.01 Kg/m²-sec [67]).

The temperature difference between inlet and outlet saline water can be minimized only by increasing the inlet temperature (for a given rate of feed water). One way of

going so is 'preheating' the feed water [66].

Figure 10.5 shows the productivity of a still with a length of 0.5 meter and a feed rate of 0.003 Kg/a2-sec as a function of ΔT . As can be seen distillation rate decreases sharply as ΔT increases. The same trend is observed for different amounts of incident solar energy.

10.4 PRODUCTIVITY OF A MODIFIED FLAT TILTED STILL

The results obtained so far in this chapter may be used for comparing the productivity of tilted solar stills. The modifications which are suggested in this work for such improvements are as follows:

- 1) Developing a recirculating flow system which the outlet flow is mixed with some fresh saline water and redirected to the entrance of the still. (The water can be recirculated using a small pump or simply by hand). This minimizes the temperature difference between outlet and inlet saline water;
- 2) Narrowing the space between the cover and the liner as much as practically possible in order to increase the insulation of the still envelope;
- 3) Providing adjustable supporting legs for the still so that the angle of inclination can be regulated (e.g. modified for winter).

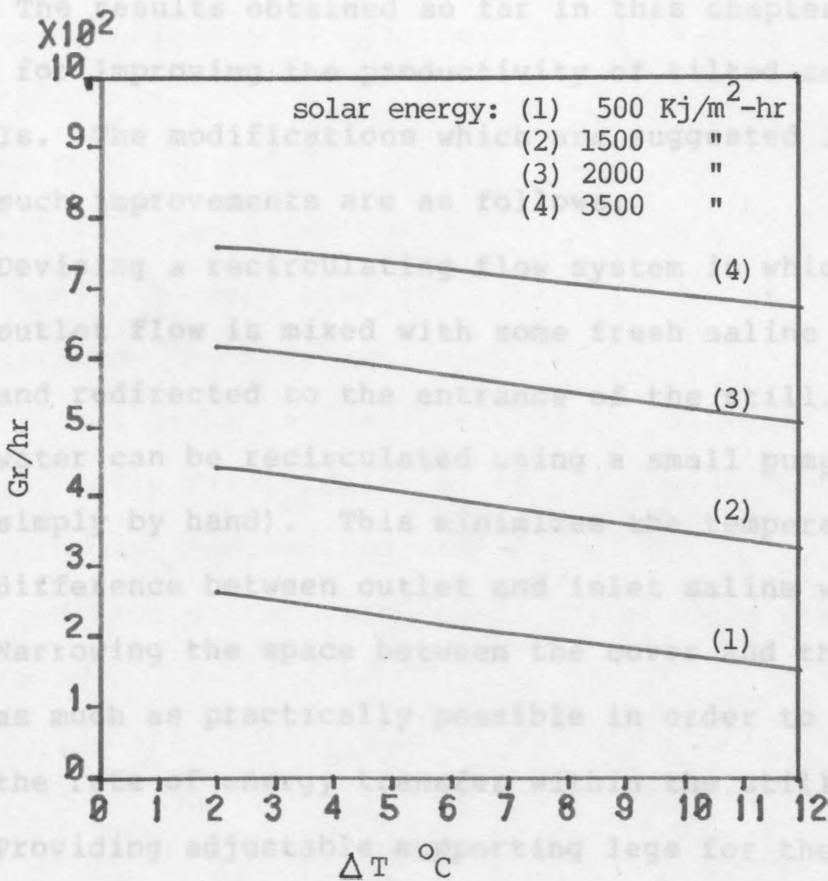


Figure 10.5 Effect of Temperature difference (Tin-Tout) on productivity

The productivity calculation for a still, with the above mentioned modifications, is given here as an example. The region chosen in this example is the Persian Gulf and the still considered is 2.0 cm deep, 50.0 cm long and 100.0 cm wide. The steps taken for calculating daily

doing so is 'preheating' the feed water [66].

Figure 10.5 shows the productivity of a still with a length of 0.5 meter and a feed rate of 0.003 Kg/m²-sec as a function of ΔT . As can be seen distillation rate decreases sharply as ΔT increases. The same trend is observed for different amounts of incident solar energy.

10.4 PRODUCTIVITY OF A MODIFIED FLAT TILTED STILL

The results obtained so far in this chapter may be used for improving the productivity of tilted solar stills. The modifications which are suggested in this work for such improvements are as follows:

- 1) Devising a recirculating flow system in which the outlet flow is mixed with some fresh saline water and redirected to the entrance of the still. (The water can be recirculated using a small pump or simply by hand). This minimizes the temperature difference between outlet and inlet saline water;
- 2) Narrowing the space between the cover and the liner as much as practically possible in order to increase the rate of energy transfer within the still envelope;
- 3) Providing adjustable supporting legs for the still so that the angle of inclination can be regulated (e.g. monthly) for maximum insolation.

The productivity calculation for a still, with the above mentioned modifications, is given here as an example. The region chosen in this example is the Persian Gulf and the still considered is 2.0 cm deep, 50.0 cm long and 100.0 cm wide. The steps taken for calculating daily

and monthly distillation rates are as follows:

- 1) The angle of inclination for each month is taken from Table 8.3. These angles correspond to the highest insolation in each month given that $10.0 < \alpha < 40.0$ deg, see Table 10.1. (The restriction on the angles is to avoid the kind of difficulties encountered in operating stills with very low or high inclinations.);
- 2) Program SOLAR is employed to estimate the hourly and daily insolations available to the still. The input data are:
Azimuth angle=0.0,
Latitude =26.0 deg north,
Vegetation type constant (a)=0.54,
Climate type constant (b)=0.18
- 3) Program STILL is then executed to calculate the hourly and daily distillation rates for a wide range of wind velocity, ambient temperature and ΔT .

The averaged monthly and annual figures are presented in Table 10.1.

Month	Jan	Feb	Mar	Apr	May	Jun	Jul	Aug	Sep	Oct	Nov	Dec
Angle (deg)	40.	40.	20.	10.	10.	10.	10.	10.	20.	30.	40.	40.
Insolation rates Kw-hr/m ²	127.	118.	141.	161.	174.	173.	179.	182.	174.	165.	147.	126.
Distillation rates(lit/m ²)	137.	130.	157.	180.	194.	194.	203.	201.	194.	185.	160.	141.
Annual Distillation=2076. lit/m ²												

Table 10.1 Monthly and annual distillation rates for an adjustable tilted solar still with recirculating system of feeding (Locality: the Persian Gulf; Latitude: 26.0 deg; Azimuth angle=0.0)

DISCUSSION

PART I

a) Pure Heat Transfer

The numerical results obtained by applying the numerical method (presented in Chapter 3) to the problem of pure heat transfer across a rectangular cavity filled with air, are given in Tables 4.1 and 4.2. Comparisons with the most consistent reported experimental data, for the vertical (Table 4.1), inclined and horizontal positions of the cavity (Table 4.2), show good agreement. This proves that when the buoyancy effect is caused by temperature inequalities in the fluid, the method of solution produces correct results.

DISCUSSION, CONCLUSIONS AND RECOMENDATION FOR FURTHER WORK

b) Water Distillation (Vertical Cavity)

Sample numerical solutions of Set 2 of the equations of change (Equations 2.13-2.17 derived under assumptions 1-6 in Chapter 2) for the problem of water distillation in a vertical cavity are given in Tables 5.2 - 5.7. As can be seen from these tables, comparisons with the reported data of Davis [1] show a close agreement for the conduction regime: the average deviation for the heat transfer rates is 4.86% (Table 5.5) and for mass transfer rates is 3.78% (Table 5.2). However, for the convective regime the deviation of the predicted from the reported data is much higher: for the heat transfer rates 13.66% and 14.37% (Tables 5.6 and 5.7 respectively), and for the mass transfer rates 23.55% and 27.62% (Tables 5.3 and 5.4 respectively). Such discrepancies warrant improvement of the theory.

DISCUSSION

PART 1

a) Pure Heat Transfer

The numerical results obtained by applying the numerical method (presented in Chapter 3) to the problem of pure heat transfer across a rectangular cavity filled with air, are given in Tables 4.1 and 4.2. Comparisons with the most consistent reported experimental data, for the vertical (Table 4.1), inclined and horizontal positions of the cavity (Table 4.2), show good agreements. This proves that when the natural convection in the cavity is caused by temperature inequalities in the field, the method of solution produces correct results.

b) Water Distillation (Vertical Cavity)

Sample numerical solutions of Set 2 of the equations of change (Equations 2.13-2.17 derived under assumptions 1-8 in Chapter 2) for the problem of water distillation in a vertical cavity are given in Tables 5.2 - 5.7. As can be seen from these tables, comparisons with the reported data of Davis [1] shows a close agreement for the conduction regime: the average deviation for the heat transfer rates is 4.96% (Table 5.5) and for mass transfer rates is 1.76% (Table 5.2). However, for the convective regimes the deviation of the predicted from the reported data is much higher: for the heat transfer rates 13.66% and 16.37% (in Tables 5.6 and 5.7 respectively), and for the mass transfer rates 23.56% and 27.42% (in Tables 5.3 and 5.4 respectively). Such discrepancies warrant improvement of the theory.

The effect of the evaporating film velocity on mass transfer rates (as a consequence of its effect on natural convection within the cavity) is presented in Table 5.8. The downward movement of the water film produces some resistance to the flow of humid air which moves upward next to the hot wall. Hence, as is observed from the table, an increase in the film velocity produces a decrease in the mass transfer rate. For the actual magnitude of the film velocity in Run 62, the effect is only a 6.6% improvement. This suggests that ignoring tangential velocity at the hot boundary is not the main origin of error in the calculation as Hu [2] suggests in his work.

The effect of physical and transport property variation on the flow characteristics and consequently on the mass transfer rate is presented in Table 5.9 (Run 62 has been chosen as an example). As can be seen, Equation Set 1 (Equations 2.1 - 2.5 derived under assumptions 1 - 6 allowing variable properties) and Equation Set 2 produce almost identical results, hence justifying the usual Boussinesq approximation undertaken in solving this type of problem.

From the equations of change it is understood that natural convection in an enclosure is generated by temperature inequalities (pure heat transfer), or by combined mass fraction and temperature inequalities in the field (simultaneous heat and mass transfer). Because the problem of pure heat transfer in Chapter 4 was satisfactorily solved, errors involved in solving the problem of simultaneous heat and mass transfer should be

due to incorrect mass fraction distribution in the cavity. Over saturation, which was observed by comparison of the water vapour mass fraction field (obtained from Set 2) with the corresponding saturated mass fractions, supports this opinion.

The reason for over saturation can be attributed to assumption 3 (Chapter 2) which states 'no phase change' in the field. There is no evidence experimentally or theoretically to prove this assumption and it is only to simplify the governing equations (Set 1 and Set 2) that one phase flow is assumed: neither is there any proof that condensation or evaporation occurs in the field. However, there must be some restriction on the water vapour mass fraction to prevent it exceeding its maximum saturated value. One form of such restriction on the diffusion equation (5.1) is presented in (5.2).

The numerical solutions of Set 3 of the equations of change (Equations 2.13 -2.15 and 5.8 which assumes the mixture is saturated) are given in Tables 5.10 and 5.11. An improvement of 10% in mass transfer rates (Table 5.10) and 4% in heat transfer rates (Table 5.11) have been achieved. Further improvement is observed when the tangential velocity is also accounted for in the calculations. The results are presented in the same tables, where the average deviations are 5.67% for heat transfer rates and 7.97% for mass transfer rates. These values are considered to be low enough to verify Set 3 of the equations and their subsequent numerical solution.

c) Water Distillation (inclined Cavity)

Tables 6.2 - 6.5 give two types of heat and mass transfer correlations obtained from the solution of Set 3 for an inclined cavity (with different angles of inclination; 0 to 90 degrees with 10 degrees intervals). In type 1, the correlations are based on the dimensionless variables which appeared in Set 3 and thus their applications may be extended to other binary mixtures as well as water vapour-air.

In type 2, the correlations are strictly true for water distillation since the properties of the humid air are implicit in the constants of the correlations.

It should be noticed that the results in Chapter 6 are unique and there is no comparable experimental or theoretical work in the literature to date. However the findings are expected to be valid because:

- 1) The satisfactory results obtained in Chapter 4, proves that the description of natural convection in the process of water distillation is correct for all angles of inclination (0 to 90 degrees). (Note: the mass fraction inequalities in the field make a relatively small contribution to the generation of free convection in the cavity in comparison to the temperature inequalities.);
- 2) The results obtained in Chapter 5 suggest that the mathematical modelling of the mass transfer mechanism works satisfactorily, and since the angle of inclination has no effect on the diffusion equation, it is concluded that for all angles of inclination the above is true.

PART 2

a) Solar Energy Estimation

The findings of Chapter 8 illustrate the use of an estimation method for availability prediction of solar energy. The use of the program SOLAR for calculation of monthly average radiation received by a tilted surface ($\alpha = 35.0$ degrees) is shown in Figure 8.1. A close agreement is observed between the predicted and reported insulations.

Table 8.2 shows the monthly incident radiation on a tilted surface, with different angles of inclination, situated in the Persian Gulf region. As is observed, the amount of radiation received is a function of inclination angle. Thus the best angle of inclination for collecting maximum insolation varies from month to month. On an annual basis, however, an angle of 10.0 degrees seems to be the optimum value.

Transmission of radiation through a tilted transparent cover is presented in Table 8.3. Although a reduction in the total amount of insolation is observed, the general distribution of energy with respect to inclination angle is similar to Table 8.2.

The figures given in Tables 8.2 and 8.3 are useful when designing a solar still to be operated in the Persian Gulf region.

b) Performance of a Tilted Solar Still

The results obtained from The program STILL are compared in Table 9.1 with the reported data for a given

tilted solar still. The close agreement observed in this table, substantiates the reliability of STILL.

Figures 10.1 - 10.5 show the effects of the important variables on the productivity of a tilted solar still. As can be seen from the figures with an increase in insolation rate and inlet temperature of the saline water (for a given feed rate), the productivity is enhanced. The wind velocity and ambient temperature have relatively minor effects on the performance.

For the modified, adjustable still with a system of recirculating flow (suggested in this work) the monthly and annual rates of productivity are presented in Table 10.1. For this still which is situated in the Persian Gulf, an annual distillation rate of 2076 liter per square meter has been predicted; which is considerable. This result, however, has to be verified by a future experimental program in the location for which the calculation has been carried out, i.e., the Persian Gulf.

- 1) The numerical method used in this work (based on the finite difference scheme devised by Spalding [16]) can be successfully applied to the problem of combined heat and mass transfer (as well as pure heat transfer) across an inclined rectangular cavity. (See Appendix [2] for the print-out of the computer program.)
- 2) In the process of water distillation in an enclosure the usual approximations of Boussinesq are justified (see Table 5.3).
- 3) Water film velocity affects the natural convection within a cavity and hence must be taken into account

CONCLUSIONS

The main achievements of the present work are:

- 1) It gives an insight into the process of simultaneous heat and mass transfer in a binary mixture. In doing so, it removes the main obstacle to the design improvement of solar stills;
- 2) It provides improved equations and computer simulation methods which can be used to enhance the performance of tilted solar stills;
- 3) It gives some useful data for future use when designing a solar still to be operated in the Persian Gulf region.

Although the geometrical shape considered is that of a rectangular cavity, the procedures presented in both parts of the work are flexible and can be extended to other geometries as well.

The conclusions which can be drawn from PART 1 of the work are as follows:

- 1) The numerical method used in this work (based on the finite difference scheme devised by Spalding [16] can be successfully applied to the problem of combined heat and mass transfer (as well as pure heat transfer) across an inclined rectangular cavity. (See Appendix [2] for the print-out of the computer program.);
- 2) In the process of water distillation in an enclosure the usual approximation of Boussinesq are justified (see Table 5.9);
- 3) Water film velocity affects the natural convection within a cavity and hence must be taken into account

in the calculations (see Table 5.8);

- 4) The assumption of 'no phase change' leads to considerable error in the results of mass transfer. Hence some restriction on the diffusion equation is necessary. Improvements are made by considering a modified form of the diffusion equation (see equation 5.8 and Tables 5.10 - 5.11 for the results obtained);
- 5) Two types of heat and mass transfer correlation have been found for water distillation in an inclined cavity (with inclination angles from 0.0 to 90.0 degrees): Type 1 is in a relatively general form (see Tables 6.2 and 6.3) and hence might be expected to produce a reasonable approximation for other gaseous systems with Prandtl and Schmidt numbers in the range of 0.5 - 1.0; Type 2 is a form valid for air-water vapour systems only (see Tables 6.4 and 6.5).

The findings of PART 2 of the work are:

- 1) A method for prediction of solar energy availability (Appendix [9] gives the print out of Program SOLAR);
- 2) The prediction of solar energy available in the persian Gulf region (received and transmitted through a transparent cover, see Tables 8.2 and 8.3 respectively);
- 3) A solution for the problem of solar distillation in a tilted flat still (see Appendix [10] for STILL print-out).

From the application of STILL it is concluded that the

factors most affecting the productivity of a tilted still are: amount of available insolation; angle of inclination and inlet temperature of the saline water (see Figures 10.1-10.5). For a suggested modified still (with recirculating system of feeding and adjustable angle of inclination), an annual productivity of 2076.0 Lit/Sq meter has been predicted (see Table 10.1).

- a) examine if the water vapour changes phase while transferring across the cavity.
- 2) A more accurate analysis of the diffusion equation in its complete form taking into consideration the possibility of phase change is also required.
- 3) An experimental investigation of water distribution in a tilted disc still is required.
 - a) verify the reliability of the proposed model.
 - b) examine the performance of the proposed disc still with recirculating feeding system and adjustable angle of inclination.
- 4) The design of new types of still using different types of multiple-effect stills and compare their performance with the use of different sized horizontal tubes are also required.

RECOMENDATION FOR FURTHER WORK

Further work which could ultimately lead to the design of cost effective solar stills include:

- 1) An experimental investigation into the problem of water distillation in an inclined rectangular cavity in order to:
 - a) test the corresponding correlations given in the present work;
 - b) examine if the water vapour changes phase while transferring across the cavity.
- 2) A more accurate analysis of the diffusion equation in its complete form taking into consideration the possibility of phase change in the field;
- 3) An experimental investigation of solar distillation in a tilted flat still in order to:
 - a) verify the reliability of the program STILL;
 - b) examine the performance of the suggested flat still with recirculating feeding system and adjustable angle of inclination.
- 4) The design of new types of still (e.g. different types of multiple effect stills) and assess their performance with the use of STILL, until improved models are discovered.

Insertion of Boundary Conditions in Finite Difference Equations

In the problem of simultaneous heat and mass transfer in a binary mixture the boundary conditions can be inserted into the corresponding finite difference equations in several different ways. Some of these are discussed here. The derived finite difference equation of energy is given below, first for a typical node in the field, and then for a node next to one of the boundaries.

By referring to Figure A-1, the energy fluxes crossing the control volume (shaded rectangular) are given as:

APPENDIX [1]

FINITE DIFFERENCE EQUATIONS FOR BOUNDARIES

$$\begin{aligned}
 & \frac{CT_D \rho c_p}{\Delta x} (T_1 - T_0) + \frac{CT_D \rho c_p}{\Delta x} (T_2 - T_1) + \dots \\
 & - \frac{1}{2} (h_w + h_c) \rho c_p \Delta x (T_1 - T_0) + \dots \\
 & \frac{CT_D \rho c_p}{\Delta x} (T_2 - T_1) + \dots
 \end{aligned}$$

Equation (A1.1)

$$\begin{aligned}
 & \frac{CT_D \rho c_p}{\Delta x} (T_1 - T_0) + \dots \\
 & - \frac{1}{2} (h_w + h_c) \rho c_p \Delta x (T_1 - T_0) + \dots \\
 & \frac{CT_D \rho c_p}{\Delta x} (T_2 - T_1) + \dots
 \end{aligned}$$

Equation (A1.2)

$$\begin{aligned}
 & \frac{CT_D \rho c_p}{\Delta x} (T_1 - T_0) + \dots \\
 & - \frac{1}{2} (h_w + h_c) \rho c_p \Delta x (T_1 - T_0) + \dots \\
 & \frac{CT_D \rho c_p}{\Delta x} (T_2 - T_1) + \dots
 \end{aligned}$$

Equation (A1.3)

Insertion of Boundary Conditions in Finite Difference Equations

In the problem of simultaneous heat and mass transfer in a binary mixture the boundary conditions can be inserted into the corresponding finite difference equations in several different ways. Some of these are discussed here. The derived finite difference equation of energy is given below, first for a typical node in the field, and then for a node next to one of the boundaries.

By referring to Figure A.1, the energy fluxes crossing the control volume (shaded rectangular) are given as:

$$\begin{aligned}
 & \text{CT}_{Pe} \\
 q_e = & \overbrace{[1/2(D_e + |F_e| + |D_e - |F_e||) + F_e]}^{\text{CT}_{Pe}} T_P + \\
 & \underbrace{-[1/2(D_e + |F_e| + |D_e - |F_e||) - F_e]}_{\text{CT}_{Ee}} T_E
 \end{aligned}
 \tag{A1.1}$$

$$\begin{aligned}
 & \text{CT}_{Pw} \\
 -q_w = & \overbrace{[1/2(D_w + |F_w| + |D_w - |F_w||) + F_w]}^{\text{CT}_{Pw}} T_P + \\
 & \underbrace{-[1/2(D_w + |F_w| + |D_w - |F_w||) - F_w]}_{\text{CT}_{Ww}} T_W
 \end{aligned}
 \tag{A1.2}$$

$$\begin{aligned}
 & \text{CT}_{Pn} \\
 q_n = & \overbrace{[1/2(D_n + |F_n| + |D_n - |F_n||) + F_n]}^{\text{CT}_{Pn}} T_P + \\
 & \underbrace{-[1/2(D_n + |F_n| + |D_n - |F_n||) - F_n]}_{\text{CT}_{Nn}} T_N
 \end{aligned}
 \tag{A1.3}$$

$$\begin{aligned}
 & \overbrace{CT_{Ps}} \\
 -q_s = & \left[\frac{1}{2} (D_s + |F_s| + |D_s - |F_s||) + F_s \right] T_P + \\
 & \left[\frac{1}{2} (D_s + |F_s| + |D_s - |F_s||) - F_s \right] T_S \\
 & \underbrace{CT_S}
 \end{aligned}$$

Equation (Al.4)

where $F_w = 0.5(\rho u C_p A)_w$
 $D_w = (K A / \delta x)_w$
 q_w is energy flux

and other variables are defined similarly. (In deriving the above equations, the hybrid central-upwind difference scheme has been employed.)

From conservation of energy flux, Equations Al.1-Al.4 are linked as:

$$q_e - q_w + q_n - q_s = ST = 0.0 \quad (Al.5)$$

hence

$$\begin{aligned}
 & \overbrace{CT_P} \\
 & [CT_{Pe} + CT_{Pw} + CT_{Pn} + CT_{Ps}] T_P + \\
 -CT_E \cdot T_E - CT_W \cdot T_W - CT_N \cdot T_N - CT_S \cdot T_S = ST
 \end{aligned}$$

(Al.6)

From conservation of mass flux:

$$F_e - F_w + F_n - F_s = 0.0 \quad (Al.7)$$

Substituting Equation Al.7 in Al.6 gives (by referring to definition of CT_{Pe} , CT_{Pw} , ... in Equations Al.1 to Al.4):

$$CT_P = CT_E + CT_W + CT_N + CT_S \quad (Al.8)$$

For a set of linear algebraic equations with constant coefficients such as

$$CT_P \cdot T_P = CT_E \cdot T_E + CT_W \cdot T_W + CT_N \cdot T_N + CT_S \cdot T_S + ST \quad (A1.9)$$

The matrix theory states that such a set will converge to a solution in an iterative solution if

$$CT_E + CT_W + CT_N + CT_S \leq CT_P \quad (A1.10)$$

(with strict inequalities for at least one node).

Since CT_E , CT_W , CT_N and CT_S are always positive, condition A1.10 is satisfied. (The under relaxation method, suggested by Gosman [34], can be employed in order to make sure that at least for one node the inequality in A1.10 is satisfied.).

For control volumes next to the liquid films the above procedure is not applicable, since the energy fluxes take different forms from those given in A1.1 or A1.2. For this situation the energy flux, e.g., q_w (energy crossing the hot wall), is expressed as:

$$-q_w = T_P \underbrace{(2 D)_w}_{CT_{Pw}} - T_l \underbrace{(2 D)_w}_{ST_w} + n_{vap} \cdot h_{vap} \quad (A1.11)$$

To link q_w with q_e , q_s and q_n , the "false source" method of Gosman [34] states that:

- 1) $CT_W = 0.0$;
- 2) CT_{Pw} (coefficient of T_P in A1.11) is added to CT_P (coefficient of T_P in A1.9);
- 3) ST_w (in A1.11) is added to ST (in A1.9).

This method although simple to apply, does not

satisfy Equation Al.7 (conservation of mass flux) when Al.8 is to be substituted in Al.6.

To overcome this difficulty, two alternative methods are suggested in the present work.

Method a)

Equation Al.11 is rearranged as:

$$-q_w = T \left[\underbrace{(2 D_w - F_w)}_{CT_{Pw}} + F_w \right] - Tl \left[\underbrace{(2 D_w + F_w) - F_w}_{CT_w} \right] + n_{vap} \cdot h_{vap} \quad (Al.12)$$

and

$$-q_w = T_P \cdot CT_{Pw} - Tl \cdot CT_w - \underbrace{[n_{vap} \cdot h_{vap} - F_w \cdot Tl]}_{ST_w} \quad (Al.13)$$

In Equation Al.13, ST_w is added to ST (in Equation Al.9), and CT_{Pw} and CT_w are defined in Al.12. In this way Equation Al.7 is satisfied. Because mass flux is very low at the boundary, Al.10 is also satisfied. (n.b. C_p , contained in F_w at the boundary, is heat capacity of humid air and not of water vapour.).

Method b)

Equation Al.11 may be also rearranged in another form as:

$$-q_w = T_P (2 D_w) - Tl [(2 D_w + 2 F_w) - 2 F_w] + n_{vap} \cdot h_{vap} \quad (Al.14)$$

and

$$\begin{aligned}
 -q_w = & T_P \overbrace{(2 D_w)}^{CT_{Pw}} - T_l \overbrace{(2 D_w + 2 F_w)}^{CT_w} + \\
 & - \underbrace{[n_{vap} \cdot h_{vap} - 2 F_w \cdot T_l]}_{ST_w}
 \end{aligned}$$

(A1.15)

In this equation CT_{pw} , CT_w and ST_w are also defined.

Methods a) and b) are both useful and can be equally adopted. However, method b) is easier to be applied especially when the finite difference equations of momentum and diffusion are considered. As an example the application of b) to the diffusion equation is given below:

$$\begin{aligned}
 -n_w = & W_P \overbrace{(2 D_w)}^{CW_{Pw}} - W_l \overbrace{(2 D_w + 2 F_w)}^{CW_w}
 \end{aligned}$$

(A1.16)

where n_w = mass flux

$$F_w = 0.5(\rho u A)_w$$

$$D_w = (D_{GV} A / \delta x)_w$$

As can be seen in Equation A1.16 there is no extra term to be added to ST in Equation A1.9.

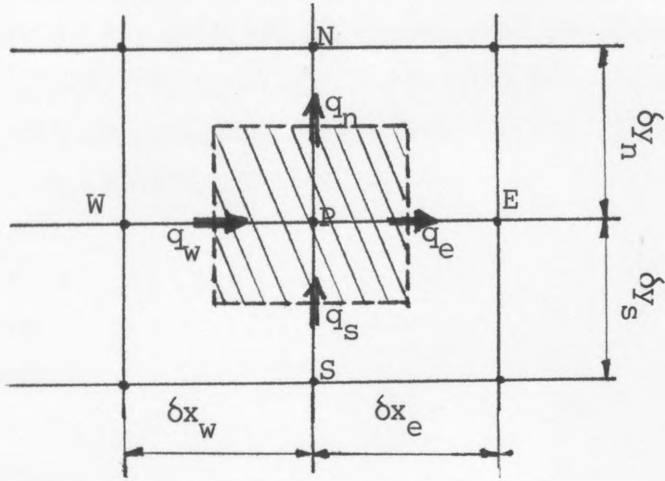


Figure A.1 Notation for a scalar control volume

APPENDIX (2)

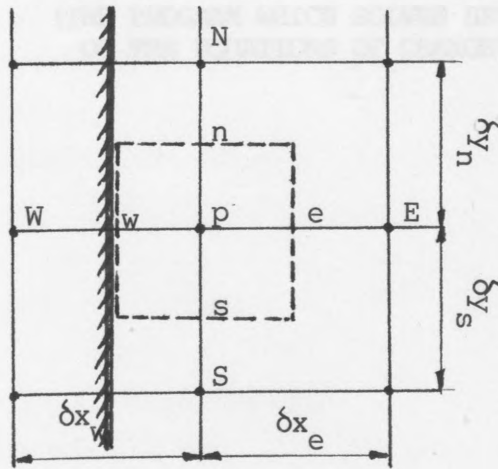


Figure A.2 Notation for a scalar control volume next to the hot boundary

Physical Properties

Fuzuda [75] reported values of the physical properties of both air and water-vapor saturated air. Since a little difference between the quantities related to dry and saturated air is observed, the physical and transport properties of humid air can be assumed to be equal to those of saturated air. On this basis, Davis [1] produced a number of equations which closely approximate the physical properties of humid air (with a degree of saturation from 0 to 1) as a function of temperature. The range of temperature is $25 - 55^{\circ}\text{C}$ and the equations are reproduced as follows: (All of the quantities appearing in this section are converted to SI units.)

APPENDIX [3] PHYSICAL PROPERTIES

1) thermal conductivity, $\text{W/m}^{\circ}\text{K}$

$$k = 1.73 [0.01345 + 14.5 T - 1374.175]/10^{-3} \quad (A3-1)$$

2) kinematic viscosity, m^2/s

$$\nu = 0.0379 [0.594 + 11.892 T - 1131.493]/10^{-3} \quad (A3-2)$$

3) thermal diffusivity, m^2/s

$$\alpha = 0.0925 [0.830 + 14.714 T - 1382.715]/10^{-3} \quad (A3-3)$$

4) air-water vapor diffusivity, m^2/s

$$D_{AW} = 0.0925 [0.875 + 16.215 T - 2023.339]/10^{-3} \quad (A3-4)$$

The molar heat capacity of water vapor as a function of temperature, given by Vose [1], is reproduced below:

$$C_{pV} = 4186.6 [7.958 + 13.175 T - 1458.800/10^3 + 0.780 T^2 - 2112.332/10^6 + 0.435 T^3 - 0.6114 T^4/10^9] \quad (A3-5)$$

Physical Properties

Kusuda [70] reported values of the physical properties of both air and water-vapour saturated air. Since a little difference between the quantities related to dry and saturated air is observed, the physical and transport properties of humid air can be assumed to be equal to those of saturated air. On this basis, Davis [1] produced a number of equations which closely approximate the physical properties of humid air (with a degree of saturation from 0 to 1) as a function of temperature. The range of temperature is 26 - 55°C and the equations are reproduced as follows: (All of the equations appearing in this section are converted to SI units when the original equations are in other units.).

1) thermal conductivity, W/m-°K

$$K = 1.73 [0.01545 + (4.5 T - 1374.175)/10^{-5}] \quad (\text{A3.1})$$

2) kinematic viscosity, m²/s

$$\nu = 0.0929 [0.588 + (3.852 T - 1133.493)/10^{-3}]/3600 \quad (\text{A3.2})$$

3) thermal diffusivity, m²/s

$$\alpha = 0.0929 [0.830 + (4.716 T - 1387.735)/10^{-3}]/3600 \quad (\text{A3.3})$$

4) air-water vapour diffusivity, m²/s

$$D_{AW} = 0.0929 [0.979 + (6.876 T - 2023.339)/10^{-3}]/3600 \quad (\text{A3.4})$$

The molar heat capacity of water vapour as a function of temperature, given by Kobe [71], is reproduced below:

$$\begin{aligned} C_{pW} = & 4186.6 (7.968 + (3.175 T - 1459.010) \cdot 10^{-4} + \\ & + (5.750 T - 2643.102) \cdot 10^{-7} + \\ & - (1.472 T - 676.634) \cdot 10^{-10}) / 18.0 \end{aligned} \quad (\text{A3.5})$$

where C_{pW} is in J/Kg mole $^{\circ}K$.

Based on the values reported by Lang [72] and Hougén et al [73], Davis [1] gives a relation for the latent heat of vaporization of water. This equation is reproduced as follows:

$$h_{\text{vap}} = 716.0 (1.0 - T/648)^{0.332} \cdot 4186.8 \quad (\text{A3.6})$$

where h_{vap} is in J/Kg.

APPENDIX 241

SOLUTION OF ENERGY EQUATION (3.9)
(SEE 2 OF THE NOTATIONS OF CHANGE)

3460C

4000C CALCULATION OF TEMPERATURE

4010C

4020 DO 236 J=2, N

4030 DO 236 I=2, M

4040 DXW=DELX(I)

4050 DXE=DELX(I+1)

4060 DX=0.5*(DELX(I)+DELX(I+1))

4070 AY=DX*HEADPTH

4080 DYS=DELT(J)

4090 DYE=DELT(J+1)

4100 DY=0.5*(DELT(J)+DELT(J+1))

4110 AX=DY*HEADPTH

4120 D1=CON*AX/DXW

4130 D2=CON*AX/DXE

4140 D3=CON*AY/DYS

4150 D4=CON*AY/DYE

4160 VOL=AX*DX

APPENDIX [4]

4170 FX1=DENSITY*V(J, I)*AX

4180 DX1=AX*DENSITY*DI*(W(J, I)-W(J, I-1))/DX

4190 F1W=FX1 - SOLUTION OF ENERGY EQUATION (5.8)

4195 IF(1 - (SET 3 OF THE EQUATIONS OF CHANGE)

4200 F1A=F11-F1W

4210 F1=(F1W*CPW+F1A*CPA)/3.0

4220 FX2=DENSITY*V(J, I)*AX

4240 DX2=AX*DENSITY*DI*(W(J, I)-W(J, I-1))/DX

4250 F2W=FX2*(0.5*(W(J, I)+W(J, I-1))-DX)

4255 IF(1.EQ.0) F2W=FX2

4260 F2A=FX2-F2W

4270 F2=(F2W*CPW+F2A*CPA)/3.0

4280 FY3=DENSITY*V(J, I)*AY

4300 DY3=AY*DENSITY*DI*(W(J, I)-W(J, I-1))/DY

4310 F3W=FY3*(0.5*(W(J, I)+W(J, I-1))-DY)

4325 IF(1.EQ.0) F3W=FY3

4330 F3A=FY3-F3W

4340 F3=(F3W*CPW+F3A*CPA)/3.0

4350 IF(1.EQ.0) F3=FY3

4360 FY4=DENSITY*V(J+1, I)*AY

4380 DY4=AY*DENSITY*DI*(W(J+1, I)-W(J, I))/DY

4390 F4W=FY4*(0.5*(W(J+1, I)+W(J, I))-DY)

```

3460C
4000C CALCULATION OF TEMPERATURE
4010C
4020 DO 236 J=2,N
4030 DO 236 I=2,M
4040 DXW=DELX(I)
4050 DXE=DELX(I+1)
4060 DX=0.5*(DELX(I)+DELX(I+1))
4070 AY=DX*BREADTH
4080 DYS=DELY(J)
4090 DYN=DELY(J+1)
4100 DY=0.5*(DELY(J)+DELY(J+1))
4110 AX=DY*BREADTH
4120 D1=CON*AX/DXW
4130 D2=CON*AX/DXE
4140 D3=CON*AY/DYS
4150 D4=CON*AY/DYN
4160 VOL=AX*DX
4170 FX1=DENSIT*U(J,I)*AX
4180 DX1=AX*DENSIT*DIF*(W(J,I)-W(J,I-1))/DXW
4190 F1W=FX1*(W(J,I)+W(J,I-1))/2.0-DX1
4195 IF(I.EQ.2) F1W=FX1
4200 F1A=FX1-F1W
4210 F1=(F1W*CPW+F1A*CPA)/2.0
4230 FX2=DENSIT*U(J,I+1)*AX
4240 DX2=AX*DENSIT*DIF*(W(J,I+1)-W(J,I))/DXE
4250 F2W=FX2*(0.5*(W(J,I)+W(J,I+1)))-DX2
4255 IF(I.EQ.M) F2W=FX2
4260 F2A=FX2-F2W
4270 F2=(F2W*CPW+F2A*CPA)/2.0
4290 FY3=DENSIT*V(J,I)*AY
4300 DY3=AY*DENSIT*DIF*(W(J,I)-W(J-1,I))/DYS
4310 F3W=FY3*(0.5*(W(J,I)+W(J-1,I)))-DY3
4315 IF(J.EQ.2) F3W=0.0
4320 F3A=FY3-F3W
4330 F3=(F3W*CPW+F3A*CPA)/2.0
4340 IF(J.EQ.2) F3=0.0
4350 FY4=DENSIT*V(J+1,I)*AY
4360 DY4=AY*DENSIT*DIF*(W(J+1,I)-W(J,I))/DYN
4370 F4W=FY4*(0.5*(W(J,I)+W(J+1,I)))-DY4

```

```

4375 IF (J.EQ.N) F4W=0.0
4380 F4A=FY4-F4W
4390 F4=(F4W*CPW+F4A*CPA)/2.0
4400 IF (J.EQ.N) F4=0.0
4410 SMP=2.0*(F4-F3+F2-F1)
4420 CP=0.0
4430 IF (SMP.GT.0.0) CP=SMP
4440 CPO=CP
4450 CU1(J,I)=AMAX1 (ABS (F1) ,D1)+F1
4460 CU2(J,I)=AMAX1 (ABS (F2) ,D2)-F2
4470 CU3(J,I)=AMAX1 (ABS (F3) ,D3)+F3
4480 CU4(J,I)=AMAX1 (ABS (F4) ,D4)-F4
4490 IF (I.EQ.2) CU1(J,I)=2.0*D1+F1
4500 IF (I.EQ.M) CU2(J,I)=2.0*D2-F2
4510 SU(J,I)=CPO*T(J,I)
4520 SP(J,I)=-CP
4530 IF (J.EQ.2) CU3(J,I)=0.0
4540 IF (J.EQ.N) CU4(J,I)=0.0
4550 IF (I.EQ.2) SU(J,I)=SU(J,I)-F1*(T(J,2)-T1)
4560 IF (I.EQ.M) SU(J,I)=SU(J,I)+F2*(T(J,M)-T2)
4570 CU(J,I)=CU1(J,I)+CU2(J,I)+CU3(J,I)+CU4(J,I)-SP(J,I)
4571C
4572C ADDITIONAL HEAT DUE TO RAIN
4573C
4850 RAIN(J,I)=- (F4W-F3W+F2W-F1W)
4851 SU(J,I)=SU(J,I)+RAIN(J,I)*(HVAP-CPW*TBAR)
4899C
4900C UNDER RELAXATION
4902 CU(J,I)=CU(J,I)/URFT
4904 SU(J,I)=SU(J,I)+(1.-URFT)*CU(J,I)*T(J,I)
4906 236 CONTINUE
4908 DO 1003 K3=1,10
4910 DO 248 J=2,N
4912 DO 249 I=2,M
4914 B(I)=CU3(J,I)*T(J-1,I)+CU4(J,I)*T(J+1,I)+SU(J,I)
4916 A1(I)=CU1(J,I)
4918 A2(I)=CU2(J,I)
4920 A(I)=CU(J,I)
4922 249 CONTINUE
4924 X(MX)=T(J,MX)

```

```

4926 X(1)=T(J,1)
4928 CALL MAN(M,A1,A2,A,B,X)
4930 DO 250 I=2,M
4932 T(J,I)=X(I)
4934 250 CONTINUE
4936 248 CONTINUE
4938 1003 CONTINUE
4940C
5630 DO 268 J=2,N
5640 U(J,2)=(-1.0/(1.0-W1))*DIF*(W(J,2)-W1)/(0.5*DELX(2))
5650 U(J,MX)=(-1.0/(1.0-W2))*DIF*(W2-W(J,M))/(0.5*DELX(MX))
5660 FLUXW(J)=U(J,2)*DENSIT*0.5*(DELY(J)+DELY(J+1))*BREADTH
5670 FLUXE(J)=U(J,MX)*DENSIT*0.5*(DELY(J)+DELY(J+1))*BREADTH
5680 268 continue
5690 FLXW=0.0
5700 FLXE=0.0
5710 DO 270 J=2,N
5720 FLXW=FLXW+FLUXW(J)*1000.0*3600.0
5730 FLXE=FLXE+FLUXE(J)*1000.0*3600.0
5740 270 continue
5750C
5760c
5770C CALCULATION OF W(J,I)=WSAT & RAIN(J,I)
5780C
5790 DO 662 J=2,N
5800 DO 662 I=2,M
5810 PH2O=10.** (8.10765-1750.286/(235.+T(J,I)-273.15))*133.32
5820 XWSAT=PH2O/P(J,I)
5830 W(J,I)=XWSAT*18.0/(XWSAT*18.0+(1.0-XWSAT)*28.97)
5840 662 CONTINUE

```

DEFINITION OF NUSSELT AND SHERWOOD NUMBERS

1) Average Nusselt number

Nusselt number is defined in two different ways:

$$a) Nu_{cond-conv} = h_c d / \lambda \quad (A5.1)$$

where:

$$h_c = q_{cond-conv} / (A_s (T_1 - T_2)) \quad (A5.2)$$

where $q_{cond-conv}$ is heat transfer through conduction and convection only.

$$b) Nu_{cond-conv,lat} = \dot{m} d / \lambda \quad (A5.3)$$

where:

$$\dot{m} = q_{cond-conv,lat} / (A_s (T_1 - T_2)) \quad (A5.4)$$

where $q_{cond-conv,lat}$ is heat transfer through conduction, convection as well as latent heat of evaporation.

APPENDIX [5]

DEFINITION OF NUSSELT AND SHERWOOD NUMBERS

2) Average Sherwood number

$$Sh = (K_x d) / (C_o v_{av}) \quad (A5.5)$$

where:

$$a) K_x = J^* / (A_s (X_1 - X_2)) \quad (A5.6)$$

where J^* is molar flux of water vapour with respect to molar average velocity, and is defined as:

$$J^* = N_{vap} (1 - X_1) \quad (A5.7)$$

$$= N_{vap} / N_{g20} (1 - X_1) \quad (A5.8)$$

b) C_o is molar density of solution and may be obtained from the equation of state as:

$$p = C_o R / M v_c \quad (A5.9)$$

Definition of Nusselt and Sherwood numbers

1) Average Nusselt number

Nusselt number is defined in two different ways:

$$a) \text{Nu}_{\text{cond-conv}} = h \cdot d / K \quad (\text{A5.1})$$

where:

$$h = q_{\text{cond-conv}} / (A \cdot (T_1 - T_2)) \quad (\text{A5.2})$$

where $q_{\text{cond-conv}}$ is heat transfer through conduction and convection only.

$$b) \text{Nu}_{\text{cond-conv, lat}} = \dot{h} \cdot d / K \quad (\text{A5.3})$$

where:

$$\dot{h} = q_{\text{cond-conv, lat}} / (A \cdot (T_1 - T_2)) \quad (\text{A5.4})$$

where $q_{\text{cond-conv, lat}}$ is heat transfer through conduction, convection as well as latent heat of evaporation.

2) Average Sherwood number

$$\text{Sh} = (K_x \cdot d) / (C_o \cdot D_{GV}) \quad (\text{A5.5})$$

where:

$$a) K_x = J^* / (A \cdot (X_{W1} - X_{W2})) \quad (\text{A5.6})$$

where J^* is molar flux of water vapour with respect to molar average velocity, and is defined as:

$$J^* = N_{\text{vap}} (1 - X_{W1}) \quad (\text{A5.7})$$

$$= n_{\text{vap}} / M_{\text{H}_2\text{O}} (1 - X_{W1}) \quad (\text{A5.8})$$

b) C_o is molar density of solution and may be obtained from the equation of State as:

$$P = C_o \bar{R} / M T_o \quad (\text{A5.9})$$

or

$$P = C_o \bar{R} T_o \quad (A5.10)$$

hence

$$C_o = P/(\bar{R} T_o) \quad (A5.11)$$

(\bar{R} is Molar universal gas constant = 8.3143 KJ/Kmol^oK)

Substituting A5.11, A5.8 and A5.6 in A5.5 gives:

$$Sh = \frac{(1-XW1) n_{vap} / M_{H2O}}{A (XW1-XW2)} \cdot \frac{d}{C_o D_{GV}} \quad (A5.12)$$

APPENDIX (6)

PHYSICAL PROPERTY DATA

Calculation of declination position of the Sun

The Earth's orbit is almost circular. (The distance from the Sun to the Earth varies between 91.25 and 94.50 million miles). The Earth's equator is inclined to plane of orbit at an angle of 23.45. This angle is also the inclination between the plane of orbit and the plane normal to the Earth's axis. Figure 23.1 shows the situation of these planes relative to each other, where:

δ is declination varying from 23.45 (21st July) to -23.45 (21st Dec) during a year. (δ is positive when the Earth is below the plane normal to the Earth's axis in the figure);
 w is angular position of the Earth.

APPENDIX [8]

δ is in the form:

$$\delta = 23.45 \sin(w) \quad \text{CALCULATION OF DECLINATION} \quad (A8.1)$$

where w is given as:

$$w = 1360.0 (n+284)/365 \quad (A8.2)$$

where n is the day of the year and the number 284 derived from: 365-91-284 (8) represents the day of birth of March when δ is equal to zero).

In deriving Equation A8.1, it has been assumed that the formula expressing the variation of day lengths throughout a year, is in a sine form. This assumption is not quite accurate. A more accurate relationship between w and δ can be obtained by referring to figure A8.1. In this figure, OECA is the plane normal to the Earth's axis and ODOB is the plane of orbit. It can be seen that:

$$\text{for } \angle OED : \sin(w) = OD/OE \quad (A8.3)$$

$$\text{for } \angle OAB : \sin(23.45) = AB/OB \quad (A8.4)$$

$$\text{for } \angle ODB : \sin(\delta) = OD/OB = AB/OB \quad (A8.5)$$

Calculation of angular position of the Sun

The Earth's orbit is almost circular. (The distance from the Sun to the Earth varies between 91.25 and 94.50 million miles). The Earth's equator is inclined to plane of orbit at an angle of $23,27^{\circ}$. This angle is also the inclination between the plane of orbit and the plane normal to the Earth's axis. Figure A8.1 shows the situation of these planes relative to each other, where:

δ is declination varying from $23,27$ (21th July) to $-23,27$ (21th Dec) during a year. (δ is positive when the Earth is below the plane normal to the Earth's axis in the figure);
 w is angular position of the Earth.

The equation suggested by Cooper [49] to approximate

δ is in the form:

$$\delta = 23.45 \sin(w) \quad (\text{A8.1})$$

where w is given as:

$$w = [360.0 (n+284)/365] \quad (\text{A8.2})$$

where n is the day of the year and the number 284 derived from: $365-81=284$ (81 represents the day of 21th of March when δ is equal to zero).

In deriving Equation A8.1, it has been assumed that the formula expressing the variation of day lengths throughout a year, is in a sine form. This assumption is not quite accurate. A more accurate relationship between w and δ can be obtained by referring to Figure A8.2. In this figure, OECA is the plane normal to the Earth's axis and OEDB is the plane of orbit. It can be shown that:

$$\text{for } \triangle OBD : \sin(w) = OB/OD \quad (\text{A8.3})$$

$$\text{for } \triangle OAB : \sin(23.45) = AB/OB \quad (\text{A8.4})$$

$$\text{for } \triangle COD : \sin(\delta) = CD/OD = AB/OB \quad (\text{A8.5})$$

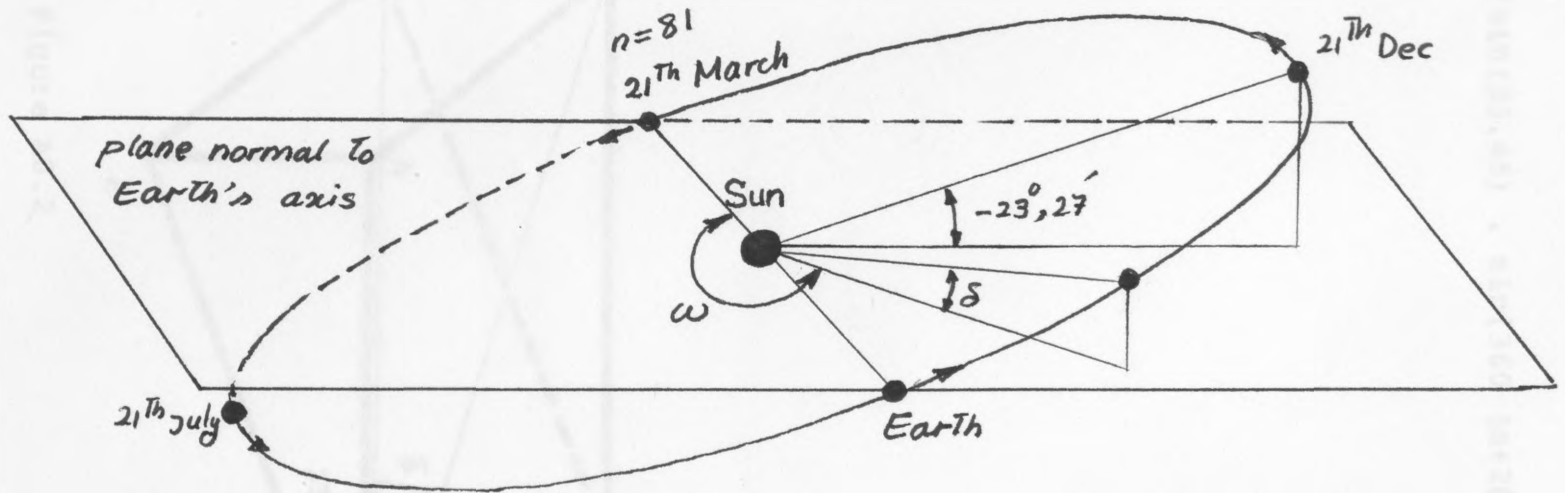


Figure A8.1 Declination and Hour angles

substituting Equations A8.3 and A8.4 in A8.5 results in:

$$\sin(\delta) = \sin(23.45) \cdot \sin[360 (n+284)/365] \quad (\text{A8.6})$$

or

$$\delta = \sin^{-1} [\sin(23.45) \cdot \sin[360 (n+284)/365]] \quad (\text{A8.7})$$

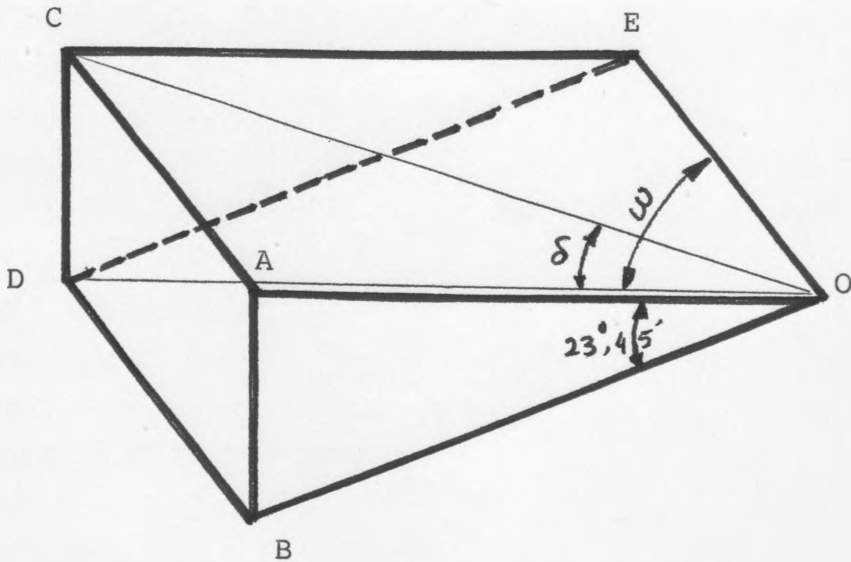


Figure A8.2

WV H/B	Specific R/42	A C2	Ts C2	ΔT C2	Distil Gr/hr
2.	200.00	0.01	20.00	2.00	57.92
2.	200.00	0.01	30.00	4.00	79.80
4.	200.00	0.01	20.00	2.00	62.67
4.	200.00	0.01	25.00	5.00	46.02
6.	200.00	0.01	25.00	3.00	105.29
6.	200.00	0.01	35.00	4.00	85.82
6.	200.00	0.01	35.00	4.00	68.72
6.	200.00	0.01	25.00	8.00	51.65
6.	200.00	0.01	30.00	1.00	113.63
6.	200.00	0.01	30.00	4.00	93.79
6.	200.00	0.01	30.00	6.00	78.68
6.	200.00	0.01	35.00	2.00	54.55
6.	200.00	0.01	35.00	2.00	121.04
6.	200.00	0.01	35.00	4.00	106.48
6.	200.00	0.01	35.00	6.00	80.47
6.	200.00	0.01	35.00	8.00	61.39
6.	200.00	0.01	40.00	2.00	127.77
6.	200.00	0.01	40.00	4.00	106.58
6.	200.00	0.01	40.00	6.00	85.90
6.	200.00	0.01	40.00	8.00	65.98
6.	200.00	0.01	20.00	2.00	93.16
6.	200.00	0.01	20.00	4.00	75.36
6.	200.00	0.01	20.00	6.00	59.82
6.	200.00	0.01	20.00	8.00	43.62
6.	200.00	0.01	25.00	2.00	101.19
6.	200.00	0.01	25.00	4.00	82.64
6.	200.00	0.01	25.00	6.00	65.10
6.	200.00	0.01	25.00	8.00	48.51
6.	200.00	0.01	30.00	2.00	109.82
6.	200.00	0.01	30.00	4.00	89.61
6.	200.00	0.01	30.00	6.00	71.14
6.	200.00	0.01	30.00	8.00	53.54
6.	200.00	0.01	25.00	2.00	116.43
6.	200.00	0.01	25.00	4.00	96.33
6.	200.00	0.01	25.00	6.00	78.92
6.	200.00	0.01	25.00	8.00	58.42
6.	200.00	0.01	40.00	2.00	123.37
6.	200.00	0.01	40.00	4.00	102.66

APPENDIX [11]

PREDICTED DISTILLATION RATES
IN A TILTED FLAT SOLAR STILL

Wv M/S	Qsolar W/M2	d Cm	Ta oC	ΔT oC	Distil Gr/hr
0.	200.00	0.01	20.00	2.00	97.92
0.	200.00	0.01	20.00	4.00	79.80
0.	200.00	0.01	20.00	6.00	62.67
0.	200.00	0.01	20.00	8.00	46.62
0.	200.00	0.01	25.00	2.00	105.89
0.	200.00	0.01	25.00	4.00	86.82
0.	200.00	0.01	25.00	6.00	68.72
0.	200.00	0.01	25.00	8.00	51.65
0.	200.00	0.01	30.00	2.00	113.63
0.	200.00	0.01	30.00	4.00	93.79
0.	200.00	0.01	30.00	6.00	74.68
0.	200.00	0.01	30.00	8.00	56.55
0.	200.00	0.01	35.00	2.00	121.04
0.	200.00	0.01	35.00	4.00	100.46
0.	200.00	0.01	35.00	6.00	80.47
0.	200.00	0.01	35.00	8.00	61.39
0.	200.00	0.01	40.00	2.00	127.77
0.	200.00	0.01	40.00	4.00	106.58
0.	200.00	0.01	40.00	6.00	85.90
0.	200.00	0.01	40.00	8.00	65.98
0.	200.00	0.03	20.00	2.00	93.16
0.	200.00	0.03	20.00	4.00	75.56
0.	200.00	0.03	20.00	6.00	59.02
0.	200.00	0.03	20.00	8.00	43.62
0.	200.00	0.03	25.00	2.00	101.19
0.	200.00	0.03	25.00	4.00	82.64
0.	200.00	0.03	25.00	6.00	65.10
0.	200.00	0.03	25.00	8.00	48.61
0.	200.00	0.03	30.00	2.00	109.02
0.	200.00	0.03	30.00	4.00	89.61
0.	200.00	0.03	30.00	6.00	71.14
0.	200.00	0.03	30.00	8.00	53.54
0.	200.00	0.03	35.00	2.00	116.49
0.	200.00	0.03	35.00	4.00	96.36
0.	200.00	0.03	35.00	6.00	76.92
0.	200.00	0.03	35.00	8.00	58.42
0.	200.00	0.03	40.00	2.00	123.33
0.	200.00	0.03	40.00	4.00	102.66

0	0.00	0.03	40.00	8.00	63.06
0.	200.00	0.05	20.00	2.00	90.82
0.	200.00	0.05	20.00	4.00	73.50
0.	200.00	0.05	20.00	6.00	57.29
0.	200.00	0.05	20.00	8.00	42.21
0.	200.00	0.05	25.00	2.00	98.84
0.	200.00	0.05	25.00	4.00	80.63
0.	200.00	0.05	25.00	6.00	63.33
0.	200.00	0.05	25.00	8.00	47.17
0.	200.00	0.05	30.00	2.00	106.65
0.	200.00	0.05	30.00	4.00	87.53
0.	200.00	0.05	30.00	6.00	69.30
0.	200.00	0.05	30.00	8.00	52.09
0.	200.00	0.05	35.00	2.00	114.23
0.	200.00	0.05	35.00	4.00	94.29
0.	200.00	0.05	35.00	6.00	75.20
0.	200.00	0.05	35.00	8.00	56.91
0.	200.00	0.05	40.00	2.00	121.20
0.	200.00	0.05	40.00	4.00	100.59
0.	200.00	0.05	40.00	6.00	80.72
0.	200.00	0.05	40.00	8.00	61.66
0.	200.00	0.07	20.00	2.00	89.28
0.	200.00	0.07	20.00	4.00	72.15
0.	200.00	0.07	20.00	6.00	56.09
0.	200.00	0.07	20.00	8.00	41.26
0.	200.00	0.07	25.00	2.00	97.29
0.	200.00	0.07	25.00	4.00	79.22
0.	200.00	0.07	25.00	6.00	62.10
0.	200.00	0.07	25.00	8.00	46.19
0.	200.00	0.07	30.00	2.00	105.12
0.	200.00	0.07	30.00	4.00	86.17
0.	200.00	0.07	30.00	6.00	68.12
0.	200.00	0.07	30.00	8.00	51.12
0.	200.00	0.07	35.00	2.00	112.61
0.	200.00	0.07	35.00	4.00	92.91
0.	200.00	0.07	35.00	6.00	74.03
0.	200.00	0.07	35.00	8.00	55.96
0.	200.00	0.07	40.00	2.00	119.72
0.	200.00	0.07	40.00	4.00	99.28
0.	200.00	0.07	40.00	6.00	79.56
0.	200.00	0.07	40.00	8.00	60.64

Wv M/S	Qsolar W/M2	d Cm	Ta oC	ΔT oC	Distil Gr/hr
0.50	200.00	0.01	20.00	2.00	96.37
0.50	200.00	0.01	20.00	4.00	78.72
0.50	200.00	0.01	20.00	6.00	62.00
0.50	200.00	0.01	20.00	8.00	46.30
0.50	200.00	0.01	25.00	2.00	104.50
0.50	200.00	0.01	25.00	4.00	85.88
0.50	200.00	0.01	25.00	6.00	68.19
0.50	200.00	0.01	25.00	8.00	51.36
0.50	200.00	0.01	30.00	2.00	112.44
0.50	200.00	0.01	30.00	4.00	92.99
0.50	200.00	0.01	30.00	6.00	74.24
0.50	200.00	0.01	30.00	8.00	56.32
0.50	200.00	0.01	35.00	2.00	120.03
0.50	200.00	0.01	35.00	4.00	99.79
0.50	200.00	0.01	35.00	6.00	80.14
0.50	200.00	0.01	35.00	8.00	61.15
0.50	200.00	0.01	40.00	2.00	127.03
0.50	200.00	0.01	40.00	4.00	106.03
0.50	200.00	0.01	40.00	6.00	85.59
0.50	200.00	0.01	40.00	8.00	65.78
0.50	200.00	0.03	20.00	2.00	91.63
0.50	200.00	0.03	20.00	4.00	74.52
0.50	200.00	0.03	20.00	6.00	58.40
0.50	200.00	0.03	20.00	8.00	43.35
0.50	200.00	0.03	25.00	2.00	99.77
0.50	200.00	0.03	25.00	4.00	81.69
0.50	200.00	0.03	25.00	6.00	64.50
0.50	200.00	0.03	25.00	8.00	48.32
0.50	200.00	0.03	30.00	2.00	107.72
0.50	200.00	0.03	30.00	4.00	88.82
0.50	200.00	0.03	30.00	6.00	70.62
0.50	200.00	0.03	30.00	8.00	53.32
0.50	200.00	0.03	35.00	2.00	115.38
0.50	200.00	0.03	35.00	4.00	95.61
0.50	200.00	0.03	35.00	6.00	76.53
0.50	200.00	0.03	35.00	8.00	58.22
0.50	200.00	0.03	40.00	2.00	122.54
0.50	200.00	0.03	40.00	4.00	102.06

0.50	200.00	0.03	40.00	6.00	82.18
0.50	200.00	0.03	40.00	8.00	62.91
0.50	200.00	0.05	20.00	2.00	89.29
0.50	200.00	0.05	20.00	4.00	72.50
0.50	200.00	0.05	20.00	6.00	56.62
0.50	200.00	0.05	20.00	8.00	41.88
0.50	200.00	0.05	25.00	2.00	97.41
0.50	200.00	0.05	25.00	4.00	79.65
0.50	200.00	0.05	25.00	6.00	62.75
0.50	200.00	0.05	25.00	8.00	46.87
0.50	200.00	0.05	30.00	2.00	105.46
0.50	200.00	0.05	30.00	4.00	86.71
0.50	200.00	0.05	30.00	6.00	68.81
0.50	200.00	0.05	30.00	8.00	51.85
0.50	200.00	0.05	35.00	2.00	113.16
0.50	200.00	0.05	35.00	4.00	93.54
0.50	200.00	0.05	35.00	6.00	74.74
0.50	200.00	0.05	35.00	8.00	56.76
0.50	200.00	0.05	40.00	2.00	120.33
0.50	200.00	0.05	40.00	4.00	100.12
0.50	200.00	0.05	40.00	6.00	80.42
0.50	200.00	0.05	40.00	8.00	61.47
0.50	200.00	0.07	20.00	2.00	87.73
0.50	200.00	0.07	20.00	4.00	71.09
0.50	200.00	0.07	20.00	6.00	55.45
0.50	200.00	0.07	20.00	8.00	40.95
0.50	200.00	0.07	25.00	2.00	95.91
0.50	200.00	0.07	25.00	4.00	78.26
0.50	200.00	0.07	25.00	6.00	61.54
0.50	200.00	0.07	25.00	8.00	45.92
0.50	200.00	0.07	30.00	2.00	103.90
0.50	200.00	0.07	30.00	4.00	85.36
0.50	200.00	0.07	30.00	6.00	67.66
0.50	200.00	0.07	30.00	8.00	50.85
0.50	200.00	0.07	35.00	2.00	111.53
0.50	200.00	0.07	35.00	4.00	92.17
0.50	200.00	0.07	35.00	6.00	73.61
0.50	200.00	0.07	35.00	8.00	55.78
0.50	200.00	0.07	40.00	2.00	118.84
0.50	200.00	0.07	40.00	4.00	98.72
0.50	200.00	0.07	40.00	6.00	79.20
0.50	200.00	0.07	40.00	8.00	60.54

Wv	Qsolar	d	Ta	ΔT	Distil
M/S	W/M2	Cm	oC	oC	Gr/hr
0.	400.00	0.01	20.00	2.00	263.40
0.	400.00	0.01	20.00	4.00	240.22
0.	400.00	0.01	20.00	6.00	217.32
0.	400.00	0.01	20.00	8.00	194.81
0.	400.00	0.01	25.00	2.00	275.14
0.	400.00	0.01	25.00	4.00	251.63
0.	400.00	0.01	25.00	6.00	228.51
0.	400.00	0.01	25.00	8.00	205.67
0.	400.00	0.01	30.00	2.00	285.96
0.	400.00	0.01	30.00	4.00	262.33
0.	400.00	0.01	30.00	6.00	238.86
0.	400.00	0.01	30.00	8.00	216.00
0.	400.00	0.01	35.00	2.00	294.95
0.	400.00	0.01	35.00	4.00	271.57
0.	400.00	0.01	35.00	6.00	248.28
0.	400.00	0.01	35.00	8.00	225.09
0.	400.00	0.01	40.00	2.00	302.43
0.	400.00	0.01	40.00	4.00	279.09
0.	400.00	0.01	40.00	6.00	256.18
0.	400.00	0.01	40.00	8.00	232.99
0.	400.00	0.03	20.00	2.00	255.83
0.	400.00	0.03	20.00	4.00	232.74
0.	400.00	0.03	20.00	6.00	210.16
0.	400.00	0.03	20.00	8.00	188.16
0.	400.00	0.03	25.00	2.00	267.53
0.	400.00	0.03	25.00	4.00	244.40
0.	400.00	0.03	25.00	6.00	221.49
0.	400.00	0.03	25.00	8.00	199.07
0.	400.00	0.03	30.00	2.00	278.24
0.	400.00	0.03	30.00	4.00	255.17
0.	400.00	0.03	30.00	6.00	232.02
0.	400.00	0.03	30.00	8.00	209.27
0.	400.00	0.03	35.00	2.00	287.62
0.	400.00	0.03	35.00	4.00	264.48
0.	400.00	0.03	35.00	6.00	241.62
0.	400.00	0.03	35.00	8.00	218.65
0.	400.00	0.03	40.00	2.00	295.11
0.	400.00	0.03	40.00	4.00	272.52

0.	400.00	0.03	40.00	6.00	249.66
0.	400.00	0.03	40.00	8.00	226.82
0.	400.00	0.05	20.00	2.00	251.96
0.	400.00	0.05	20.00	4.00	229.06
0.	400.00	0.05	20.00	6.00	206.61
0.	400.00	0.05	20.00	8.00	184.72
0.	400.00	0.05	25.00	2.00	263.77
0.	400.00	0.05	25.00	4.00	240.77
0.	400.00	0.05	25.00	6.00	218.09
0.	400.00	0.05	25.00	8.00	195.85
0.	400.00	0.05	30.00	2.00	274.56
0.	400.00	0.05	30.00	4.00	251.57
0.	400.00	0.05	30.00	6.00	228.60
0.	400.00	0.05	30.00	8.00	206.14
0.	400.00	0.05	35.00	2.00	284.12
0.	400.00	0.05	35.00	4.00	261.01
0.	400.00	0.05	35.00	6.00	238.07
0.	400.00	0.05	35.00	8.00	215.55
0.	400.00	0.05	40.00	2.00	291.72
0.	400.00	0.05	40.00	4.00	269.09
0.	400.00	0.05	40.00	6.00	246.31
0.	400.00	0.05	40.00	8.00	223.66
0.	400.00	0.07	20.00	2.00	249.19
0.	400.00	0.07	20.00	4.00	226.51
0.	400.00	0.07	20.00	6.00	204.30
0.	400.00	0.07	20.00	8.00	182.45
0.	400.00	0.07	25.00	2.00	261.09
0.	400.00	0.07	25.00	4.00	238.29
0.	400.00	0.07	25.00	6.00	215.67
0.	400.00	0.07	25.00	8.00	193.56
0.	400.00	0.07	30.00	2.00	271.97
0.	400.00	0.07	30.00	4.00	249.12
0.	400.00	0.07	30.00	6.00	226.38
0.	400.00	0.07	30.00	8.00	203.84
0.	400.00	0.07	35.00	2.00	281.57
0.	400.00	0.07	35.00	4.00	258.59
0.	400.00	0.07	35.00	6.00	235.86
0.	400.00	0.07	35.00	8.00	213.38
0.	400.00	0.07	40.00	2.00	289.15
0.	400.00	0.07	40.00	4.00	266.62
0.	400.00	0.07	40.00	6.00	244.24
0.	400.00	0.07	40.00	8.00	221.59

Wv	Qsolar	d	Ta	ΔT	Distil
M/S	W/M2	Cm	oC	oC	Gr/hr
1.00	400.00	0.01	20.00	2.00	239.18
1.00	400.00	0.01	20.00	4.00	217.65
1.00	400.00	0.01	20.00	6.00	196.58
1.00	400.00	0.01	20.00	2.00	250.82
1.00	400.00	0.01	20.00	4.00	228.91
1.00	400.00	0.01	20.00	6.00	207.34
1.00	400.00	0.01	20.00	8.00	186.31
1.00	400.00	0.01	25.00	2.00	264.32
1.00	400.00	0.01	25.00	4.00	241.96
1.00	400.00	0.01	25.00	6.00	219.83
1.00	400.00	0.01	25.00	8.00	198.17
1.00	400.00	0.01	30.00	2.00	276.86
1.00	400.00	0.01	30.00	4.00	253.95
1.00	400.00	0.01	30.00	6.00	231.43
1.00	400.00	0.01	30.00	8.00	209.47
1.00	400.00	0.01	35.00	2.00	287.91
1.00	400.00	0.01	35.00	4.00	265.06
1.00	400.00	0.01	35.00	6.00	242.28
1.00	400.00	0.01	35.00	8.00	219.80
1.00	400.00	0.01	40.00	2.00	297.38
1.00	400.00	0.01	40.00	4.00	274.52
1.00	400.00	0.01	40.00	6.00	251.71
1.00	400.00	0.01	40.00	8.00	228.89
1.00	400.00	0.03	20.00	2.00	243.06
1.00	400.00	0.03	20.00	4.00	221.43
1.00	400.00	0.03	20.00	6.00	200.18
1.00	400.00	0.03	20.00	8.00	179.52
1.00	400.00	0.03	25.00	2.00	256.55
1.00	400.00	0.03	25.00	4.00	234.35
1.00	400.00	0.03	25.00	6.00	212.73
1.00	400.00	0.03	25.00	8.00	191.44
1.00	400.00	0.03	30.00	2.00	269.11
1.00	400.00	0.03	30.00	4.00	246.63
1.00	400.00	0.03	30.00	6.00	224.50
1.00	400.00	0.03	30.00	8.00	202.75
1.00	400.00	0.03	35.00	2.00	280.42
1.00	400.00	0.03	35.00	4.00	257.84
1.00	400.00	0.03	35.00	6.00	235.34
1.00	400.00	0.03	35.00	8.00	213.31
1.00	400.00	0.03	40.00	2.00	290.09
1.00	400.00	0.03	40.00	4.00	267.62

1.00	400.00	0.03	40.00	6.00	244.91
1.00	400.00	0.03	40.00	8.00	222.64
1.00	400.00	0.05	20.00	2.00	239.18
1.00	400.00	0.05	20.00	4.00	217.65
1.00	400.00	0.05	20.00	6.00	196.58
1.00	400.00	0.05	20.00	8.00	176.19
1.00	400.00	0.05	25.00	2.00	252.70
1.00	400.00	0.05	25.00	4.00	230.70
1.00	400.00	0.05	25.00	6.00	209.20
1.00	400.00	0.05	25.00	8.00	188.01
1.00	400.00	0.05	30.00	2.00	265.33
1.00	400.00	0.05	30.00	4.00	242.98
1.00	400.00	0.05	30.00	6.00	221.06
1.00	400.00	0.05	30.00	8.00	199.45
1.00	400.00	0.05	35.00	2.00	276.60
1.00	400.00	0.05	35.00	4.00	254.30
1.00	400.00	0.05	35.00	6.00	231.95
1.00	400.00	0.05	35.00	8.00	210.00
1.00	400.00	0.05	40.00	2.00	286.61
1.00	400.00	0.05	40.00	4.00	264.10
1.00	400.00	0.05	40.00	6.00	241.73
1.00	400.00	0.05	40.00	8.00	219.43
1.00	400.00	0.07	20.00	2.00	236.54
1.00	400.00	0.07	20.00	4.00	215.19
1.00	400.00	0.07	20.00	6.00	194.23
1.00	400.00	0.07	20.00	8.00	173.87
1.00	400.00	0.07	25.00	2.00	250.07
1.00	400.00	0.07	25.00	4.00	228.22
1.00	400.00	0.07	25.00	6.00	206.78
1.00	400.00	0.07	25.00	8.00	185.82
1.00	400.00	0.07	30.00	2.00	262.69
1.00	400.00	0.07	30.00	4.00	240.46
1.00	400.00	0.07	30.00	6.00	218.70
1.00	400.00	0.07	30.00	8.00	197.18
1.00	400.00	0.07	35.00	2.00	274.15
1.00	400.00	0.07	35.00	4.00	251.72
1.00	400.00	0.07	35.00	6.00	229.68
1.00	400.00	0.07	35.00	8.00	207.75
1.00	400.00	0.07	40.00	2.00	284.06
1.00	400.00	0.07	40.00	4.00	261.60
1.00	400.00	0.07	40.00	6.00	239.30
1.00	400.00	0.07	40.00	8.00	217.37

Wv M/S	Qsolar W/M2	d Cm	Ta oC	ΔT oC	Distil Gr/hr
0.	600.00	0.01	20.00	2.00	451.72
0.	600.00	0.01	20.00	4.00	427.01
0.	600.00	0.01	20.00	6.00	402.62
0.	600.00	0.01	20.00	8.00	378.02
0.	600.00	0.01	25.00	2.00	460.88
0.	600.00	0.01	25.00	4.00	436.79
0.	600.00	0.01	25.00	6.00	412.88
0.	600.00	0.01	25.00	8.00	388.92
0.	600.00	0.01	30.00	2.00	466.97
0.	600.00	0.01	30.00	4.00	444.27
0.	600.00	0.01	30.00	6.00	421.16
0.	600.00	0.01	30.00	8.00	397.47
0.	600.00	0.01	35.00	2.00	470.40
0.	600.00	0.01	35.00	4.00	448.67
0.	600.00	0.01	35.00	6.00	426.38
0.	600.00	0.01	35.00	8.00	404.12
0.	600.00	0.01	40.00	2.00	469.67
0.	600.00	0.01	40.00	4.00	449.47
0.	600.00	0.01	40.00	6.00	428.95
0.	600.00	0.01	40.00	8.00	407.26
0.	600.00	0.03	20.00	2.00	441.68
0.	600.00	0.03	20.00	4.00	417.48
0.	600.00	0.03	20.00	6.00	393.10
0.	600.00	0.03	20.00	8.00	368.95
0.	600.00	0.03	25.00	2.00	451.16
0.	600.00	0.03	25.00	4.00	427.61
0.	600.00	0.03	25.00	6.00	403.69
0.	600.00	0.03	25.00	8.00	379.86
0.	600.00	0.03	30.00	2.00	457.56
0.	600.00	0.03	30.00	4.00	435.05
0.	600.00	0.03	30.00	6.00	412.27
0.	600.00	0.03	30.00	8.00	389.08
0.	600.00	0.03	35.00	2.00	461.12
0.	600.00	0.03	35.00	4.00	439.64
0.	600.00	0.03	35.00	6.00	417.74
0.	600.00	0.03	35.00	8.00	395.57
0.	600.00	0.03	40.00	2.00	460.90
0.	600.00	0.03	40.00	4.00	440.95

0.00	600.00	0.03	40.00	6.00	420.33
0.00	600.00	0.03	40.00	8.00	399.23
0.00	600.00	0.05	20.00	2.00	436.92
0.00	600.00	0.05	20.00	4.00	412.72
0.00	600.00	0.05	20.00	6.00	388.39
0.00	600.00	0.05	20.00	8.00	364.37
0.00	600.00	0.05	25.00	2.00	446.41
0.00	600.00	0.05	25.00	4.00	422.85
0.00	600.00	0.05	25.00	6.00	399.28
0.00	600.00	0.05	25.00	8.00	375.31
0.00	600.00	0.05	30.00	2.00	453.04
0.00	600.00	0.05	30.00	4.00	430.48
0.00	600.00	0.05	30.00	6.00	407.73
0.00	600.00	0.05	30.00	8.00	384.63
0.00	600.00	0.05	35.00	2.00	456.60
0.00	600.00	0.05	35.00	4.00	435.08
0.00	600.00	0.05	35.00	6.00	413.57
0.00	600.00	0.05	35.00	8.00	391.12
0.00	600.00	0.05	40.00	2.00	456.56
0.00	600.00	0.05	40.00	4.00	436.52
0.00	600.00	0.05	40.00	6.00	415.92
0.00	600.00	0.05	40.00	8.00	394.94
0.00	600.00	0.07	20.00	2.00	433.42
0.00	600.00	0.07	20.00	4.00	409.52
0.00	600.00	0.07	20.00	6.00	385.26
0.00	600.00	0.07	20.00	8.00	361.12
0.00	600.00	0.07	25.00	2.00	442.92
0.00	600.00	0.07	25.00	4.00	419.67
0.00	600.00	0.07	25.00	6.00	396.16
0.00	600.00	0.07	25.00	8.00	372.30
0.00	600.00	0.07	30.00	2.00	449.79
0.00	600.00	0.07	30.00	4.00	427.24
0.00	600.00	0.07	30.00	6.00	404.54
0.00	600.00	0.07	30.00	8.00	381.54
0.00	600.00	0.07	35.00	2.00	453.50
0.00	600.00	0.07	35.00	4.00	432.36
0.00	600.00	0.07	35.00	6.00	410.49
0.00	600.00	0.07	35.00	8.00	388.49
0.00	600.00	0.07	40.00	2.00	453.49
0.00	600.00	0.07	40.00	4.00	433.84
0.00	600.00	0.07	40.00	6.00	413.26
0.00	600.00	0.07	40.00	8.00	392.32

Wv M/S	Qsolar W/M2	d Cm	Ta oC	ΔT oC	Distil Gr/hr
1.00	600.00	0.01	20.00	2.00	432.35
1.00	600.00	0.01	20.00	4.00	408.04
1.00	600.00	0.01	20.00	6.00	383.95
1.00	600.00	0.01	20.00	8.00	359.95
1.00	600.00	0.01	25.00	2.00	446.22
1.00	600.00	0.01	25.00	4.00	422.15
1.00	600.00	0.01	25.00	6.00	398.40
1.00	600.00	0.01	25.00	8.00	374.51
1.00	600.00	0.01	30.00	2.00	458.06
1.00	600.00	0.01	30.00	4.00	434.62
1.00	600.00	0.01	30.00	6.00	410.65
1.00	600.00	0.01	30.00	8.00	387.00
1.00	600.00	0.01	35.00	2.00	467.05
1.00	600.00	0.01	35.00	4.00	443.95
1.00	600.00	0.01	35.00	6.00	420.86
1.00	600.00	0.01	35.00	8.00	397.54
1.00	600.00	0.01	40.00	2.00	472.53
1.00	600.00	0.01	40.00	4.00	450.29
1.00	600.00	0.01	40.00	6.00	427.85
1.00	600.00	0.01	40.00	8.00	405.32
1.00	600.00	0.03	20.00	2.00	422.33
1.00	600.00	0.03	20.00	4.00	398.33
1.00	600.00	0.03	20.00	6.00	374.42
1.00	600.00	0.03	20.00	8.00	350.75
1.00	600.00	0.03	25.00	2.00	436.34
1.00	600.00	0.03	25.00	4.00	412.49
1.00	600.00	0.03	25.00	6.00	388.83
1.00	600.00	0.03	25.00	8.00	365.23
1.00	600.00	0.03	30.00	2.00	448.21
1.00	600.00	0.03	30.00	4.00	424.92
1.00	600.00	0.03	30.00	6.00	401.35
1.00	600.00	0.03	30.00	8.00	377.88
1.00	600.00	0.03	35.00	2.00	457.41
1.00	600.00	0.03	35.00	4.00	434.51
1.00	600.00	0.03	35.00	6.00	411.70
1.00	600.00	0.03	35.00	8.00	388.50
1.00	600.00	0.03	40.00	2.00	462.97
1.00	600.00	0.03	40.00	4.00	441.23

- 00	600.00	0.03	40.00	6.00	419.02
1.00	600.00	0.03	40.00	8.00	396.53
1.00	600.00	0.05	20.00	2.00	417.16
1.00	600.00	0.05	20.00	4.00	393.44
1.00	600.00	0.05	20.00	6.00	369.68
1.00	600.00	0.05	20.00	8.00	346.21
1.00	600.00	0.05	25.00	2.00	431.34
1.00	600.00	0.05	25.00	4.00	407.81
1.00	600.00	0.05	25.00	6.00	384.24
1.00	600.00	0.05	25.00	8.00	360.77
1.00	600.00	0.05	30.00	2.00	443.33
1.00	600.00	0.05	30.00	4.00	420.06
1.00	600.00	0.05	30.00	6.00	396.81
1.00	600.00	0.05	30.00	8.00	373.47
1.00	600.00	0.05	35.00	2.00	452.53
1.00	600.00	0.05	35.00	4.00	429.88
1.00	600.00	0.05	35.00	6.00	407.08
1.00	600.00	0.05	35.00	8.00	383.99
1.00	600.00	0.05	40.00	2.00	458.54
1.00	600.00	0.05	40.00	4.00	436.71
1.00	600.00	0.05	40.00	6.00	414.48
1.00	600.00	0.05	40.00	8.00	392.35
1.00	600.00	0.07	20.00	2.00	413.83
1.00	600.00	0.07	20.00	4.00	390.13
1.00	600.00	0.07	20.00	6.00	366.42
1.00	600.00	0.07	20.00	8.00	343.03
1.00	600.00	0.07	25.00	2.00	428.06
1.00	600.00	0.07	25.00	4.00	404.49
1.00	600.00	0.07	25.00	6.00	380.93
1.00	600.00	0.07	25.00	8.00	357.53
1.00	600.00	0.07	30.00	2.00	440.06
1.00	600.00	0.07	30.00	4.00	416.71
1.00	600.00	0.07	30.00	6.00	393.45
1.00	600.00	0.07	30.00	8.00	370.41
1.00	600.00	0.07	35.00	2.00	449.13
1.00	600.00	0.07	35.00	4.00	426.71
1.00	600.00	0.07	35.00	6.00	403.85
1.00	600.00	0.07	35.00	8.00	381.05
1.00	600.00	0.07	40.00	2.00	455.26
1.00	600.00	0.07	40.00	4.00	433.59
1.00	600.00	0.07	40.00	6.00	411.60
1.00	600.00	0.07	40.00	8.00	389.41

Wv M/S	Qsolar W/M2	d Cm	Ta oC	ΔT oC	Distil Gr/hr
0.	800.00	0.01	20.00	2.00	629.68
0.	800.00	0.01	20.00	4.00	607.81
0.	800.00	0.01	20.00	6.00	586.13
0.	800.00	0.01	20.00	8.00	563.68
0.	800.00	0.01	25.00	2.00	628.20
0.	800.00	0.01	25.00	4.00	608.52
0.	800.00	0.01	25.00	6.00	587.86
0.	800.00	0.01	25.00	8.00	566.85
0.	800.00	0.01	30.00	2.00	621.57
0.	800.00	0.01	30.00	4.00	604.07
0.	800.00	0.01	30.00	6.00	585.42
0.	800.00	0.01	30.00	8.00	566.36
0.	800.00	0.01	35.00	2.00	609.42
0.	800.00	0.01	35.00	4.00	594.80
0.	800.00	0.01	35.00	6.00	578.10
0.	800.00	0.01	35.00	8.00	560.91
0.	800.00	0.01	40.00	2.00	591.49
0.	800.00	0.01	40.00	4.00	578.96
0.	800.00	0.01	40.00	6.00	565.65
0.	800.00	0.01	40.00	8.00	550.98
0.	800.00	0.03	20.00	2.00	617.80
0.	800.00	0.03	20.00	4.00	596.55
0.	800.00	0.03	20.00	6.00	575.01
0.	800.00	0.03	20.00	8.00	552.39
0.	800.00	0.03	25.00	2.00	616.40
0.	800.00	0.03	25.00	4.00	597.46
0.	800.00	0.03	25.00	6.00	577.10
0.	800.00	0.03	25.00	8.00	556.41
0.	800.00	0.03	30.00	2.00	610.34
0.	800.00	0.03	30.00	4.00	593.16
0.	800.00	0.03	30.00	6.00	574.94
0.	800.00	0.03	30.00	8.00	555.79
0.	800.00	0.03	35.00	2.00	599.31
0.	800.00	0.03	35.00	4.00	584.41
0.	800.00	0.03	35.00	6.00	568.29
0.	800.00	0.03	35.00	8.00	551.11
0.	800.00	0.03	40.00	2.00	581.83
0.	800.00	0.03	40.00	4.00	569.17

0.00	800.00	0.03	40.00	6.00	555.79
0.00	800.00	0.03	40.00	8.00	541.20
0.00	800.00	0.05	20.00	2.00	612.18
0.00	800.00	0.05	20.00	4.00	590.82
0.00	800.00	0.05	20.00	6.00	569.21
0.00	800.00	0.05	20.00	8.00	547.00
0.00	800.00	0.05	25.00	2.00	611.01
0.00	800.00	0.05	25.00	4.00	591.47
0.00	800.00	0.05	25.00	6.00	571.50
0.00	800.00	0.05	25.00	8.00	550.85
0.00	800.00	0.05	30.00	2.00	604.93
0.00	800.00	0.05	30.00	4.00	587.65
0.00	800.00	0.05	30.00	6.00	569.87
0.00	800.00	0.05	30.00	8.00	550.74
0.00	800.00	0.05	35.00	2.00	594.08
0.00	800.00	0.05	35.00	4.00	579.12
0.00	800.00	0.05	35.00	6.00	563.00
0.00	800.00	0.05	35.00	8.00	546.41
0.00	800.00	0.05	40.00	2.00	576.52
0.00	800.00	0.05	40.00	4.00	564.44
0.00	800.00	0.05	40.00	6.00	551.08
0.00	800.00	0.05	40.00	8.00	536.52
0.00	800.00	0.07	20.00	2.00	608.01
0.00	800.00	0.07	20.00	4.00	587.16
0.00	800.00	0.07	20.00	6.00	565.64
0.00	800.00	0.07	20.00	8.00	543.18
0.00	800.00	0.07	25.00	2.00	607.17
0.00	800.00	0.07	25.00	4.00	587.74
0.00	800.00	0.07	25.00	6.00	567.89
0.00	800.00	0.07	25.00	8.00	547.38
0.00	800.00	0.07	30.00	2.00	601.29
0.00	800.00	0.07	30.00	4.00	584.13
0.00	800.00	0.07	30.00	6.00	566.03
0.00	800.00	0.07	30.00	8.00	547.09
0.00	800.00	0.07	35.00	2.00	590.49
0.00	800.00	0.07	35.00	4.00	575.68
0.00	800.00	0.07	35.00	6.00	559.73
0.00	800.00	0.07	35.00	8.00	542.82
0.00	800.00	0.07	40.00	2.00	573.38
0.00	800.00	0.07	40.00	4.00	560.89
0.00	800.00	0.07	40.00	6.00	547.70
0.00	800.00	0.07	40.00	8.00	533.39

Wv	Qsolar	d	Ta	ΔT	Distil
M/S	W/M2	Cm	oC	oC	Gr/hr
1.00	800.00	0.01	20.00	2.00	620.24
1.00	800.00	0.01	20.00	4.00	596.19
1.00	800.00	0.01	20.00	6.00	572.08
1.00	800.00	0.01	20.00	8.00	547.67
1.00	800.00	0.01	25.00	2.00	629.55
1.00	800.00	0.01	25.00	4.00	606.16
1.00	800.00	0.01	25.00	6.00	583.07
1.00	800.00	0.01	25.00	8.00	559.45
1.00	800.00	0.01	30.00	2.00	634.36
1.00	800.00	0.01	30.00	4.00	612.11
1.00	800.00	0.01	30.00	6.00	590.05
1.00	800.00	0.01	30.00	8.00	567.30
1.00	800.00	0.01	35.00	2.00	633.72
1.00	800.00	0.01	35.00	4.00	613.73
1.00	800.00	0.01	35.00	6.00	592.70
1.00	800.00	0.01	35.00	8.00	571.31
1.00	800.00	0.01	40.00	2.00	627.62
1.00	800.00	0.01	40.00	4.00	609.41
1.00	800.00	0.01	40.00	6.00	590.59
1.00	800.00	0.01	40.00	8.00	570.60
1.00	800.00	0.03	20.00	2.00	608.45
1.00	800.00	0.03	20.00	4.00	584.41
1.00	800.00	0.03	20.00	6.00	560.44
1.00	800.00	0.03	20.00	8.00	536.62
1.00	800.00	0.03	25.00	2.00	617.37
1.00	800.00	0.03	25.00	4.00	594.51
1.00	800.00	0.03	25.00	6.00	571.51
1.00	800.00	0.03	25.00	8.00	548.15
1.00	800.00	0.03	30.00	2.00	622.56
1.00	800.00	0.03	30.00	4.00	600.87
1.00	800.00	0.03	30.00	6.00	578.93
1.00	800.00	0.03	30.00	8.00	556.43
1.00	800.00	0.03	35.00	2.00	622.65
1.00	800.00	0.03	35.00	4.00	602.18
1.00	800.00	0.03	35.00	6.00	581.80
1.00	800.00	0.03	35.00	8.00	560.69
1.00	800.00	0.03	40.00	2.00	617.02
1.00	800.00	0.03	40.00	4.00	598.31

1.00	800.00	0.03	40.00	6.00	579.60
1.00	800.00	0.03	40.00	8.00	560.45
1.00	800.00	0.05	20.00	2.00	602.43
1.00	800.00	0.05	20.00	4.00	578.70
1.00	800.00	0.05	20.00	6.00	554.69
1.00	800.00	0.05	20.00	8.00	530.84
1.00	800.00	0.05	25.00	2.00	611.42
1.00	800.00	0.05	25.00	4.00	588.79
1.00	800.00	0.05	25.00	6.00	565.75
1.00	800.00	0.05	25.00	8.00	542.74
1.00	800.00	0.05	30.00	2.00	616.38
1.00	800.00	0.05	30.00	4.00	594.99
1.00	800.00	0.05	30.00	6.00	573.33
1.00	800.00	0.05	30.00	8.00	550.85
1.00	800.00	0.05	35.00	2.00	616.87
1.00	800.00	0.05	35.00	4.00	596.68
1.00	800.00	0.05	35.00	6.00	576.22
1.00	800.00	0.05	35.00	8.00	555.46
1.00	800.00	0.05	40.00	2.00	611.35
1.00	800.00	0.05	40.00	4.00	592.97
1.00	800.00	0.05	40.00	6.00	574.15
1.00	800.00	0.05	40.00	8.00	554.91
1.00	800.00	0.07	20.00	2.00	598.29
1.00	800.00	0.07	20.00	4.00	574.53
1.00	800.00	0.07	20.00	6.00	550.84
1.00	800.00	0.07	20.00	8.00	527.02
1.00	800.00	0.07	25.00	2.00	607.43
1.00	800.00	0.07	25.00	4.00	584.74
1.00	800.00	0.07	25.00	6.00	562.00
1.00	800.00	0.07	25.00	8.00	538.66
1.00	800.00	0.07	30.00	2.00	612.41
1.00	800.00	0.07	30.00	4.00	590.94
1.00	800.00	0.07	30.00	6.00	569.28
1.00	800.00	0.07	30.00	8.00	547.15
1.00	800.00	0.07	35.00	2.00	612.76
1.00	800.00	0.07	35.00	4.00	592.94
1.00	800.00	0.07	35.00	6.00	572.42
1.00	800.00	0.07	35.00	8.00	551.65
1.00	800.00	0.07	40.00	2.00	607.37
1.00	800.00	0.07	40.00	4.00	589.41
1.00	800.00	0.07	40.00	6.00	570.48
1.00	800.00	0.07	40.00	8.00	551.21

Wv M/S	Qsolar W/M2	d Cm	Ta oC	ΔT oC	Distil Gr/hr
0.	1000.00	0.01	20.00	2.00	760.18
0.	1000.00	0.01	20.00	4.00	746.25
0.	1000.00	0.01	20.00	6.00	731.82
0.	1000.00	0.01	20.00	8.00	716.26
0.	1000.00	0.01	25.00	2.00	738.79
0.	1000.00	0.01	25.00	4.00	728.64
0.	1000.00	0.01	25.00	6.00	716.39
0.	1000.00	0.01	25.00	8.00	702.92
0.	1000.00	0.01	30.00	2.00	710.14
0.	1000.00	0.01	30.00	4.00	702.91
0.	1000.00	0.01	30.00	6.00	694.27
0.	1000.00	0.01	30.00	8.00	684.39
0.	1000.00	0.01	35.00	2.00	674.68
0.	1000.00	0.01	35.00	4.00	670.11
0.	1000.00	0.01	35.00	6.00	665.11
0.	1000.00	0.01	35.00	8.00	657.82
0.	1000.00	0.01	40.00	2.00	630.18
0.	1000.00	0.01	40.00	4.00	630.04
0.	1000.00	0.01	40.00	6.00	628.46
0.	1000.00	0.01	40.00	8.00	624.53
0.	1000.00	0.03	20.00	2.00	746.83
0.	1000.00	0.03	20.00	4.00	733.77
0.	1000.00	0.03	20.00	6.00	719.50
0.	1000.00	0.03	20.00	8.00	703.51
0.	1000.00	0.03	25.00	2.00	726.16
0.	1000.00	0.03	25.00	4.00	715.57
0.	1000.00	0.03	25.00	6.00	704.38
0.	1000.00	0.03	25.00	8.00	691.35
0.	1000.00	0.03	30.00	2.00	698.32
0.	1000.00	0.03	30.00	4.00	691.50
0.	1000.00	0.03	30.00	6.00	682.61
0.	1000.00	0.03	30.00	8.00	672.50
0.	1000.00	0.03	35.00	2.00	662.80
0.	1000.00	0.03	35.00	4.00	659.73
0.	1000.00	0.03	35.00	6.00	653.72
0.	1000.00	0.03	35.00	8.00	647.20
0.	1000.00	0.03	40.00	2.00	620.09
0.	1000.00	0.03	40.00	4.00	619.83

0.00	1000.00	0.03	40.00	6.00	618.18
0.00	1000.00	0.03	40.00	8.00	614.35
0.00	1000.00	0.05	20.00	2.00	740.59
0.00	1000.00	0.05	20.00	4.00	726.97
0.00	1000.00	0.05	20.00	6.00	712.82
0.00	1000.00	0.05	20.00	8.00	697.06
0.00	1000.00	0.05	25.00	2.00	719.59
0.00	1000.00	0.05	25.00	4.00	709.80
0.00	1000.00	0.05	25.00	6.00	698.15
0.00	1000.00	0.05	25.00	8.00	685.31
0.00	1000.00	0.05	30.00	2.00	692.46
0.00	1000.00	0.05	30.00	4.00	685.14
0.00	1000.00	0.05	30.00	6.00	676.52
0.00	1000.00	0.05	30.00	8.00	666.69
0.00	1000.00	0.05	35.00	2.00	657.43
0.00	1000.00	0.05	35.00	4.00	653.85
0.00	1000.00	0.05	35.00	6.00	648.20
0.00	1000.00	0.05	35.00	8.00	641.99
0.00	1000.00	0.05	40.00	2.00	614.88
0.00	1000.00	0.05	40.00	4.00	614.94
0.00	1000.00	0.05	40.00	6.00	612.88
0.00	1000.00	0.05	40.00	8.00	609.46
0.00	1000.00	0.07	20.00	2.00	735.72
0.00	1000.00	0.07	20.00	4.00	722.58
0.00	1000.00	0.07	20.00	6.00	708.28
0.00	1000.00	0.07	20.00	8.00	692.98
0.00	1000.00	0.07	25.00	2.00	715.44
0.00	1000.00	0.07	25.00	4.00	705.50
0.00	1000.00	0.07	25.00	6.00	693.74
0.00	1000.00	0.07	25.00	8.00	680.87
0.00	1000.00	0.07	30.00	2.00	688.23
0.00	1000.00	0.07	30.00	4.00	681.48
0.00	1000.00	0.07	30.00	6.00	672.79
0.00	1000.00	0.07	30.00	8.00	662.90
0.00	1000.00	0.07	35.00	2.00	653.62
0.00	1000.00	0.07	35.00	4.00	649.95
0.00	1000.00	0.07	35.00	6.00	644.95
0.00	1000.00	0.07	35.00	8.00	638.01
0.00	1000.00	0.07	40.00	2.00	611.30
0.00	1000.00	0.07	40.00	4.00	611.32
0.00	1000.00	0.07	40.00	6.00	609.21
0.00	1000.00	0.07	40.00	8.00	605.81

Wv M/S	Qsolar W/M2	d Cm	Ta oC	ΔT oC	Distil Gr/hr
1.00	1000.00	0.01	20.00	2.00	794.31
1.00	1000.00	0.01	20.00	4.00	773.56
1.00	1000.00	0.01	20.00	6.00	751.44
1.00	1000.00	0.01	20.00	8.00	729.67
1.00	1000.00	0.01	25.00	2.00	791.35
1.00	1000.00	0.01	25.00	4.00	772.20
1.00	1000.00	0.01	25.00	6.00	752.06
1.00	1000.00	0.01	25.00	8.00	731.72
1.00	1000.00	0.01	30.00	2.00	781.87
1.00	1000.00	0.01	30.00	4.00	764.87
1.00	1000.00	0.01	30.00	6.00	746.76
1.00	1000.00	0.01	30.00	8.00	728.31
1.00	1000.00	0.01	35.00	2.00	764.38
1.00	1000.00	0.01	35.00	4.00	750.26
1.00	1000.00	0.01	35.00	6.00	734.88
1.00	1000.00	0.01	35.00	8.00	718.34
1.00	1000.00	0.01	40.00	2.00	738.78
1.00	1000.00	0.01	40.00	4.00	726.80
1.00	1000.00	0.01	40.00	6.00	714.19
1.00	1000.00	0.01	40.00	8.00	701.03
1.00	1000.00	0.03	20.00	2.00	780.50
1.00	1000.00	0.03	20.00	4.00	759.48
1.00	1000.00	0.03	20.00	6.00	738.21
1.00	1000.00	0.03	20.00	8.00	716.34
1.00	1000.00	0.03	25.00	2.00	777.53
1.00	1000.00	0.03	25.00	4.00	758.69
1.00	1000.00	0.03	25.00	6.00	739.05
1.00	1000.00	0.03	25.00	8.00	718.64
1.00	1000.00	0.03	30.00	2.00	768.32
1.00	1000.00	0.03	30.00	4.00	751.22
1.00	1000.00	0.03	30.00	6.00	733.69
1.00	1000.00	0.03	30.00	8.00	715.79
1.00	1000.00	0.03	35.00	2.00	750.95
1.00	1000.00	0.03	35.00	4.00	736.74
1.00	1000.00	0.03	35.00	6.00	721.98
1.00	1000.00	0.03	35.00	8.00	706.14
1.00	1000.00	0.03	40.00	2.00	725.83
1.00	1000.00	0.03	40.00	4.00	714.56

1.00	1000.00	0.03	40.00	6.00	701.99
1.00	1000.00	0.03	40.00	8.00	688.90
1.00	1000.00	0.05	20.00	2.00	773.21
1.00	1000.00	0.05	20.00	4.00	752.62
1.00	1000.00	0.05	20.00	6.00	731.34
1.00	1000.00	0.05	20.00	8.00	709.51
1.00	1000.00	0.05	25.00	2.00	770.61
1.00	1000.00	0.05	25.00	4.00	751.72
1.00	1000.00	0.05	25.00	6.00	732.06
1.00	1000.00	0.05	25.00	8.00	712.18
1.00	1000.00	0.05	30.00	2.00	761.43
1.00	1000.00	0.05	30.00	4.00	744.85
1.00	1000.00	0.05	30.00	6.00	727.32
1.00	1000.00	0.05	30.00	8.00	708.96
1.00	1000.00	0.05	35.00	2.00	744.39
1.00	1000.00	0.05	35.00	4.00	730.73
1.00	1000.00	0.05	35.00	6.00	715.40
1.00	1000.00	0.05	35.00	8.00	699.64
1.00	1000.00	0.05	40.00	2.00	719.84
1.00	1000.00	0.05	40.00	4.00	708.56
1.00	1000.00	0.05	40.00	6.00	696.00
1.00	1000.00	0.05	40.00	8.00	682.97
1.00	1000.00	0.07	20.00	2.00	768.73
1.00	1000.00	0.07	20.00	4.00	747.82
1.00	1000.00	0.07	20.00	6.00	726.70
1.00	1000.00	0.07	20.00	8.00	705.04
1.00	1000.00	0.07	25.00	2.00	765.72
1.00	1000.00	0.07	25.00	4.00	746.99
1.00	1000.00	0.07	25.00	6.00	727.50
1.00	1000.00	0.07	25.00	8.00	707.81
1.00	1000.00	0.07	30.00	2.00	756.47
1.00	1000.00	0.07	30.00	4.00	740.05
1.00	1000.00	0.07	30.00	6.00	722.73
1.00	1000.00	0.07	30.00	8.00	704.55
1.00	1000.00	0.07	35.00	2.00	740.28
1.00	1000.00	0.07	35.00	4.00	726.22
1.00	1000.00	0.07	35.00	6.00	711.09
1.00	1000.00	0.07	35.00	8.00	695.54
1.00	1000.00	0.07	40.00	2.00	715.17
1.00	1000.00	0.07	40.00	4.00	704.10
1.00	1000.00	0.07	40.00	6.00	691.80
1.00	1000.00	0.07	40.00	8.00	679.01

SYNTHETIC ICE AND FINE PARTICLES
IN AN ENCLOSED RECTANGULAR CAVITY AND ITS APPLICATION TO
SOLAR STILLIZATION

W. M. HADJICHAOS and J. D. COOPER

The City Polytechnic, Northampton Square, London EC1A 3AA, U.K.

In the first part of this work the results of experiments have
and were used to fit an air-water vapour mixture to experiment. The
physical model is an enclosed rectangular cavity with the two lower
parallel faces insulated or insulated and different temperatures. A
film of water film was on the lower and higher parallel face of the
cavity. Heat transfer from the film, but at the same time
radiation from the upper and lower parallel face. A natural
convection flow is established in the cavity, and the equations of
continuity, momentum, energy and diffusion are solved by an integral
diffusion method of solution. The results are compared with the
data in the cavity to show the agreement to an integral form the
procedure.

OUTLINE OF A PAPER TO BE PRESENTED IN

WORLD SOLAR FORUM
CONGRESS OF INTERNATIONAL SOLAR ENERGY SOCIETY
23-28 AUG 1981, BRIGHTON

In the second part of the work the results of the first part
are applied to the solar stillization of water, in which the
evaporative cavity face is exposed to incident solar radiation. In
conjunction with this solar radiation, reaching the water is
found to be. The empirical equation of Page (6) is used to
predict daily totals of evaporation on a horizontal surface. Then
the formula of Page (7) is modified to allow for the effects of
wind and it used to calculate hourly evaporation from the predicted
daily totals. The results of model are also used for calculating
water collection on a tilted surface. Finally, daily, weekly, and
annual evaporation on a tilted surface are calculated over the periods
in question.

The relationship between solar energy absorbed by a tilted solar
still and other parameters of energy transfer is investigated.
The distribution rate, as a function of solar radiation and other
parameters, is derived. Finally the performance of a tilted solar
still, and the effect of geometric variables, design factors, and
operation conditions are discussed.

SIMULTANEOUS HEAT AND MASS TRANSFER
IN AN INCLINED RECTANGULAR CAVITY AND ITS APPLICATION TO
SOLAR DISTILLATION

M. Bazargan and J.R. Simonson *

The City University, Northampton Square, London EC1V OHB.

In the first part of this work the problem of simultaneous heat and mass transfer in an air water vapour mixture is considered. The physical model is an inclined rectangular cavity with the two longer parallel faces maintained at constant and different temperatures. A film of water flows over the lower and hotter parallel face of the cavity. Evaporation takes place from this face, and at the same time condensation occurs on the upper and cooler parallel face. A natural recirculating flow is established in the cavity, and the equations of continuity, momentum, energy and diffusion are solved by the finite difference scheme of Spalding, Gosman, Patankar and others(1). The air in the cavity is assumed non-soluble. As an initial test the procedure is applied to pure heat transfer in a vertical rectangular cavity and a comparison is made with experimental data of Carlson (2). Secondly, the problem of water distillation in a vertical cavity is examined and results are compared with the data of Davis (3). Finally the procedure is applied to distillation in an inclined cavity at 10° increments of inclination between 0° and 90° . In each case two types of correlation model are obtained.

In the second part of the work the results of the first part are applied to the solar distillation of saline water, in which the evaporative cavity face is heated by incident solar radiation. In conjunction with this work global radiation reaching the earth is first examined. The empirical equation of Page (4) is used to estimate daily totals of radiation on a horizontal surface. Then the formula of Close (5) is modified to allow for the effects of clouds and is used to calculate hourly radiation from the estimated daily figures. The findings of Busler (6) are then used for calculating hourly radiation on a tilted surface. Finally, daily, monthly, and annual radiation on a tilted surface are calculated over the periods in question.

The relationship between solar energy absorbed by a tilted solar still and other interrelated components of energy transfer is formulated. The distillation rate, as a function of solar radiation and other parameters, is obtained. Finally the performance of a tilted solar still, and the effect of atmospheric variables, design factors, and operation conditions are examined.

- (1) DAVIS, J. E., "Simultaneous energy and mass transfer in partial pressure distillation", Ph.D. Thesis, University of Wisconsin, Madison, Wisconsin (1965).
- (2) SU, C. Y., "A theoretical and interferometric study of transport phenomena in partial pressure distillation in a rectangular enclosure", Ph.D. Thesis, University of Wisconsin (1971).
- (3) CARLSON, W. G., "Interferometric studies of convective flow phenomena in vertical plane enclosed air layers", Ph.D. Thesis, University of Minnesota (1956).
- (4) ENRETI, A. F. and CHU, N. C., "Heat transfer across vertical layers", Journal of Heat Transfer, Transactions of the American Society of Mechanical Engineers, Series C, Vol. 87, p. 110 (1965).
- * (5) HELLUMS, J. G. and CHURCHILL, S. W., "Computation of natural convection by finite difference methods", Proceedings of the International Heat Transfer Conference (1961).
- (6) HELLUMS, J. G. and CHURCHILL, S. W., "Transient and steady state, free and natural convection, numerical solutions", American Institute of Chemical Engineers, Journal, Vol. 8, p. 630 (1962).
- (7) WILSON, J. D., "The finite difference computation of natural convection in an enclosed rectangular cavity", Ph.D. Thesis, University of Michigan, Ann Arbor, Michigan (1963).
- (8) SYDANI DAVIS, G. and BENTLEYBOUGH, C. F., "Natural convection in an enclosed rectangular cavity", Mechanical and Chemical Engineering Transactions, The Institute of Mechanical Engineers, Australia, no. 12

- [1] DAVIS, J. E., "Simultaneous energy and mass transfer in partial pressure distillation", Ph.D. Thesis, University of Wisconsin, Madison, Wisconsin (1965).
- [2] HU, C. Y., "A theoretical and interferometric study of transport phenomena in partial pressure distillation in a rectangular enclosure", Ph.D. Thesis, University of Wisconsin (1971).
- [3] CARLSON, W. O., "Interferometric studies of convective flow phenomena in vertical plane enclosed air layers", Ph.D. Thesis, University of Minnesota (1956).
- [4] EMERY, A. F. and CHU, N. C., "Heat transfer across vertical layers", Journal of Heat Transfer, Transactions of American Society of Mechanical Engineers, Series C, Vol. 87, p. 110 (1965).
- [5] HELLUMS, J. D. and CHURCHILL, S. W., "Computation of natural convection by finite difference methods", Proceedings of the International Heat Transfer Conference (1961).
- [6] HELLUMS, J. D. and CHURCHILL, S. W., "Transient and steady state, free and natural convection, numerical solutions", American Institute of Chemical Engineers, Journal, Vol. 8, p. 690 (1962).
- [7] WILKES, J. O., "The finite difference computation of natural convection in an enclosed rectangular cavity", Ph.D. Thesis, University of Michigan, Ann Arbor, Michigan (1963).
- [8] DEVAHL DAVIS, G. and KETTLEBOROUGH, C. F., "Natural convection in an enclosed rectangular cavity", Mechanical and Chemical Engineering Transactions, The Institute of Mechanical Engineers, Australia, no. 43

(May 1965).

- [9] ELDER, J. W., "Laminar free convection in a vertical slot", *Journal of Fluid Mechanics*, Vol. 23, p. 77 (1965).
- [10] WILKES, J. O., CHURCHILL, S. W., "The finite difference computation on natural convection in a rectangular enclosure", *American Institute of Chemical Engineers Journal*, Vol. 12, No. 1, p. 161 (1966).
- [11] SAMUELS, M. R. and CHURCHILL, S. W., "Stability of a fluid in a rectangular region heated from below", *American Institute of Chemical Engineers*, Vol. 13, No. 1, p. 77 (1967).
- [12] DEVAHL DAVIS, G., "Laminar natural convection in an enclosed rectangular cavity", *International Journal of Heat and Mass Transfer*, Vol. 11, p. 1675, (1968).
- [13] ELDER, J. W., "Numerical experiments with free convection in a vertical slot", *Journal of Fluid Mechanics*, Vol. 24, p. 823 (1968).
- [14] PEACEMAN, D. W. and RACHFORD, J. H. H., "The numerical solution of parabolic and elliptic differential equations", *Society for Industrial Applied Mathematic*, Vol. 3, No. 1, p. 28 (1955).
- [15] SPALDING, D. B., "A novel finite-difference formulation for differential expressions involving both first and second derivatives", *International Journal for Numerical Methods in Engineering*, Vol. 4, p. 541 (1972).
- [16] CARETTO, L. S., GOSMAN, A. D., PATANKAR, S. V. and SPALDING, D. B., "Two calculation procedures for

- steady, three dimensional flows with recirculation", Proceedings of Third International Conference on Numerical Methods in Fluid Dynamics, Paris (July 1972).
- [17] TELKES, M., "Improved solar stills", Transactions of the Conference on the Use of Solar Energy, Vol. 3, Part 2, p. 145, University of Arizona Press (1955).
- [18] DUNKLE, R. V., "Solar water distillation, the roof type still and a multiple effect diffusion still", International Heat Transfer Conference, Part V, International Developements in Heat Transfer, University of Colorado, p.895 (1961).
- [19] MACLEOD, L. H. and McCracken, H. W., "Performance of greenhouse solar stills", Sea Water Conversion Program, University of California, Series 75, Issue 26, November (1961).
- [20] BAUM, V. A. and BARIRAMOV, R., "Heat and Mass Transfer Processes in Solar Stills of the Hot-Box Type", Solar Energy, Vol.8, No.3, p.78 (1964).
- [21] GRUNE, W. N., COLLINS, R. A., HUGHES, R. B. and THOMPSON, R. L., "Development of an improved solar still", United States Department of Interior, Office of Saline Water Research and Development Progress, Report No. 60 (1962).
- [22] HOLLANDS, K. G. T., "The regeneration of lithium chloride brine in a solar still for use in solar air conditioning", Solar Energy, Vol. 7, No. 2, p. 39 (1963).
- [23] MORSE, R. N. and READ, W. R. W., "A rational basis for the engineering development of a solar still",

- Solar Energy, Vol. 12, No. 1, p. 5, September (1968).
- [24] SHERIDAN, N. R., BULLOCK, K. J. and DUFFIE, J. A.,
"Study of the solar processes by analogue computer",
Solar Energy, Vol. 11, No. 2, p. 69 (1967).
- [25] CLOSE, D. J., "A design approach for solar processes",
Solar Energy, Vol.11, No.2, p.112 (1967).
- [26] COOPER, P. I., "The transient analysis of glass
covered solar stills", Ph.D Thesis, University of
Western Australia (1970).
- [27] JAKOB, M., "Heat transfer", Vol. II, John Wiley and
Sons, Inc., New York (1957).
- [28] BOWEN, I. S., "The ratio of heat loss by conduction
and by evaporation from any water surface", The
Physical Review, Vol.27, 2nd Series, p.779 (1926).
- [29] BIRD, R. B., STEWART, W. E. and LIGHTFOOT, E. N.,
"Transport phenomena", John Wiley and Sons, Inc.,
New York (1960).
- [30] SHERWOOD, T. K. and PIGFORD, R. L., "Absorption and
extraction", New York, McGraw-Hill Book Company,
Inc., (1952).
- [31] GOSMAN, A. D., PUN W. M., RUNCHAL, A. K., SPALDING,
D. B. and WOLFSHTEIN, M., "Heat and mass transfer
in recirculating flows", Academic Press, London
(1969).
- [32] PATANKAR, S. V. and SPALDING, D. B. "Numerical
predictions of three-dimensional flows" Imperial
College, Mechanical Engineering Department, Report
EF/TN/A/46 (June 1972).
- [33] PATANKAR, S. V. and SPALDING, D. B. "A calculation
procedure for heat, mass and momentum transfer in

- three-dimensional parabolic flows", International Journal of Heat and Mass Transfer, Vol. 15, p. 1787, (1972).
- [34] GOSMAN, A. D. and IDERIAH F. J. K., "A general computer program for two dimensional, turbulent, recirculating flows", Department of Mechanical Engineering, Imperial College, Unpublished manuscript (1976).
- [35] ECKERT, E. R. G. and CARLSON, W. O., "Natural convection in an air layer enclosed between two vertical plates with different temperatures", Journal of Heat and Mass transfer, Vol. 2, p. 106 (1961).
- [36] SCHINKEL, W. M. M. and HOOGENDOORN, C. J., "Interferometric study of the local heat transfer by natural convection in inclined air filled enclosure", International Heat Transfer Conference, 6th Toronto, p. 287 (1979).
- [37] LANGE, N. A., "Handbook of chemistry", 9th edition, p. 1438, Handbook publishers, Sandusky, Ohio (1956).
- [38] HARDING, J., "Apparatus for solar distillation", Proceedings of Institution of Civil Engineers, Vol. 73, p.284 (1883).
- [39] TELKES, M., "Flat, tilted solar stills", proceedings, International Seminar on Solar and Aeolian Energy, Sounian, Greece, New York, Plenum Press, p. 14 (1964).
- [40] TELKES, M., "Research on methods for solar distillation", Office of Saline Water Report No. 13, PB 161388, 66 pages (Dec 1956).
- [41] TELKES, M., "Solar still theory and new research", Proceedings, Symposium on Saline Water Conversion,

- National Academy of Sciences, National Research Council, Washington, D. C., Publication No. 568, p. 568 (Nov 1957).
- [42] TELKES, M., "New and improved methods for lower cost solar distillation", Office of Saline Water Report No. 31, PB 161402, 38 pages (Aug 1959).
- [43] TELKES, M., "Solar still construction", Office of Saline Water Report No. 33, PB161404, 18 pages (Aug 1959).
- [44] FRITZ, S., "Transmission of solar energy through the earth's clear and cloudy atmosphere", Transactions of the Conference on Use of Solar Energy, Vol.1, p.17, University of Arizona Press, Tucson, (1958).
- [45] MOON, P., "Proposed standard radiation curves for engineering use", Journal Franklin Institute, Vol. 230, p. 583 (1940).
- [46] LIU, B. Y. H. and JORDAN, R. C., "The inter-relationship and characteristic distribution of direct, diffuse and total solar radiation", Solar Energy, 4, No. 3, (1960).
- [47] BUGLER, J. W., "The determination of hourly insolation on an inclined plane using a diffuse irradiance model based on hourly measured global horizontal insolation", Solar Energy, Vol. 19, p. 477 (1977).
- [48] BENFORD, F. and BOCK, J. E., "A time analysis of sunshine", American Illuminating Engineering Society Transactions, Vol. 34, p. 200 (1939).
- [49] COOPER, P. I., "The absorption of radiation in solar

- stills", Solar Energy, Vol.12, p. 333 (1969).
- [50] NORRIS, D. J., "Solar radiation on inclined surfaces", Solar Energy, Vol. 10, No. 2, April (1966).
- [51] PAGE, J. K., "The estimation of monthly mean values of daily total short-wave radiation on vertical and inclined surfaces from sunshine records for latitudes 40 deg N - 40 deg S", Proceedings of UN Conference on New Sources of Energy, 4, 378 (1964).
- [52] DUFFIE, J. A. and BECKMAN, W. A., "Solar energy thermal processes", John Wiley and Sons, New York, (1974).
- [53] LÖF, G. O. G., DUFFIE, J. A., and SMITH, C. O., "World distribution of solar radiation", Engineering Experiment Station Report 21, University of Wisconsin, Madison (July 1966).
- [54] BRINKWORTH, B. J., "Autocorrelation and stochastic modeling of insolation sequences", Solar Energy, Vol. 19, p. 343 (1977).
- [55] LIU, B. Y. H. and JORDAN, R. C., "The long-term average performance of flat-plate solar energy collectors.", Solar Energy, 7, p. 53 (1963).
- [56] SOLAR ENERGY ORGANIZATION, IRAN, Personal communication (1978).
- [57] MCADAMS, W. H., "Heat transmission", 3rd ed., McGraw-Hill Book Company, Inc., New York (1954).
- [58] COOPER, P. I., "Digital simulation of transient solar still processes", Solar Energy, Vol. 12, p. 313 (1969).
- [59] HOWE, E. D., "Solar distillation research at the university of California", U. N. Conference on New

Sources of Energy, Paper 35/S/29, Rome, 22 pages
(Aug 1961).

- [60] BLOEMER, J. W., IRWIN, J. R. and EIBLING, J. A.,
"Second two years' progress on study and field
evaluation of solar sea-water stills", Battelle
Memorial Institute, Office of Saline Water Report
No. 147, 83 pages (July 1965).
- [61] TELKES, M., "Fresh water from sea water by solar
distillation", Industrial and Engineering Chemistry,
Vol. 45, No.5, p. 1108 (May 1953).
- [62] LÖF, G. O. G., EIBLING, J. A. and BLOEMER, J. W.,
"Energy balances in solar distillers", American
Institute of Chemical Engineers, Journal, Vol. 7,
No. 4, p. 641 (Dec 1961).
- [63] BLOEMER, J. W., EIBLING, J. A., IRWIN, J. A. and
LÖF, G. O. G., "Analog computer simulation of solar
still operation", American Society of Mechanical
Engineers, Paper 63-WA-313, 8 pages (nov 1963).
- [64] BLOEMER, J. W., "Factors affecting solar-still
performance", American Society of Mechanical
Engineers, Paper 65-WA/SOL-1, 8 pages (nov 1965).
- [65] TALBERT, S. G. and EIBLING, J. A., "Manual on solar
distillation of saline water", United states Depart-
ment of the Interior, Research and Development Progress
Report No. 546 (Apr 1970).
- [66] PROCTOR, D., "Effect of adding waste heat to a solar
still", Solar Energy, Vol. 14, No. 4, p. 433 (1973).
- [67] BEARD, J. T., LACHETTA, F. A., LILLELEHT, L. U. and
HUCKSTEP, F. L., "Design and operational influences
on thermal performance of solaris solar collector",

Journal of Engineering for Power, Vol. 100, p. 497
(1978).

- [68] COOPER, P. I. and READ, W. R. W., "Design philosophy and operating experience for Australian solar stills", International Congress the sun in the service of mankind, Report E103, (Jul 1973).
- [69] TREWARTHA, G. T., "An introduction to climate", 3rd edition, New York, McGraw-Hill (1954).
- [70] KUSUDA, T., "calculation of the temperature of a flat-plate wet surface under adiabatic conditions", Humidity and Moisture Measurement and Control in Science and Industry, Vol. 1, p. 28, Reinhold, New York (1965).
- [71] KOBE, K. A., "Thermochemistry of petrochemicals", p. 32, Reprint no. 44, University of Texas Bureau of Engineering Research, Austin (1958).
- [72] LANGE, N. A., "Handbook of chemistry", 9th edition, p. 1464, Handbook publishers, Sandusky, Ohio (1956).
- [73] HOUGEN, O. A., WATSON, K. M. and RAGATZ, R. A., "Chemical process principles", Part 1, second edition, p. 281, Jhon Wiley and Sons, New York (1956).